Det Norske Veritas

Final Report

Development of Heat-Affected Zone Hardness Limits for In-Service Welding

PHMSA Research and Development
Agreement #DTPH56-07-T-000004
Project #216

Report No./DNV Reg. No.: ENAUS826BBRUCE (20090930) – Version 1

Development of Heat-Affected Zone Hardness Limits for In-Service Welding		DNV Columbus, Inc. Asset Risk Management 5777 Frantz Road Dublin, OH 43017-1386 Tel: (614) 761-1214 Fax: (614) 761-1633 http://www.dnv.com http://www.dnvcolumbus.com	
For: PHMSA Research and Development Agreement #DTPH56-07-T-000004 Project #216			
Account Reference:	82673428		
Date of Issue:	September 29, 2009	Project No.:	82673428
Report No.:	ENAUS826BBRUCE	Organization Unit:	Asset Risk Management
Revisions No.:	1	Subject Group:	Welding & Materials Technology

Summary:

The objective of this project was to develop heat-affected zone hardness acceptance criteria that can be used to evaluate welds during the qualification of procedures for welding onto in-service pipelines. A series of graphs was developed that show proposed maximum-allowable hardness as a function of material chemical composition (CE level) for a range of thicknesses. In addition, guidance was developed for several issues related to the application of HAZ hardness limits to welds made onto in-service pipelines.

Prepared by:	William A. Bruce Director Welding & Materials Technology	
Prepared by:	Bradley C. Etheridge Staff Welding Engineer Welding & Materials Technology	
Prepared by:	Vincent R. Arnett Welding Engineer Welding & Materials Technology	
Contributions made by:	Andrew Carman University of Wollongong	
Contributions made by:	David Nolan BlueScope Steel	

☐	No distribution without permission from the client or responsible organizational unit (however, free distribution for internal use within DNV after 3 years).	Indexing Terms:	
■	No distribution without permission from the client or responsible organizational unit.	Key Words:	Welding, Heat-Affected Zone, Hardness Limits
☐	Strictly confidential.	Service Area:	Asset Risk Management
☐	Unrestricted distribution.	Market Segment:	Onshore Pipelines

Rev. No. / Date:	Reason for Issue:	Prepared by:	Approved by:	Verified by:

© 2008 DNV Columbus, Inc.
All rights reserved. This publication or parts thereof may not be reproduced or transmitted in any form or by any means, including photocopying or recording, without the prior written consent of DNV Columbus, Inc.

EXECUTIVE SUMMARY

Welding onto in-service pipelines is frequently required to facilitate a repair or to install a branch connection using the "hot tapping" technique. Welds made in-service cool at an accelerated rate as the result of the ability of the flowing contents to remove heat from the pipe wall. These welds, therefore, are likely to have hard heat-affected zones (HAZs) and an increased susceptibility to hydrogen cracking. To prevent hydrogen cracking, at least one of the three conditions necessary for its occurrence must be eliminated or reduced to below a threshold level. Beyond the use of low-hydrogen electrodes to minimize hydrogen levels, it is prudent to develop and use procedures that minimize the formation of crack-susceptible microstructures. Exactly how crack susceptible microstructures are defined, and what microstructures and hardness levels will lead to cracking for any given set of conditions, is the subject of some debate, however.

HAZ hardness is often used as an indicator of the susceptibility of a microstructure to cracking during the evaluation of procedure qualification welds. A widely used value below which it is generally agreed that hydrogen cracking is not expected to occur is 350 HV. Critical hardness level, or the hardness level below which hydrogen cracking is not expected to occur, is not a fixed value, but depends on the hydrogen level of the welding process being used and on the chemical composition (carbon content and carbon equivalent or CE level) of the materials being welded. The ability of welds to tolerate high HAZ hardness is also affected somewhat by joint restraint. The objective of this project was to develop HAZ hardness acceptance criteria that can be used to evaluate welds during the qualification of procedures for welding onto in-service pipelines.

The current work focused on the further development and validation of previously-developed criteria, particularly for modern microalloyed materials and material over a wide range of wall thicknesses. The experimental portion of this work was carried out in two parallel phases. One phase involved practical weldability trials to further develop previously established empirical limits for a wider range of conditions. The other phase involved a more fundamental approach to more confidently prescribe hardness limitations by investigating microstructural susceptibility to hydrogen cracking.

A series of graphs was developed that show proposed maximum-allowable hardness as a function of material chemical composition (CE level) for a range of thicknesses. In addition, guidance was developed for several issues related to the application of HAZ hardness limits to welds made onto in-service pipelines. This guidance focuses on the way in which HAZ hardness is measured during the qualification of welding procedures, determination of chemical composition for an in-service pipeline, and control of weld hydrogen levels.

Table of Contents

1. INTRODUCTION 1
2. BACKGROUND 1
3. FACTORS AFFECTING CRITICAL HARDNESS LEVELS 2
3.1 Weld Hydrogen Level 2
3.2 Material Chemical Composition 3
3.3 Joint Restraint 3
4. PREVIOUS WORK 3
5. CURRENT WORK 4
6. Full-Scale Weldability Trials 4
6.1 Materials 5
6.2 Weld Hydrogen Level 6
6.3 Weld Thermal Cycles 7
6.4 Experimental Matrix 7
6.5 Experimental Procedure 8
7. Results 9
8. Analysis of Results 9
9. Microstructural Susceptibility Work 10
10. Development of Criteria 10
11. Validation of Criteria during Field Trials 16
12. Development of Related Guidance 17
12.1 Measurement of HAZ Hardness during Procedure Qualification 17
12.1.1 Indenter type 18
12.1.2 Surface finish 18
12.1.3 Indentation location 18
12.1.4 Load/indentation size 18
12.1.5 Number of indentations required 19
12.1.6 Treatment of results 19
12.1.7 Proposed HAZ hardness testing procedure 19
12.2 Determination of Chemical Composition for an In-Service Pipeline 19
12.2.1 Interrogation of Records 20
12.2.2 Measurement using Portable Equipment 20
12.2.3 Removal of Small Sample for Laboratory Measurement 20

Table of Contents (continued)

12.2.4 General Rules of Thumb 20
12.3 Control of Weld Hydrogen Levels 21
12.3.1 Electrode Procurement 21
12.3.2 Electrode Packaging 21
13. DISCUSSION 22
14. SUMMARY AND CONCLUSIONS 23
15. ACKNOWLEGEMENT 24
16. REFERENCES 25

List of Tables

Table 1. List of Steel Materials for Full-Scale Weldability Trials and Small-Scale Experiments 28
Table 2. Chemical Composition Results for Materials Listed in Table 1 29
Table 3. List of Welding Consumables for Weldability Trials 30
Table 4. Diffusible Hydrogen Analysis Results for Consumables Listed in Table 3 31
Table 5. Experimental Matrix for Full-Scale Weldability Trials at DNV 32
Table 6. Welding Parameters for Full-Scale Weldability Trials at DNV 33
Table 7. Results for Full-Scale Weldability Trials at DNV 42
Table 8. Summary of Results for Full-Scale Weldability Trials 50
Table 9. General Rules of Thumb for Pipe Material Chemical Composition 55

List of Figures

Figure 1. Schematic Illustration of HAZ Microstructure in Low CE Material Consisting of 90% Martensite (%C = 0.06, HVM = 353, HV = 343)..... 56
Figure 2. Schematic Illustration of HAZ Microstructure in High CE Material Consisting of 40% Martensite (%C = 0.30, HVM = 545, HV = 368)..... 56
Figure 3. Critical Hardness Level vs. CEIIW Level from Several Previous Programs. [10]57
Figure 4. Critical Hardness Level for In-Service Welds vs. CEIIW and Weld Hydrogen Level from Previous Work..... 57
Figure 5. Example of Highly-Restrained Multi-Pass Fillet Weld from Previous Program. 58
Figure 6. Comparison of Hardness Testing Results with Hardness Evaluation Criterion from Previous Work..... 58
Figure 7. Experimental Setup for Highly-Restrained Multi-Pass Fillet Welds in Current Work. 59
Figure 8. Setup for Flowing Mineral Oil Condition..... 59
Figure 9. Three-Pass Fillet Weld being made at Target Heat Input Level..... 60
Figure 10. Example of Completed Three-Pass Fillet Weld..... 60
Figure 11. Example of metallographic section completed weld. 61
Figure 12. HAZ Hardness Indent Locations 61
62
Figure 13. Example of nick-break specimen from completed weld with root crack. 62
62
Figure 14. Example of face-bend specimen from completed weld with toe crack. 62
Figure 15. Preliminary HAZ Hardness Evaluation Criteria based on CEIIW for Thinner Materials with Carbon Contents greater than 0.10%..... 63
Figure 16. Comparison of HAZ Hardness Testing Results with Preliminary Hardness Evaluation Criterion..... 64
Figure 17. Example of Three-Dimensional HAZ Hardness Evaluation Criteria for In-Service Welds – ≤ 4 ml/100g Hydrogen Level..... 65
Figure 18. HAZ Hardness Evaluation Criteria for In-Service Welds – ≤ 4 ml/100g Hydrogen Level 66
Figure 19. HAZ Hardness Evaluation Criteria for In-Service Welds – ≤ 8 ml/100g Hydrogen Level 67
Figure 20. HAZ Hardness Evaluation Criteria for In-Service Welds – ≤ 16 ml/100g Hydrogen Level 68

List of Figures (continued)

Figure 21. HAZ Hardness Evaluation Criteria for In-Service Welds – Cellulosic-Coated Electrodes 69
Figure 22. Comparison of HAZ Hardness Testing Results with Hardness Evaluation Criteria shown in Figures 21 through 24 70
Figure 23. Columbia Gas Line 1804 with Eventual Hot Tap Location Marked 71
Figure 24. Completed Confirmation Welds on Line 1804 71
Figure 25. Hot Tap Branch Welded Over Completed Confirmation Welds 72
Figure 26. Hot Tap Coupons with Confirmation Welds after Removal 72
Figure 27. Typical Metallographic Section through Completed Confirmation Welds 73
Figure 28. E7018-H4R Electrodes in 10-lb (4.5-kg) Hermetically Sealed Can 73

List of Appendices

Appendix A. Review of Previous Work Related to the Development of HAZ Hardness Evaluation Criteria
Appendix B. Results of Small-Scale Experimental Simulations at University of Wollongong
Appendix C. Control of Weld Hydrogen Levels for Welds Made onto In-Service Pipelines

1. INTRODUCTION

Welding onto in-service pipelines is frequently required to facilitate a repair or to install a branch connection using the "hot tapping" technique. There are significant economic and environmental incentives for performing pipeline repair and maintenance without removing the pipeline from service. From an economic viewpoint, a shutdown involves revenue loss from the loss of pipeline throughput, in addition to that from the gas lost to the atmosphere. Since methane is a so-called "greenhouse gas", there are also environmental incentives for avoiding the venting of large quantities of gas into the atmosphere.

Welds made in-service cool at an accelerated rate as the result of the ability of the flowing contents to remove heat from the pipe wall. These welds, therefore, are likely to have hard heat-affected zones (HAZs) and an increased susceptibility to hydrogen cracking. To prevent hydrogen cracking, at least one of the three conditions necessary for its occurrence must be eliminated or reduced to below a threshold level. Beyond the use of low-hydrogen electrodes to minimize hydrogen levels, it is prudent to develop and use procedures that minimize the formation of crack-susceptible microstructures. Exactly how crack susceptible microstructures are defined, and what microstructures and hardness levels will lead to cracking for any given set of conditions, is the subject of some debate, however.

The objective of this project was to develop HAZ hardness acceptance criteria that can be used to evaluate welds during the qualification of procedures for welding onto in-service pipelines.

2. BACKGROUND

Hydrogen cracking in welds made onto in-service pipelines, like other welds, requires that three primary, independent conditions be satisfied simultaneously. These conditions are as follows:

- Hydrogen in the weld. All arc welding processes introduce hydrogen into the weld to some extent. Hydrogen can originate from moisture in electrode coatings, in the atmosphere (humidity) or on the pipe surface (condensation). Hydrogen can also originate from hydrocarbons or other organic contaminants on the pipe or on the welding consumables.

- Susceptible weld microstructure. In general, hard HAZ microstructures are most susceptible to hydrogen cracking. Such microstructures are promoted by steel that has a high carbon equivalent (CE) value and by rapid weld cooling rates. Weld cooling rates are determined by welding heat input and pipeline operating conditions. Operating conditions that influence weld cooling rates include product type, flow rates, ambient temperatures, and pipe wall thickness. Weld metal microstructures can also be susceptible to hydrogen cracking.

- Tensile stresses acting on the weld. Tensile stresses can be either applied or residual. Applied stresses can result from movement of a pipeline due to soil settlement. Residual stresses arise from the restraint of the welded connection and strains imposed by the contraction of the weld on cooling.

HAZ hardness is often used as an indicator of the susceptibility of a microstructure to cracking during the evaluation of procedure qualification welds. A widely used value below which it is generally agreed that hydrogen cracking is not expected to occur is 350 HV. Both API 1104 Appendix B [1] and the Canadian code CSA Z662 [2] indicate that procedures for in-service welding that produce HAZ hardness greater than 350 HV should be evaluated with regard to the risk of hydrogen cracking. Neither of these codes provides guidance pertaining to how this evaluation should be performed. The Australian standard AS 2885.2 [3] prohibits HAZ hardness greater than 350 HV for in-service welds.

The generally-regarded notion that 350 HV is a hardness level below which hydrogen cracking is not expected dates back to work by Dearden and O'Neill in the 1940s [4]. This notion was validated by Bailey in the early 1970s for welds with a diffusible hydrogen content of approximately 16 ml/100 g of deposited weld metal [5]. Bailey also noted that for welds with a diffusible hydrogen content of approximately 8 ml/100 g, the critical hardness, or the hardness level below which hydrogen cracking is not expected, is on the order of 400 HV. The 350 HV limit was used in work by Graville and Read in the mid-1970s [6]. This limit was later adopted by Kiefner, et al., during work that resulted in the development of the Battelle thermal analysis computer model for hot tap welding [7]. The Battelle work mentions that this value is especially pertinent to pipelines, as a previous study [8] showed that accidental hard spots (un-tempered martensite) in line pipe will crack during service when exposed to mild hydrogen charging (typical of cathodic protection) if the hardness is in excess of 360 Brinell (equivalent to 380 HV).

3. FACTORS AFFECTING CRITICAL HARDNESS LEVELS

Critical hardness level, or the hardness level below which hydrogen cracking is not expected to occur, is not a fixed value, but depends on the hydrogen level of the welding process being used (as suggested by Bailey) and on the chemical composition (carbon content and CE level) of the materials being welded. The ability of welds to tolerate high HAZ hardness is also affected somewhat by joint restraint.

3.1 Weld Hydrogen Level

The risk of hydrogen cracking increases as hydrogen level increases. Lower limits on hardness are required where higher hydrogen levels are anticipated. Conversely, closer control of hydrogen level allows higher hardness to be tolerated. Many modern low-hydrogen (AWS EXX18-type) electrodes, particularly those with the "H4R" supplemental designator (e.g., E7018-H4R) produce weld hydrogen levels of less than 4 ml/100 g. For this reason, a hardness limit of 350 HV may be highly conservative for some applications.

3.2 Material Chemical Composition

While HAZ hardness is often used as an indicator of cracking susceptibility, the true susceptibility depends on the microstructures present in the HAZ. A better indicator of cracking susceptibility might be the volume fraction of crack-susceptible microstructures, such as martensite, in the HAZ. For a material of a given chemical composition, HAZ hardness is a good indicator of the relative amount of martensite present in the HAZ. The hardness of martensite depends on the carbon level of the material being welded, however. One formula for determining the hardness of martensite [9] is:

$$HM = 802\ (C) + 305 \qquad (1)$$

The measured hardness in the HAZ of a low carbon material that consists mostly of martensite (schematically illustrated in Figure 1) may be lower than the measured hardness in a higher carbon material with a much lower volume fraction of martensite (Figure 2), yet the cracking susceptibility in the lower carbon material might be higher. In other words, lower carbon content materials tend to crack at lower hardness levels. Conversely, higher hardness can be tolerated when welding higher carbon content materials. Several previous programs by others have attempted to address this issue [10-14].

3.3 Joint Restraint

Welds in more-highly-restrained joints are more susceptible to cracking than welds in less-highly restrained joints. For the type of welds that are typically made onto in-service pipelines, joint restraint is primarily governed by material thicknesses.

4. PREVIOUS WORK

A comprehensive review of previous work related to the development of HAZ hardness evaluation criteria is shown in Appendix A and is summarized below.

Critical hardness level is shown as a function of CE_{IIW} level from several previous programs in Figure 3. The data shown in this figure are for fillet welds made at a hydrogen level of approximately 12 ml/100 g. In subsequent work [15], this figure was used as a starting point for the development of a HAZ hardness evaluation criterion for welds made onto in-service pipelines. This hardness evaluation criterion was developed to quantify the trade-offs that can be made between hardness, hydrogen level, and chemical composition. This hardness evaluation criterion was later incorporated into the users' manual for the PRCI Thermal Analysis Model for Hot Tap Welding [16].

A hardness evaluation criterion for in-service welds that is loosely based on Figure 3 is shown in Figure 4. This figure shows HAZ hardness limits as a function of CE_{IIW} for three different weld hydrogen levels. For each CE level, the critical hardness level for the 8 ml/100 g hydrogen level is roughly that extrapolated from a lower bound of the data shown in Figure 3 from several previous programs. A 25 HV increase in the critical hardness was allowed for the 4 ml/100 g hydrogen level. A 50 HV decrease was imposed for the welds made using cellulosic-coated electrodes.

To evaluate this criterion, highly-restrained multi-pass fillet welds were made under simulated in-service conditions (Figure 5) on materials with a variety of chemical compositions using a variety of different hydrogen levels, after which they were metallography sectioned to measure hardness at the weld toe and to examine for the presence of cracks. A comparison of the hardness testing results with the evaluation criterion is shown in Figure 6. This figure indicates that the criterion has accurately predicted the occurrence of cracking (i.e., welds that are cracked tend not to meet the criterion), although there is some conservatism.

While this criterion has been effective for the conditions that were evaluated [0.375-inch (9.5-mm)-thick materials with a carbon content greater than 0.10%], additional data was required to further validate this criterion and to expand its applicability to a broader range of materials, which is the objective of the current work. The use of such a criterion is useful in determining how close the use of a certain procedure in a specific application is to the hydrogen cracking threshold.

5. CURRENT WORK

The current work, which was sponsored in part by the US Department of Transportation – Pipeline and Hazardous Materials Safety Administration, focused on the further development and validation of these previously-developed criteria, particularly for modern microalloyed materials and material over a wide range of wall thicknesses. The experimental portion of this work was carried out in two parallel phases. One phase (work carried out under the direction of DNV Columbus [formerly CC Technologies]) involved practical weldability trials to further develop previously established empirical limits for a wider range of conditions. The other phase (work carried out under the direction of University of Wollongong) involved a more fundamental approach to more confidently prescribe hardness limitations by investigating microstructural susceptibility to hydrogen cracking.

6. FULL-SCALE WELDABILITY TRIALS

In this phase of the work, full-scale hydrogen cracking tests, which also allow measurement of resulting hardness levels, were performed. An experimental procedure similar to that used in the previous work was used. This procedure involves highly restrained multi-pass fillet welds that are made under simulated in-service conditions. The use of multiple passes allows residual stresses to develop fully and allows tempering from subsequent passes to be considered. Trials

were carried out on materials with a variety of chemical compositions and thicknesses using a variety of different hydrogen levels. Welds were made using two thermal severity levels, which were simulated using either flowing water or flowing mineral oil on the inside of the pipe material.

6.1 Materials

Table 1 contains a summary of the steel materials for the full-scale weldability trials at DNV Columbus (DNV) and the small-scale experiments at University of Wollongong (UoW). Many of these are new materials to the program, although some are common to previous work in this area. A description of these materials is given below.

- Material N3A – This material is an SA516 Grade 70 plate material with a chemical composition and microstructure similar to older vintage line pipe material. It is similar in composition (CE_{IIW} of 0.42) and thickness (0.375 inch [9.5 mm]) to a material in previous work [15]. It was used to validate the new setup for the full-scale trials by duplicating results from this previous work.

- Material A1 – This material is an Australian-produced API 5LX-60 (20-inch-diameter by 0.339-inch [8.6 mm] wall thickness). It has a carbon content of 0.17% and a carbon equivalent (CE_{IIW}) of 0.38. Some small scale experimental data are available for this material from previous work. This material was used primarily for the initial development work for the new small-scale experimental procedure (e.g., Gleeble specimen configuration, hydrogen charging procedure, fracture toughness testing protocol, etc.).

- Material P6 – This material is an older vintage API 5LX-52 that is thinner than the materials used in the original program (0.312 inch [7.9 mm] as opposed to 0.375 inch [9.5 mm]). Full-scale test data for this material is available from subsequent work. It was used for the small-scale experiments, the results of which were used to develop a relationship between full-scale weldability trials and small-scale experiments.

- Material P2 – This material is a relatively modern API 5LX-65 (36-inch-diameter by 0.375-inch [9.5 mm] thick) that has relatively low carbon content (0.14%) but above the 0.10% carbon content threshold that separated the modern and conventional compositions in the previous programs. Full-scale test data for this material is available from previous work. This material was used for the small-scale experiments, the results of which were used to develop a relationship between full-scale weldability trials and small-scale experiments.

- Material GTN – This material is a 1961 vintage API 5LX-52 (36-inch-diameter by 0.437-inch [11.1 mm] wall thickness) that is representative of an older material in the TransCanada PipeLines (TCPL) system. It has a carbon content of 0.21% and a CE_{IIW} of 0.40. It was used for both full-scale weldability trials and small-scale experiments.

- Material TC2 – This material is a modern API 5LX-80 (36-inch-diameter by 0.543-inch [13.8 mm] wall thickness) microalloyed material that is representative of what TCPL has used in the recent past. This material was used for both full-scale weldability trials and small-scale experiments.
- Material EB5 – This material is an older vintage API 5LX-52 (34-inch diameter by 0.281-inch [7.1 mm] wall thickness). It has a carbon content of 0.27% and a CE_{IIW} of 0.48 and was used to generate additional full-scale weldability trial data.
- Material EB5-S – This is a 0.500 inch [12.7 mm] wall thickness full-encirclement sleeve material that was installed on an older vintage API 5LX-52 (34-inch diameter) pipeline. It has a carbon content of 0.14 % and a CE_{IIW} of 0.39 and was used to generate additional full-scale weldability trial data.
- Material EX1 – This is a limited production experimental X120 line pipe material (36-inch diameter by 0.636-inch [16.2 mm] wall thickness). It has a carbon content of 0.025%, a manganese content of 2.14%, a CE_{IIW} of 0.55, and a Pcm carbon equivalent of 0.20. It was used to generate additional full-scale weldability trial data.

Chemical composition results for these materials are given in Table 2.

Some of the materials are common to both phases of the work. This was intended to develop a link between the results of the full-scale hydrogen cracking tests and the small-scale fracture behavior experiments. The primary material variables of interest for the full-scale weldability trials were chemical composition and thickness. The primary material variable of interest for the small-scale tests was chemical composition. For the full-scale weldability trials, restraint levels are affected by material thickness. For the small-scale experiments, restraint level is simulated by the application of load during testing.

6.2 Weld Hydrogen Level

Welding consumables that were procured for the full-scale weldability trials at DNV are summarized in Table 3. These include standard AWS E7018-H4R (low hydrogen) electrodes, specially prepared E7018 electrodes, and standard cellulosic-coated electrodes (i.e., AWS E-6010 type). Standard E7018-H4R electrodes were used in the as-received condition for welds intended to have a hydrogen level of 4 ml/100 g or less. Standard E6010 electrodes were used for welds intended to have a hydrogen level of approximately 40-60 ml/100 g. Two separate batches of low hydrogen electrodes were procured for welds intended to have an elevated hydrogen level (initially hoped to be approximately 8 ml/100 g). One was a batch of partially-dried E7018 electrodes that was procured from the manufacturer. The other is a batch of E7018 electrodes from a second-tier manufacturer that was procured from a local supplier. Diffusible hydrogen testing was carried out to confirm diffusible hydrogen levels for the latter and for the standard E7018 electrodes. The results indicate that the standard E7018-H4R electrodes indeed have a hydrogen level of less than 4 ml/100 g and that the second-tier E7018

electrodes have a hydrogen level nearer to 16 ml/100 g. As opposed to searching for or formulating (by re-drying) electrodes that produce a hydrogen level of approximately 8 ml/100 g, it was recognized that data for welds with a hydrogen level of approximately 16 ml/100 g would be a useful complement to the existing data. Therefore, the second-tier E7018 electrodes that were procured from a local supplier were used for welds intended to have an elevated hydrogen level.

Confirmation of hydrogen levels was carried out using the AWS A4.3-93 method [17] and gas chromatography equipment. This was carried out at two separate stages of the experimental work at DNV. The results are given in Table 4.

For the small-scale experiments at UoW, artificial hydrogen charging was used to produce hydrogen levels in specimens composed of simulated HAZ microstructure that are representative of those used in the full-scale weldability trials.

6.3 Weld Thermal Cycles

In both phases of the experimental program, a variety of HAZ microstructures were produced for each material by simulating thermal conditions (accelerated weld cooling) experienced in the field. In the full-scale weldability trials at DNV, welds were made using two thermal severity levels, which were simulated using either flowing water or flowing mineral oil on the inside of the pipe material. In the small-scale experiments at UoW, time at peak temperature and weld cooling rates (i.e., weld cooling times from 800 to 500°C) were varied so that the microstructures that are produced are representative of those produced during the full-scale weldability trials at DNV.

6.4 Experimental Matrix

For the full-scale weldability trials at DNV, the goal of the experimental matrix was to generate combinations of HAZ hardness and hydrogen level that result in welds that are just above and below the hydrogen cracking threshold. For a given material, heat input and thermal severity level combine to determine weld cooling rates and subsequent HAZ hardness. For the lowest of the three hydrogen levels (4 ml/100 g), it was necessary to generate HAZ hardness that is at the upper end of the range for each material. For the highest of the three hydrogen levels (50 ml/100 g), welds will crack at lower levels of HAZ hardness. These factors were taken into account in the development of the preliminary experimental matrix for the full-scale weldability trials at DNV, which is given in Table 5. Some combinations of heat input and thermal severity level combine to result in the same level of HAZ hardness. Therefore, some of the welds originally proposed for the experimental matrix were eliminated to avoid duplicate conditions.

For the small-scale experiments at UoW, the goal of the experimental matrix was to produce specimens in the Gleeble thermo-mechanical simulator that have microstructures and hardness levels that are representative of those in the HAZs from the full-scale weldability trials. These specimens were then tested to measure fracture toughness as a function of hydrogen charging

conditions. As no standard protocol existed for this type of testing, the parameters for both specimen production and hydrogen charging needed to be developed during the initial stages of the experimental work at UoW. Parameters that were included in the matrix for producing specimens include time at peak temperature and weld cooling rate (i.e., weld cooling time from 800 to 500°C).

6.5 Experimental Procedure

The setup for the full-scale weldability trials at DNV involved the fabrication of a vessel from a length of 20-inch (508.0-mm)-diameter pipe into which panels of the materials of interest were welded (Figure 7). The panels replaced one quadrant of the vessel circumference. Sections of material equal in wall thickness and chemical composition were anchor-welded to each of the panels so that a range of fillet welds, simulating the fillet weld between the end of a full-encirclement sleeve and the pipe, could be deposited. The width of the section anchor-welded to each panel was 6 inches (152.4 mm). A controlled gap of 1/16 inch (1.6 mm) was provided so that the geometry (i.e., stress concentration) at the root of each weld would be consistent.

Trials were carried out under the previously-established flowing water and flowing oil procedure qualification conditions [18]. The flowing water procedure qualification condition involved circulating cold tap water [70°F (21°C)] through the vessel at approximately 10 gal/min (38 l/min). The flowing oil procedure qualification condition (Figure 8) involved circulating mineral oil [80°F (27°C)] through the vessel at approximately 5 gal/min (19 l/min).

The full-scale weldability trials consisted of making short (approximately 6 inch [150 mm] long), three-pass fillet welds at the target heat input level (Figure 9). A total of 52 experimental welds were made. Arc current and voltage were monitored using an ammeter and a volt meter, and travel speed was monitored using a stopwatch and a linear scale. Target heat input levels were achieved only by varying the travel speed, which was carefully controlled by prompting the welder with designated marks over the weld length and by calling out the time interval over which the marks should be encountered. Welding parameters that were used are given in Table 6. A typical completed weld is shown in Figure 10.

Following welding, the welds are allowed to sit for at least 24 hours, after which they were subjected to visual and magnetic particle inspection. The experimental welds are then subjected to metallographic examination and mechanical testing to investigate for the presence of cracks (Figure 11). The welds are sectioned, mounted, ground, polished, and etched using standard metallographic procedures and examined at 200X magnification. HAZ hardness measurements are made using a previously-developed procedure [19]. Using this procedure, hardness measurements are made at the toe of the weld in the coarse-grain HAZ on the pipe side of the joint. Five indents are made using a Vickers indenter and a 10-kg load. The indents are spaced 0.6 mm (0.024 inch) from each other and 0.2 mm (0.008 inch) from the fusion line. The use of this procedure is illustrated in Figure 12. The results were reported as an average for this region

of anticipated maximum hardness. The metallographic sections are also used to characterize HAZ microstructures.

Test specimens were also extracted from each weld and used for face bend and nick-break testing as specified in API 1104 Appendix B and CSA Z662. A shallow saw cut was provided in the face of the weld after which the top portion of the coupon was removed by fracturing the weld through the throat. This was accomplished by first driving a chisel into the gap between the top and bottom portions of the coupon and then bending the top portion away using a wrench. The fracture surfaces were visually examined for cracking in the weld root area and suspect areas were further examined using a binocular light microscope. A typical hydrogen crack that was found is shown in Figure 13.

The bottom portion of each coupon was then used for the face/toe bend test. The remainder of the weld metal was removed from the coupon using a belt sander. Care was taken so as not to remove the weld toe. The weld toe was then put into tension using a bend tester with a 2t radius mandrel. Following bending, the weld toes were visually examined for cracking and suspect areas were further examined using a binocular light microscope. A typical hydrogen crack that was found is shown in Figure 14.

7. RESULTS OF FULL-SCALE WELDABILITY TRIALS

The results of destructive testing are given in Table 7. A wide range of HAZ hardness was produced, as were welds with and without HAZ cracks. Several welds made using cellulosic-coated electrodes and with elevated hydrogen level low-hydrogen electrodes also contain weld metal hydrogen cracks. Since the objective of the current projects was to develop hardness limits to avoid HAZ hydrogen cracking, weld metal hydrogen cracks were ignored. Unexpected results for experiments conducted on Materials TC2 and EX1 are described in Section 10.

8. ANALYSIS OF RESULTS

The results of the initial full-scale weldability trials on Materials N3A, GTN, and EB5 were compared to the previously-developed HAZ hardness evaluation criteria based on the IIW carbon equivalent formula (CE_{IIW}) for thinner materials with carbon contents greater than 0.10%. These criteria were also modified to include a weld hydrogen level of 16 ml/100 g of deposited weld metal (Figure 15). Comparison of the HAZ hardness testing results with the evaluation criteria (Figure 16) indicates that, for the initial trials, the criteria have accurately predicted the occurrence of cracking. The experimental welds that contain HAZ hydrogen cracks tend not to meet the criteria (i.e., the data points for welds with HAZ cracks lie above and to the left of the 1:1 line in the Figure 16). The results of these initial trials and the later trials were further analyzed to account for the effect of thickness and to investigate the use of alternative carbon equivalent formulas as described in Section 10.

9. MICROSTRUCTURAL SUSCEPTIBILITY WORK

This phase of the work investigated the relationship between pipe composition, hardness, microstructure, and fracture behavior arising as a result of in-service welding procedures. This more fundamental work was intended to complement the full-scale weldability trials described above and give support in understanding the procedural "operating windows" with respect to effect of hydrogen content, composition, etc., on hydrogen cracking susceptibility.

Coarse grain HAZ (CGHAZ) microstructures were produced in small samples using a Gleeble 3500 thermomechanical processing machine. Thermal cycles were calibrated so that the microstructures that are produced are representative of those produced during the weldability trials described above.

A range of fracture specimen configurations were tested. These included notched cylinders for tensile testing and notched bars for bend testing, etc. This preliminary testing established the most appropriate configuration for the problem.

Following this, samples of CGHAZ in the optimum configuration were charged with known concentrations of diffusible hydrogen (calibrated against charging conditions, etc). Fracture testing of specimens was performed as a function of hydrogen content. The resulting fracture mechanisms were studied using standard metallographic and fractographic procedures.

The results of these small-scale experimental simulations, which are provided in Appendix B, provide insight into the interrelationship between hydrogen content, microstructure, hardness, composition, and embrittlement behavior.

10. DEVELOPMENT OF CRITERIA

The initial effort in this phase of the work focused on using existing data from previous work to develop HAZ hardness acceptance criteria using the CEN carbon equivalent formula. It is thought that the use of this formula may allow for both conventional and low carbon steels to be evaluated together (i.e., using criteria based on a single carbon equivalent formula). Effort has also focused on the development of criteria for intermediate thicknesses. It was anticipated that a sliding scale for thickness could be developed as opposed to the use of a stepwise increase as was used in the earlier work.

The susceptibility of a given steel composition to hardening in the HAZ as a result of the weld thermal cycle is often predicted by the use of carbon equivalent (CE) formulas. These formulas describe the compositional (weight %) effect on hardenability, or the tendency to form crack-susceptible weld microstructures, and when combined with the effects of pipe wall thickness, weld configuration, and heat input on cooling time, they can be used in procedures for estimating the heat input requirements or preheat conditions necessary to avoid hydrogen cracking. There are a number of such formulas used in this way as a measure of weldability [20], but perhaps the most widely used is the International Institute of Welding formula (CE_{IIW}):

$$CE_{IIW} = C + Mn/6 + (Cu+Ni)/15 + (Cr+Mo+V)/5 \quad (2)$$

The CE_{IIW} formula is generally considered to be more relevant for evaluating the weldability of older steel types, such as steels produced prior to thermomechanical controlled processing, with higher carbon contents from 0.10-0.3%. Another widely used formula, Pcm, regards the effect of carbon as much more significant than that of the alloying elements, and is generally considered to be more appropriate for the more modern, carbon-reduced or microalloyed steels:

$$Pcm = C + Si/30 + (Mn+Cu+Cr)/20 + Ni/60 + Mo/15 + V/10 + 5B \quad (3)$$

For example, the American Welding Society (AWS) method for determining the minimum necessary preheat to avoid HAZ cracking recommends Pcm be used for steels with C < 0.11% and CE_{IIW} for steels with C ≥ 0.11% [21].

Another formula, developed by Yurioka et al as a weldability index for a range of low carbon, high strength, and carbon-manganese steels, incorporates an interactive term for carbon and alloying elements [22]. The CEN formula approaches the values of CE_{IIW} when applied to higher carbon steels and the values of Pcm when applied to lower carbon steels:

$$CEN = C + A(C)\ \{Si/24 + Mn/6 + Cu/15 + Ni/20 + (Cr+Mo+Nb+V)/5 + 5B\} \quad (4)$$

where: $A(C) = 0.75 + 0.25 \tanh [20(C-0.12)]$

The following correlations between the formulae have been established:

$$CEN = 2\ Pcm - 0.092 \qquad (\text{where } C \leq 0.17\%) \quad (5)$$

and,

$$CEN = CE_{IIW} + 0.12 \qquad (\text{where } C > 0.17\%) \quad (6)$$

In the initial project that resulted in the development of the existing criteria, an extensive amount of data was generated for two wall thicknesses; 0.375 and 0.750 inch (9.5 and 19.1 mm). In a subsequent project, limited data was generated for one additional wall thickness (0.312 inch [7.9 mm]. In the current project, data was generated for several additional wall thicknesses. The

majority of the materials from the previous projects were lower-strength conventionally alloyed line pipe steels, typical of those for which in-service welding is common, although the initial project did include an early-generation X80 material. The materials in the current project include a modern X80 and an experimental X120 material. A material typical of that used for full-encirclement repair sleeves was also included in the current project. In the previous projects, welds were made using consumables that produced three different nominal hydrogen levels. In addition to these, data was generated in the current project for one additional hydrogen level.

A total of 52 full-scale weldability trials were made in the current project. A summary of the results is given in Table 8. The trials that were conducted allow continuity to be established between the current project and the previous projects, and allow the results to be extended to include modern microalloyed materials and material over a wide range of wall thicknesses.

The procedure for evaluating candidate criteria is iterative in nature. For each set of experimental data, the candidate criteria are used to determine whether or not cracking is predicted. Graphs of measured HAZ hardness vs. maximum-allowable hardness according to the candidate criteria are then made. Experimental data for which cracks were produced are given a solid-color data point. Experimental data for which the welds were found to be free from cracks are given an open data point. A 1:1 line is then provided on the graphs. If the criteria have been accurate in predicting the occurrence of cracking, all of the solid-color data points will be above the 1:1 line. If some of the solid-color data points lie below the 1:1 line, the candidate criteria are adjusted and the process is repeated. Ideally, some of the solid-color data points will lie just above the 1:1 line, indicating that the criteria have been accurate, but not overly conservative.

Several options were pursued to incorporate the effect of wall thickness into the criteria. One involved the use of a three-dimensional graph with maximum-allowable hardness shown as a function of material chemical composition (CE level) and thickness. Another involved the use of correction factors for material thicknesses that differ from 0.375 and 0.750 inch (9.5 and 19.1 mm).

The wall thicknesses for the materials in the experiments on which the existing criteria were developed were chosen based on the thermal severity. During in-service welding, the effect of the flowing contents on weld cooling rate diminishes as pipe wall thickness increases. The flowing contents have a significant effect on welds made onto relatively thin in-service pipelines (e.g., less than 0.5 inch [6.4 mm] thick). When the wall thickness exceeds 0.5 inch (12.7 mm) or so, the effect of the flowing contents diminishes, as does the effect of increasing the wall thickness beyond 0.5 inch (12.7 mm). The 0.375 inch (9.5 mm) wall thickness was chosen to represent conditions where the pipe contents have a significant effect on weld cooling rate. The 0.750 inch (19.1 mm) wall thickness was chosen to represent conditions where the pipe contents have a diminished effect on weld cooling rate. Wall thickness not only affects thermal severity, but also restraint level. Welds made onto relatively thin in-service pipelines are less highly restrained than welds made onto relatively thick in-service pipelines. When welds are more highly restrained, the residual stress level that results from thermal contraction as the weld cools

tends to be higher. Therefore, for a given weld microstructure and hydrogen level, the risk of cracking is greater for in-service welds made onto thicker materials.

In the previous work, a 50 HV reduction in maximum-allowable HAZ hardness was imposed for welds made onto 0.750 inch (19.1 mm) thick material compared to welds made onto 0.375 (9.5 mm) thick material. In the current project, experimental data was generated for materials with several additional wall thicknesses (0.281, 0.437, 0.543, and 0.650 inch [7.1, 11.1, 13.8, and 16.5 mm]. To incorporate the effect of wall thickness into the criteria, a set of three-dimensional graphs was developed. These graphs show proposed maximum-allowable hardness as a function of material chemical composition (CE level) and thickness. One graph is required for each of the held hydrogen levels that have been evaluated. In the previous work, welds were made using consumables that produced three different nominal hydrogen levels; 4, 8 and 50 ml/100 gm of deposited weld metal. In addition to these, data was generated in the current project for welds made using consumables that produced a nominal hydrogen level of 16 ml/100 gm. An example of a three-dimensional graph for the ≤ 4 ml/100g hydrogen level is shown in Figure 17.

The three-dimensional graphs, while containing the necessary information, are somewhat difficult to navigate. An alternative method of presenting this information is shown in Figures 18 through 21. These are two-dimensional graphs that show proposed maximum-allowable hardness as a function of material chemical composition (CE level) for a range of thicknesses (≤ 0.375, 0.500, 0.625, and ≥ 0.750 inch [≤ 9.5, 12.7, 15.9, and ≥ 19.1 mm]). Interpolation can be used for wall thicknesses not shown on the graphs.

The experimental data on which the previously-developed criteria are based are for sleeve fillet welds where the sleeve material is identical to the pipe material. In practice, sleeve material will have a different chemical composition to that of the pipe material and will often be thicker than the pipe material. In the current project, one series of experiments was conducted using Material EB5 as the pipe material (0.281 inch [7.1 mm] thick and 0.48 CE_{IIW}) and Material EB5-S (0.500 inch [12.7 mm] thick and 0.39 CE_{IIW}) as the sleeve material. To account for differences in chemical composition between the pipe and sleeve material, determination of the maximum-allowable HAZ hardness using Figures 18 through 21should be made based on the less favorable of the two materials (i.e., the material with the higher CE level). To account for differences in thickness between the pipe and sleeve (or branch) material, the following formula was developed to determine the 'effective' thickness:

$$t_e = (2t_p + t_s)/3 \qquad (7)$$

where: t_e = *the effective thickness,* t_p = *pipe wall thickness, and* t_s = *sleeve thickness*

The use of the effective thickness takes the additional restraint when using a thicker sleeve material into account. If the sleeve thickness is equal to the pipe wall thickness, then the effective thickness is simply the pipe wall thickness.

The results of the full-scale weldability trials on materials with carbon contents greater than 0.10% (N3A, GTN, EB5 and EB5/EB5-S) were compared to the criteria shown in Figures 18 through 21. Comparison of the HAZ hardness testing results with the evaluation criteria is shown in Figure 22. This figure indicates that, in general, the criteria have accurately predicted the occurrence of cracking. The experimental welds that contain HAZ hydrogen cracks tend not to meet the criteria (i.e., the data points for welds with HAZ cracks lie above and to the left of the 1:1 line in the Figure 22). The one exception to this is the data point for Weld No. D42. One of the face bend test specimens taken from this weld contains a small hydrogen crack at the weld toe. The source of this anomaly is not clear. On possible explanation is a local difference in hydrogen level. This weld was made with properly conditioned low hydrogen electrodes, but moisture under the sleeve, for example, may have resulted in a local hydrogen level increase in this area.

It was anticipated that experimental data generated for modern microalloyed materials in the current project could be used to develop criteria using the CEN carbon equivalent formula, which would allow for both conventional and low carbon steels to be evaluated using criteria based on a single carbon equivalent formula. Unfortunately, the experiments conducted on Materials TC2 and EX1 produced unexpected results.

Nearly all of the welds for Materials TC2 and EX1 contained HAZ hydrogen cracks. The measured average HAZ hardness for the experiments conducted on Material EX1 ranged from a low of 300 HV to a high of 322 HV (a difference of only 22 HV). This range resulted in spite of the welds having been made over a wide range of heat input levels and at both severe (simulated using flowing water) and less severe (simulated using flowing mineral oil) thermal conditions. Since nearly all of the welds contain hydrogen cracks, it is apparent that HAZ hardness is not a useful indicator of susceptibility in this material. The same is true, but to a lesser extent, for Material TC2, where the measured average HAZ hardness ranged from a low of 287 HV to a high of 333 HV (a difference of 46 HV).

The presence of hydrogen cracks in nearly all of the welds made using properly-conditioned low-hydrogen electrodes on Materials TC2 and EX1 was an unexpected result. Several experimental difficulties were encountered with these welds. Difficulty was experienced establishing a consistent root gap during fabrication of the test setup using these materials, as both are relatively thick and high strength (X80 and X120 for Materials TC2 and EX1, respectively). The presence of an excessive root gap made welding of the root pass difficult, particularly at low heat input levels which resulted in very small fillet weld throat thicknesses. Many unintended workmanship defects in these welds were produced as a result.

Another difficulty was also related to the thickness of these two modern microalloyed materials (0.543 and 0.636 inch [13.8 and 16.2 mm] for Materials TC2 and EX1, respectively). In the previous work, most of the materials were 0.375 inch (9.5 mm) thick. For thicker material (0.75 inch [19.1 mm]), the bend test specimens were machined down to 0.375 inch (9.5 mm) thick. A rather severe 2t radius mandrel (1-1/2 inch [38 mm] diameter for 0.375 inch [9.5 mm]

thick materials) was used to ensure that any toe cracks that might be present are exposed. In the current work, a 1-1/2 inch (38 mm) diameter mandrel was also used but the bend test specimens were not machined down. This would have certainly exposed any toe cracks that might have been present, but also caused some tears that may have been misinterpreted as toe cracks. None of the welds made on Materials TC2 and EX1 were condemned solely based on face bend test results, however.

As with the anomaly described above for Weld No. D42, it is possible that elevated weld hydrogen levels were produced by what were thought to be properly-conditioned low-hydrogen electrodes. Diffusible hydrogen testing was carried out at two different stages of the project; once at the beginning of the full-scale weldability trials (February 7, 2008) and once at the end (December 4, 2008). For the properly-conditioned low-hydrogen electrodes, this testing resulted in values of 1.76 and 3.78 ml/100 g of deposited weld metal, respectively (Table 4). Experiments on Materials TC2 and EX1 were conducted later in the program than other experiments (September 29, 2008, and November 11-12, 2008, respectively). While an increase in weld hydrogen level did seem to occur for the properly-conditioned low-hydrogen electrodes, both results were less than 4 ml/100 g. While these electrodes were stored at an appropriate temperature in an electrode holding oven, deviations from the expected weld hydrogen level can occur during welding as the result of changes in ambient atmospheric conditions.

In addition to HAZ hydrogen cracks in the welds made on Materials TC2 and EX1, some of these welds, particularly those made at elevated hydrogen levels, also contained weld metal hydrogen cracks (this is also true for some of the welds made on the other materials). All of the full-scale weldability trials were conducted using E7018 electrodes, which undermatches (or in the case of Material EX1, grossly undermatches) the strength of the two modern microalloyed materials. The use of undermatching strength weld metal is generally considered to be adventurous in preventing HAZ hydrogen cracking, as shrinkage strains tend to be accommodated in the generally less crack susceptible weld metal (as opposed to the HAZ). Selection of weld metal strength for in-service welds on these materials, and the design of hot tap fitting for large diameter, high pressure pipelines using these materials (strength level, thickness, etc.), are issues worthy of additional consideration

As the result of the difficulties described above, it was not possible to investigate the CEN carbon equivalent formula for both conventional and low carbon steels. It is clear, however, that HAZ hardness may not be a useful indicator of susceptibility to hydrogen cracking in modern microalloyed materials. The results also illustrate that protection against hydrogen cracking is not necessarily provided by limiting HAZ hardness to 350 HV for these materials. A useful step forward was made in incorporating the effect of thickness into the HAZ hardness acceptance criteria for materials with carbon contents greater than 0.10%, however.

11. VALIDATION OF CRITERIA DURING FIELD TRIALS

The developed criteria was validated during a series of field trials that involved welds made onto actual in-service pipelines. This was accomplished using the confirmation weld scheme. This scheme involves making a series of experimental welds onto the portion of the pipeline that were subsequently removed by the hot-tap cutter. After removal of the hot tap 'coupon', metallographic examination and hardness testing were performed so a comparison could be made with the results of welds made under simulated in-service conditions to validate the criteria.

Access to two gas transmission pipelines that were scheduled for hot tap installations, along with the necessary support for the field trials, was provided by Columbia Gas Transmission. One line (Line 1804) was 20 inch diameter by 0.250 inch (6.4 mm) wall thickness APL 5LX-52 that was manufactured in 1960. The other (Line 10240) was 24 inch nominal diameter by 0.260 inch (6.6 mm) wall thickness APL 5LX-60 that was manufactured in 1982. The normal operating pressure for both lines is approximately 745 psi. The normal flow rate for Line 1804 was 100 MMSCFD (equivalent to 10.29 ft/sec at 745 psi) and for Line 10240 was 149 MMSCFD (equivalent to 10.58 ft/sec at 745 psi).

Line 1804 is shown in Figure 23 prior to commencement of the field trials. An outline of the hot tap cutter is shown. The inside diameter of the cutter was 7.125 inch (181.0 mm) and the pilot drill diameter was 1.25 inch (31.8 mm) diameter. Strips of line pipe material that were 1.75 inch (44.5 mm) wide were cut to fit the geometric constraints of the hot-tap cutter and tack welded to the pipeline on the top and bottom of the strips. Experimental fillet welds, simulating the fillet welds made between a pipeline and the edge of a full-encirclement fitting, were then made along the long sides of the strips (Figure 24). These welds were made using properly conditioned low hydrogen (E7018-H4R) electrodes over a range of heat input levels so that a range of heat-affected zone hardness would be produced. Welding parameters that were used are given in Table 9. After completing the confirmation welds, the hot tap branch was welded over confirmation welds (Figure 25) and a full-encirclement reinforcement was installed. This procedure was then repeated on Line 10240. After the hot tap cuts were made (several weeks later), the hot tap coupons with the confirmation welds were sent to DNV for analysis (Figure 26).

Analysis of the hot tap coupons included chemical analysis of the line pipe material, metallographic examination to investigate for the presence of cracks, and HAZ hardness testing. Two metallographic sections were removed from each experimental weld. The sections were mounted, ground, polished, and etched using standard metallographic procedures and examined at 200X magnification. HAZ hardness measurements are made using a previously-developed procedure.

Chemical analysis results are given in Table 10. Both of the line pipe materials have carbon contents much greater than 0.10% and relatively high CE levels. A typical metallographic

section is shown in Figure 27. The results of HAZ hardness testing, along with metallographic examination results, are given in Table 11.

The HAZ hardness testing results were compared with the criteria for welds made using properly conditioned low hydrogen electrodes (≤ 4 ml/100g hydrogen level) shown in Figure 18. For an effective thickness ≤ 0.375 inch (9.5 mm) and materials with CE_{IIW} of 0.47 and 0.45, the criteria indicate that HAZ hardness should be limited to 414 and 408 HV, respectively. Unfortunately, the flow conditions during the field validation trials were such that HAZ hardness levels approaching these limits could not be produced even at the lowest manageable heat input levels, in spite of the relatively high CE values of the materials. None-the-less, the results indicate that that the criteria have accurately predicted the absence of cracking.

12. DEVELOPMENT OF RELATED GUIDANCE

Guidance was developed for several issues related to the application of HAZ hardness limits to welds made onto in-service pipelines. This guidance focuses on three primary issues; 1.) the way in which HAZ hardness is measured during the qualification of procedures for welding onto in-service pipelines, 2.) determination of chemical composition for an in-service pipeline, and 3) control of weld hydrogen levels.

12.1 Measurement of HAZ Hardness during Procedure Qualification

HAZ hardness testing is often used as a performance indicator for welds. The way in which HAZ hardness is measured is the topic of considerable debate. Factors that may affect the measurement results include surface finish, indenter type (Vickers, Knoop, Rockwell, Brinell, etc.), indentation location (along the fusion line, distance from the fusion line, etc.), load/indentation size (for methods that involve a choice of loads), number of indentations required (number of specimens required, number of hardness indents per specimen, etc.), and treatment of results (maximum single result, average of results from area of maximum hardness, etc.). For multi-pass welds, the wide variety of microstructures that can result from tempering and re-transformation from subsequent passes provides an additional complication. Consequently, indentation location with respect to microstructure type, treatment of the results (average or peak value), significance of localized hard zones, etc., are important for multi-pass welds.

Some generalized rules for the measurement of heat affected zone hardness levels exist [24-29], although there are no universally-accepted specific procedures. In order to apply the HAZ hardness limits that were developed in this project, it is important to measure HAZ during procedure qualification in a way that is consistent with how it was measured during the experimental portion of this project. Guidance related to the various aspects of HAZ hardness measurement is discussed below.

12.1.1 Indenter type

Common hardness measurement methods for metallic materials include Vickers, Knoop, Rockwell, and Brinell. The Vickers hardness testing method is the predominant measurement technique for welds and HAZs. The diamond indentation can be made using loads ranging from 1 to 120 kg. For homogeneous materials, the resulting hardness measurement is relatively independent of the load used. For a material of a given hardness, the size of the indentation produced by a Vickers indenter is proportional to the load used. Smaller loads produce relatively small indentations that are appropriate for investigating the hardness of small (i.e., microscopic) areas or of individual microstructural constituents. Larger loads produce larger indentations and tend to produce an averaging effect for areas consisting of mixed microstructures. Intermediate loads produce indentations that tend to be appropriate for HAZs.

12.1.2 Surface finish

The relatively small impression made by a Vickers indenter requires that the surface be flat and perpendicular to the indenter and the surface have a surface finish finer than 300 grit. Vickers hardness measurements should be made on a metallographically prepared surface. The surface of the specimen should be prepared in such a way that the ends of the indentation diagonals are clearly defined. Care should be taken in preparing the surface so that tempering during grinding or work-hardening during polishing is avoided.

12.1.3 Indentation location

HAZ hydrogen cracks tend to occur in areas where hard microstructures coincide with stress concentrations. For welds made onto in-service pipelines (e.g., hot tap and repair sleeve welds), these areas tend to occur at the toe of the weld in the pipe material. The root region of typical in-service welds can also represent a stress concentration, particularly for sleeve fillet welds where gaps exist between the sleeve and the pipeline, but hard microstructures that develop in this region initially are often tempered or refined by subsequent passes. Therefore, the region of most interest with regard to HAZ hardness measurement is the weld toe region in the pipe material. If the full-encirclement sleeve or hot tap fitting material has a higher carbon equivalent (CE) than the pipe material, it may be useful to supplement HAZ hardness measurement at the weld toe region of the pipe material with measurements at the weld root region of the sleeve or fitting material.

12.1.4 Load/indentation size

As noted above, the size of the indentation produced by a Vickers indenter is proportional to the load used. To evaluate hydrogen cracking risk, it is common to ignore the hardness of individual microstructural constituents by using a load that is high enough to produce some averaging within the coarse-grained region of the HAZ. It is important to use a load that is low enough to produce an indentation that is small enough to fit within the confines of the coarse-grained region, however. For the size of HAZ produced by welding processes and heat input levels

typically used for in-service welding (e.g., shielded-metal arc welding at 15 to 40 kJ/inch [0.6 to 1.6 kJ/mm]), a Vickers indentation produced using a load of 10 kg has been shown to be appropriate. For reference, the diagonal of a Vickers indentation produced using a load of 10 kg in a material with a hardness of 350 HV is 0.23 mm (0.009 inch).

12.1.5 Number of indentations required

Various methodologies exist for measuring hardness in welds. Many of these involve conducting a hardness measurement traverse across the weld to locate areas of high hardness. If the locations of areas with high hardness are already known, as is the case with welds made onto in-service pipelines, a better approach is to concentrate hardness measurements in these areas. There is considerable variation that can occur when measuring HAZ hardness, so multiple indentations should be made. There is a limit to the number of hardness indentations that can be placed in the coarse-grained region of the HAZ near the weld toe, however. ASTM E92 [30] indicates that Vickers hardness indentations should not be made closer to another indentation than a distance equal to two and one half times the length of diagonal of the indentation. For the size of HAZ produced by welding processes and heat input levels typical used for in-service welding, a minimum of five measurements has been found to be appropriate. The measurements should follow the fusion boundary using the contour method. To further account for variations that can occur when measuring HAZ hardness, measurements should be made on at least two metallographic sections from each weld of interest.

12.1.6 Treatment of results

In order to assess the overall hydrogen cracking susceptibility of in-service welds, averaging the results of the five measurements taken in the coarse-grained region of the HAZ near the weld toe has been found to be appropriate. Consideration can be given to excluding measurements that deviate from the median value. The results are then reported as an average for this region of anticipated maximum hardness.

12.1.7 Proposed HAZ hardness testing procedure

The procedure that is being used during the experimental portion of this project involves making hardness measurements at the toe of the weld in the coarse-grained HAZ on the pipe side of the joint. Five Vickers 10-kg indents are spaced 0.6 mm (0.024 inch) from each other and 0.2 mm (0.008 inch) from the fusion line. The results for these five measurements in the area of maximum hardness are then averaged. This technique is the same as that illustrated in Figure 12.

12.2 Determination of Chemical Composition for an In-Service Pipeline

Selection of welding procedures for avoiding hydrogen cracking is often made based on the chemical composition of the pipe and fitting materials being welded. Knowledge of the pipe material chemical composition is necessary for applying the HAZ hardness limits that were developed in this project. Several methods exist for determining the chemical composition of an

in-service pipeline. These, along with examples and related factors, include interrogation of records that contain chemical composition information for existing pipelines (database development, statistical treatment of data, etc.), measurement using portable equipment (equipment type, manufacturer, etc.), and removal of small sample for laboratory measurement (collection of filings, analysis methods, etc.). Estimates can also be made using general rules of thumb. Guidance related to the various aspects of chemical composition determination is discussed below.

12.2.1 Interrogation of Records

Many companies do not have records that contain chemical composition information for older, existing pipelines and make conservative estimates of chemical composition (e.g., based on the maximum allowable limits of the specification to which the materials were produced). This usually results in an overestimation of the tendency for unacceptably high hardness levels to result and can be restrictively over-conservative. Pipeline operating companies should develop a database of chemical composition information for material in their system for this purpose. Chemical analysis results for pipe material removed from existing pipelines (e.g., hot tap coupons and cut-outs) can be used to populate such a database.

12.2.2 Measurement using Portable Equipment

The most promising technique for performing a chemical composition analysis in the field is optical emission spectrography (OES) via a fiber-optic umbilical cord. Several companies offer systems that can be used in the field, although these are relatively expensive. Several OES analyzers claim to be capable of analyzing for elements down to atomic number 5 (boron), some with accuracy of 0.001% at 0.04% quoted for carbon [31].

12.2.3 Removal of Small Sample for Laboratory Measurement

Chemical composition determination by removal of samples for laboratory analysis is relatively simple and can be quite accurate provided that care is taken in removing the samples and that they are properly analyzed. Filings can be removed from an in-service pipeline using a high-speed rotary file (burr grinder). The rotary file should be inspected following use to insure that teeth have not broken off. The inclusion of teeth in the filings can raise the apparent content of certain elements, particularly carbon. The filings can be analyzed using traditional wet chemistry (i.e., titration methods) or using the inductively coupled plasma (ICP) method. The combustion-in-oxygen method using a LECO analyzer should be used to accurately determine carbon and sulfur levels of samples composed of filings.

12.2.4 General Rules of Thumb

In the absence of other information, estimates of pipe material chemical composition can be made. Some very general rules of thumb pertaining to pipe material chemical composition are provided in Table 9. It should be noted that there are many exceptions to these rules. In general,

the highest CE materials that are encountered in North America are API 5L-X52 grades that were manufactured in the 1950's and early 1960's.

12.3 Control of Weld Hydrogen Levels

The ability to tolerate HAZ hardness levels that are higher than the limits that have been traditionally imposed (e.g., 350 HV) depends on the ability to closely control weld hydrogen levels. The importance of controlling hydrogen levels for welds made onto in-service pipelines is well established. Some companies simply specify the use of low hydrogen electrodes without providing additional guidance. Storage and handling of low-hydrogen electrodes is an in-exact science at best, even though general guidelines for their use are available [32-35]. The hydrogen level of welds made using low-hydrogen electrodes can vary widely depending on a range of factors. These include the manufacturer, classification/supplemental designation, packaging, storage conditions, handling, atmospheric exposure, and drying/re-conditioning practices. Guidance related to the various aspects of weld hydrogen level control is summarized below. Detailed guidance is provided in Appendix C.

12.3.1 Electrode Procurement

Many of the potential problems associated with minimizing hydrogen levels for welds made onto in-service pipelines can be addressed at the electrode procurement stage. Many modern low-hydrogen electrodes (EXX18-type) produce weld hydrogen levels that are less than 4 to 5 ml/100 g in the as-received condition. With the amount of moisture in the electrode coating that is permissible (0.6% according to AWS A5.1 [36]), hydrogen levels in welds made using low-hydrogen electrodes can be as high as 16 ml/100 g, which is excessive for many in-service welding applications. Supplementary designators are now available that allow a specific maximum-allowable hydrogen level to be specified. In AWS A5.1, these designators are H4, H8, and H16, where "H" indicates hydrogen and "4, 8, and 16" refer to the average maximum-allowable hydrogen level in ml/100 g in the "as-received" condition. In addition, AWS has introduced an "R" designator that allows a moisture resistant coating to be specified. The R designator indicates that the electrodes have passed an absorbed moisture test after exposure to an environment of 80ºF (26.7ºC) and 80% relative humidity for a period of not less than 9 hr. Electrodes that meet this requirement have coating moisture limits that are lower than their non-moisture-resistant counterparts.

For in-service welding applications, pipeline operators should consider specifying electrodes with the H4R designator. These are becoming more common and, while there may be a price premium, this is negligible compared to the cost for remedial action that would be required following the discovery or failure of an in-service weld with hydrogen cracks.

12.3.2 Electrode Packaging

For in-service welding applications, the use of electrodes that are packaged in hermetically-sealed cans (i.e., appropriate for use in the as-received condition) would seem to be preferable.

If electrodes packaged in cardboard cartons are used, care must be taken to ensure that drying is not required by the manufacturer prior to their use in the as-received condition. If drying is required, care must be taken to ensure that the drying is carried out properly. If the electrodes are intended to be used in the as-received condition and they are packaged in plastic-sealed cardboard containers, care should be taken to ensure that the plastic wrap is not damaged.

For in-service welding applications, it may be advantageous to purchase and use low-hydrogen electrodes in smaller quantities (e.g., 10-lb [4.5-kg] cans), an example of which is shown in Figure 28. This is particularly true for smaller jobs (e.g., small diameter lines) where it would be difficult to use an entire 50-lb (22.7-kg) can. There is also a price premium for this type of packaging, however.

13. DISCUSSION

Others use or have proposed using HAZ hardness evaluation criteria that are variable depending on the chemical composition of the materials being welded [37]. These criteria may not be suitable for in-service welds; however, as welds made under in-service conditions tend to cool more quickly than other welds. The diffusion rate of hydrogen in steel is strongly influenced by temperature. Hydrogen in welds that are allowed to cool slowly can diffuse away soon after welding. For in-service welds, any hydrogen that enters the weld tends to become trapped there. This is one reason a limit of 350 HV may not be sufficient for in-service welds made using cellulosic-coated (EXX10 type) electrodes.

The results of this and previous work directed specifically at welds made onto in-service pipelines [15, 23, 38-40] indicate that the widely-used limit of 350 HV is overly conservative for some applications and non-conservative for others. Hardness evaluation criteria were developed that can be used to quantify the trade-offs that can be made between HAZ hardness, hydrogen level, and the chemical composition and thickness of the materials being welded for welds made onto in-service pipelines. The previously-developed criteria were previously shown to be accurate for predicting the occurrence of cracking for the narrow range of conditions that were investigated [9.5-mm (0.375-inch)-thick materials with a carbon content greater than 0.10%]. The results of the current work further developed and validated these previously-developed criteria for material over a wide range of wall thicknesses and produced data for modern microalloyed materials. The current work also further investigated the relationship between composition, hardness, microstructure, and fracture resistance of the coarse-grained HAZ arising from simulated in-service welding procedures.

Excluding the anomaly described in Section 10 for Weld No. D42, only one other full-scale weldability trial conducted on materials with carbon contents greater than 0.10% using properly-conditioned low hydrogen electrodes produced HAZ hydrogen cracking (Weld No. D40). This was a low heat input weld made on a high CE material (0.48 CE_{IIW} and 0.269 %C) under flowing water conditions. The resulting HAZ hardness was measured to be over 450 HV (i.e., did not meet the acceptance criteria). The absence of cracks in other welds made using

properly-conditioned low hydrogen electrodes illustrates the benefits of close control of weld hydrogen levels when welding onto in-service pipelines.

While a better indicator of cracking susceptibility might be the volume fraction of crack-susceptible microstructure (e.g., martensite) in the HAZ, or even the actual fracture toughness of the HAZ microstructure, these are difficult to measure during the qualification of welding procedures. In contrast, HAZ hardness is relatively simple to measure. Therefore, it is anticipated that HAZ hardness will remain the preferred method of evaluating procedure qualification welds with regard to cracking susceptibility.

Some concern has been expressed pertaining to the risk of cracking in subsequent service when hard HAZ microstructures are exposed to hydrogen charging from cathodic protection. In recent work pertaining to weld deposition repair [41], specimens of welded line pipe steel were subjected to a tensile stress at yield level while a cathodic current was applied. No cracks initiated in the HAZ in spite of the fact that the HAZ hardness levels were as high as 400 HV.

Results of small scale experiments provide insight into the interrelationship between hydrogen content, microstructure, hardness, composition, and embrittlement behavior. As with the results of the full-scale weldability trials, these results also emphasize the importance of close control of weld hydrogen levels when welding onto in-service pipelines.

Unexpected results from the experiments conducted on Materials TC2 and EX1 highlight several issues for that remain to be addressed for modern microalloyed materials. It is apparent from these results that HAZ hardness is not a useful indicator of susceptibility in these materials, Material EX1 in particular. Selection of weld metal strength for in-service welds on these materials and hot tap fitting design for large diameter, high pressure pipelines using these materials are also issues worthy of additional consideration.

14. SUMMARY AND CONCLUSIONS

The aim of this work was to contribute toward a more complete understanding of the relationship between maximum HAZ hardness, diffusible hydrogen content, restraint, and cracking behavior for in-service welding applications. The results of this and previous work indicates that a relaxation of the widely used hardness limit of 350 HV is certainly feasible for some materials, which may result in an increased use of in-service welding and the realization of significant economic and environmental benefits. However, for other applications (e.g., welds made on low carbon materials at high hydrogen levels), it may be prudent to further restrict allowable hardness levels to reduce the risk of cracking. This would result in increased safety and reliability of completed welds. Results of full-scale weldability trials further developed and validated previously developed criteria for conventional materials. These results, and the results of the small-scale experiments, illustrate the benefits of close control of weld hydrogen levels when welding onto in-service pipelines. For modern, microalloyed materials, several issues remain to be addressed.

15. ACKNOWLEGEMENT

The authors would like to thank the sponsors of the current work, who are US Department of Transportation – Pipeline and Hazardous Materials Safety Administration, TransCanada PipeLines, BlueScope Steel, and University of Wollongong, and Columbia Gas Transmission for providing a site and the support for the field validation trials.

16. REFERENCES

[1]. API Standard 1104 – Twentieth Edition, "Welding of Pipelines and Related Facilities," American Petroleum Institute, Washington, DC, November 2005.

[2]. CSA Z662-07, "Oil and Gas Pipeline Systems," CSA International, June 2007.

[3]. AS 2885.2-2007, Pipelines–Gas and liquid petroleum, Part 2: Welding, Standards Australia, March 2007.

[4]. Dearden, J. and O'Neill, H., "A Guide to the Selection and Welding of Low Alloy Structural Steels," Institute of Welding Transactions, Vol. 3, October 1940.

[5]. Bailey, N., "Welding Procedures for Alloy Steels," The Welding Institute, Abington Hall, Cambridge, July 1970.

[6]. Graville, B. A. and Read, J. A., "Optimization of Fillet Weld Sizes," Welding Research Supplement, Welding Journal, April 1974.

[7]. Kiefner, J. F., Fischer, R. D., and Mishler, H. W., "Development of Guidelines for Repair and Hot Tap Welding on Pressurized Pipelines," Final Report, Phase 1, to Repair and Hot Tap Welding Group, Battelle Columbus Division, Columbus, OH, September 1981.

[8]. Groeneveld, T. P., "Hydrogen Stress Cracking," 5th Symposium on Line Pipe Research, American Gas Association, Catalog No. L30174, November 1974.

[9]. Lorenz, K. and Düren, C., "C-Equivalent for Evaluation of Large Diameter Pipe Steels." Conference on Steels for Line-Pipe and Pipe Line Fittings, London, October 1981.

[10]. Matharu, I. S. and Hart, P.H.M., "Heat Affected Zone (HAZ) Hydrogen Cracking Behaviour of Low Carbon Equivalent C-Mn Structural Steels," The Welding Institute, Report No. 290/1985, Abington Hall, Cambridge, November 1985.

[11]. Boothby, P. J. and Rodgerson, P., "Offshore Structural Steels: Weldability and Hardenability," "Towards Rational and Economic Fabrication of Offshore Structures – Overcoming the Obstacles," London, November 1984

[12]. Watkins, F. and Bodger P., "The Advantages of Low-Hydrogen Welding (Processes and Consumables) for Higher Strength Steels," Welding Research International, Vol. 5, No. 3, 1975.

[13]. Hart, P.H.M., "The Influence of Steel Cleanliness on HAZ Hydrogen Cracking: The Present Position," IIW Document No. IX-1308-84, 1984.

[14]. Hart, P.H.M., Matharu, I. S., and Jones, A. R., "The Influence of Reduced Carbon Equivalent on HAZ Cracking in Structural Steels," 7th International Conference on Offshore Mechanics and Arctic Engineering (OAME), Houston, February 1988.

16. REFERENCES (continued)

[15]. Bruce, W. A., "Qualification and Selection of Procedures for Welding onto In-Service Pipelines and Piping Systems," Final Report to a Group of Sponsors, Edison Welding Institute, Columbus, OH, January 1996.

[16]. Bruce, W. A., Li, V., Citterberg, R., Wang, Y.-Y., and Chen, Y., "Improved Cooling Rate Model for Welding on In-Service Pipelines," PRCI Contract No. PR-185-9633, EWI Project No. 42508CAP, Edison Welding Institute, Columbus, OH, July 2001.

[17]. AWS A4.3-93:R2006, "Standard Methods for Determination of the Diffusible Hydrogen Content of Martensitic, Bainitic, and Ferritic Steel Weld Metal Produced by Arc Welding," American Welding Society, Miami, Florida, 2006.

[18]. Bruce, W. A. and Threadgill, P. L., "Evaluation of the Effect of Procedure Qualification Variables for Welding onto In-Service Pipelines," Final Report to A.G.A. Pipeline Research Committee for PR-185-9329, EWI Project No. J7141, Edison Welding Institute, Columbus, OH, July 1994.

[19]. Lazor, R. B., Private Communication, Interprovincial Pipe Line Company, 1995.

[20]. Yurioka, N., "Physical metallurgy of steel weldability", ISIJ International, 2001, Vol.41, No.6, 566-570.

[21]. AWS D1.1-86, Structural welding code – Steel, 1986, American Welding Society.

[22]. Yurioka, N., Suzuki, H., and Ohshita, S., Welding Journal, 1983, 62(6), 147-153.

[23]. Bruce, W. A., and Boring, M. A., "Realistic Hardness Limits for In-Service Welding," Final Report to PRCI for Contract No. GRI-8758, Edison Welding Institute, Columbus, OH, March 2005.

[24]. Stout, R. D., "Hardness as an Index of the Weldability and Service Performance of Steel Weldments," WRC Bulletin 189, Welding Research Council, November 1973.

[25]. Brooks, T. L., and Hart, P. H. M., "Do Hardness Measurements Impress You?," The Welding Institute Research Bulletin, March 1977.

[26]. WTIA Technical Note TGN-PE-01, "Hardness Testing of Welds," WTIA TGN-PE-01, Welding Technology Institute of Australia, Silverwater, NSW, March 2006.

[27]. BS 7363:1990, Method for bead-on-plate (BOP) test for welds, British Standards Institute, 1990.

[28]. API RP 582, Recommended Practice and Supplementary Welding Guidelines for the Chemical, Oil, and Gas Industries, First Edition, American Petroleum Institute, March 2001.

16. REFERENCES (continued)

[29]. API RP 2Z, Recommended Practice for Preproduction Qualification for Steel Plates for Offshore Structures, Fourth Edition, American Petroleum Institute, September 2005.

[30]. ASTM E92, Standard Test Method for Vickers Hardness of Metallic Materials, American Society for Testing and Materials, 2003.

[31]. Product Literature, Belec Compact Port Optical Emission Spectrometer, Georgsmarienhütte, Germany, http://www.belec.de/english/emain.htm.

[32]. Unknown, Storing and Re-drying Electrodes, The Lincoln Electric Company, Cleveland, OH, http://lincolnelectric.com/knowledge/articles/content/storing.asp.

[33]. Unknown, Recommendations for the Storage, Re-drying and Handling of ESAB Consumables, ESAB AB, Göteborg, Sweden, http://www.esab.com/ESABHtml/pdf/Handling%20&Storage%20of%20Consumables(1).pdf.

[34]. AWS D1.1:2004, Structural Welding Code – Steel, American Welding Society, Miami, FL, 2004.

[35]. WTIA Technical Note 3, Care and Conditioning of Arc Welding Consumables, WTIA TN-3-94, Welding Technology Institute of Australia, Silverwater, NSW, 1994.

[36]. AWS A5.1-91, Specification for Carbon Steel Electrodes for Shielded Metal Arc Welding, American Welding Society, Miami, FL, 1991.

[37]. Kiefer, J., Private Communication, ConocoPhillips, July 2004.

[38]. Bruce, W. A., "Qualification of Procedures for Welding Onto In-Service Pipelines," International Pipeline Conference – IPC 2002 (Calgary), 2002.

[39]. Bruce, W. A., Nolan, D., and Dunne, D., "Weldability Issues for In-Service Pipeline Welding," International Conference on Pipeline Repairs and In-Service Welding (Wollongong, Australia), Welding Technology Institute of Australia, 2003.

[40]. Bruce, W. A., Nolan, D., Sterjovski, Z., and Dunne, D., "Effect of Steel Composition and Cooling Rate on Microstructure and Hardness of the HAZ for In-Service Welding of Pipelines," International Pipeline Integrity and Repairs Conference (Sydney), Welding Technology Institute of Australia, 2004.

[41]. Oguchi, N., Sakai, J., Inoue, H., and Komukai, S., Critical Hardness for HSC in Deposit Welding on Steel Line Pipes under Cathodic Protection, International Pipeline Conference – IPC 2006 (Calgary), 2006.

Table 1. List of Steel Materials for Full-Scale Weldability Trials and Small-Scale Experiments

Material	Purpose	Form	Specification	Source
N3A	DNV	Plate – 0.375 inch thick	SA 516-70	Steel supplier in the US (American Alloy Steel)
A1	UoW	Pipe – 20-inch-diameter by 0.339-inch-wall thickness	API 5LX-60	Pipeline operating company in Australia
P6	UoW	Pipe – 20-inch-diameter by 0.312-inch-wall thickness	API 5LX-52	Pipeline operating company in the US
P2	UoW	Pipe – 36-inch-diameter by 0.375-inch-wall thickness	API 5LX-65	Pipeline operating company in the US
GTN	DNV/UoW	Pipe – 36-inch-diameter by 0.437-inch wall thickness	API 5LX-52	Pipeline operating company in the US
TC2	DNV/UoW	Pipe – 36-inch-diameter by 0.543-inch wall thickness	API 5LX-80	Pipeline operating company in Canada
EB5	DNV	Pipe – 34-inch diameter by 0.281-inch wall thickness	API 5LX-52	Pipeline operating company in Canada
EB5-S	DNV	Sleeve – 34-inch diameter by 0.500-inch wall thickness	Unknown	Pipeline operating company in Canada
EX1	DNV	Pipe – 36-inch-diameter by 0.636-inch wall thickness	Experimental X120	Pipeline operating company in the US

Table 2. Chemical Composition Results for Materials Listed in Table 1

Element	Composition, Wt. %								
	Sample ID								
	N3A	A1	P6	P2	GTN	TC2	EB5	EB5-S	EX1
C (Carbon)	0.2250	0.1700	0.3200	0.1450	0.2140	0.0560	0.2690	0.1410	0.0250
Mn (Manganese)	1.0300	1.2300	0.9500	1.4100	1.0200	1.6900	1.2000	1.3000	2.1370
P (Phosphorus)	0.0100	0.0080	0.0160	0.0070	0.0130	0.0100	0.0030	0.0050	0.0040
S (Sulfur)	0.0020	0.0050	0.0230	0.0070	0.0210	0.0040	0.0230	0.0220	0.0160
Si (Silicon)	0.2570	0.2500	0.0100	0.3600	0.0420	0.2450	0.0360	0.2490	0.0690
Cu (Copper)	0.0180	0.0090	0.0400	0.3600	0.0920	0.2410	0.0190	0.0300	0.3200
Sn (Tin)	0.0010	--	--	--	0.0080	0.0100	--	--	--
Ni (Nickel)	0.0110	0.0090	0.0300	0.0330	0.0790	0.1310	0.0250	0.0820	0.6060
Cr (Chromium)	0.0130	0.0260	0.0300	0.0630	0.0160	0.1060	0.0430	0.0630	0.2670
Mo (Molybdenum)	0.0020	0.0050	0.0100	0.0090	0.0010	0.2750	0.0050	0.0120	0.2330
Al (Aluminum)	0.0280	0.0210	0.0100	0.0320	0.0010	0.0340	0.0030	0.0380	0.0100
V (Vanadium)	0.0020	0.0050	0.0100	0.0020	0.0020	0.0080	0.0010	0.0510	0.0590
Nb (Niobium)	0.0010	0.0460	0.0100	0.0310	0.0010	0.0880	0.0020	0.0090	0.0180
Zr (Zirconium)	0.0010	--	--	--	0.0010	0.0030	--	--	--
Ti (Titanium)	0.0030	0.0050	0.0100	0.0030	0.0010	0.0120	0.0010	0.0010	0.0140
B (Boron)	0.0001	0.0000	0.0000	0.0000	0.0001	0.0001	0.0004	0.0000	0.0010
Ca (Calcium)	0.0014	--	--	--	0.0000	0.0022	--	--	--
Co (Cobalt)	0.0040	--	--	--	0.0240	0.0080	--	--	--
CE_{IIW}	0.40	0.38	0.49	0.42	0.40	0.44	0.48	0.39	0.55
Pcm	0.29	0.24	0.37	0.25	0.27	0.19	0.34	0.23	0.20
CSA Ceq	0.41	0.39	0.49	0.40	0.40	0.27	0.49	0.36	0.31

Table 3. List of Welding Consumables for Full-Scale Weldability Trials

Consumable Designation	Intended Hydrogen Level	Specification	Manufacturer	Diameter, inch (mm)	Source
E04	< 4 ml/100 g	AWS E7018-H4R	Lincoln	1/8 (3.2)	Local supplier
E05	Elevated	AWS E7018*	Lincoln	3/32 (2.8)	Manufacturer
E03	Elevated	AWS E7018	Not specified.	1/8 (3.2)	Local supplier
CEL	40-60 ml/100 g	AWS E6010	Lincoln	1/8 (3.2)	Local supplier

* Specially formulated for experimental purposes only.

Table 4. Diffusible Hydrogen Analysis Results for Consumables Listed in Table 3

Consumable Designation	Analysis Date	Sample Number	Total Hydrogen Vol. at STP, ml	Deposit Weight, g	Diffusible Hydrogen, ml/100 g
E03	February 7, 2008	08-4652-01	1.046	7.9	13.27
		08-4652-02	1.041	7.5	13.90
		08-4652-03	1.022	7.7	13.33
		08-4652-04	1.027	7.6	13.47
		Average (Standard Deviation)			13.49 (0.28)
E04	February 7, 2008	08-4653-01	0.154	8.1	1.90
		08-4653-02	0.131	8.1	1.61
		08-4653-03	0.134	7.4	1.80
		08-4653-04	0.147	8.4	1.75
		Average (Standard Deviation)			1.76 (0.12)
E03	December 4, 2008	08-5350-01	0.920	8.3	11.15
		08-5350-02	0.884	8.6	10.32
		08-5350-03	0.945	8.5	11.07
		08-5350-04	0.895	8.5	10.56
		Average (Standard Deviation)			10.77 (0.40)
E04	December 4, 2008	08-5351-01	0.329	8.7	3.78
		08-5351-02	0.367	9.3	3.93
		08-5351-03	0.338	9.7	3.49
		08-5351-04	0.351	8.9	3.93
		Average (Standard Deviation)			3.78 (0.21)
CEL	December 4, 2008	08-5352-01	3.634	6.6	55.32
		08-5352-02	2.463	6.4	38.68
		08-5352-03	2.326	6.5	36.07
		08-5352-04	3.910	6.2	62.61
		Average (Standard Deviation)			48.17 (12.86)

Table 5. Experimental Matrix for Full-Scale Weldability Trials at DNV

Material	Hydrogen Level, ml/100 g	Thermal Severity Level	Heat Input		
			Low	Med.	High
N3A	<4	Water	**D12**	**D11**	**D06**
		Motor Oil	--	--	--
	~16	Water	--	**D14**	**D07**
		Motor Oil	--	--	
	~50	Water	--	--	**D13**
		Motor Oil	--	--	--
GTN	<4	Water	**D20, D21**	**D22**	**D23**
		Motor Oil	--	--	--
	~16	Water	**D24**	**D25**	**D26**
		Motor Oil	--	--	
	~50	Water	--	--	**D27**
		Motor Oil	--	--	--
EB5	<4	Water	**D30, D31**	**D32**	**D33**
		Motor Oil	--	--	--
	~16	Water	**D34**	**D35**	**D36**
		Motor Oil	--	--	
	~50	Water	--	--	**D37**
		Motor Oil	--	--	--
EB5-S	<4	Water	**D40**	**D41**	**D42**
		Motor Oil	--	--	--
	~16	Water	--	**D43**	**D44, D45**
		Motor Oil	--	--	
	~50	Water	--	--	**D46**
		Motor Oil	--	--	--
TC2	<4	Water	**D50**	**D51**	**D52**
		Motor Oil	--	--	--
	~16	Water	--	**D53, D54**	**D55**
		Motor Oil	--	--	
	~50	Water	--	--	**D56**
		Motor Oil	--	--	--
EX1	<4	Water	**D60**	**D61**	**D62**
		Motor Oil	**D70, D71**	**D72, D73**	--
	~16	Water	**D63**	**D64, D65**	**D66, D67**
		Motor Oil	**D74**	**D75**	**D76**
	~50	Water	--	--	**D68**
		Motor Oil	--	--	--

Table 6. Welding parameters for Full-Scale Weldability Trials at DNV

Weld No./ Description	Pass/Run No.	Welding Parameters					Heat Input (kJ/inch)		
		Amps	Volts	Length (inch)	Time (sec)	Travel Speed (inch/min)	Run	Pass Average	Weld Average
D12 - N3A - Water - <4ml/100gm - Low heat input	1 - 1	135	24	4.125	61	4.06	47.91	40.44	34.39
	1 - 2	134	25	4.375	56	4.69	42.88		
	1 - 3	134	25	4.500	41	6.59	30.52		
	2 - 1	136	24	4.250	47	5.43	36.10	31.34	
	2 - 2	135	24	4.250	42	6.07	32.02		
	2 - 3	135	24	4.250	34	7.50	25.92		
	3 - 1	134	25	5.750	59	5.85	34.37	29.89	
	3 - 2	135	24	6.375	50	7.65	25.41		
D11 - N3A - Water - <4ml/100gm - Medium heat input	1 - 1	135	24	3.625	61	3.57	54.52	51.57	41.88
	1 - 2	134	24	3.000	56	3.21	60.03		
	1 - 3	135	23	3.250	55	3.55	52.55		
	1 - 4	135	23	3.250	41	4.76	39.17		
	2 - 1	136	24	5.125	59	5.21	37.58	33.67	
	2 - 2	136	24	6.688	61	6.58	29.77		
	3 - 1	135	23	5.250	52	6.06	30.75	34.44	
	3 - 2	135	23	5.750	57	6.05	30.78		
	3 - 3	136	24	1.875	24	4.69	41.78		
D06 - N3A - Water - <4ml/100gm - High heat input	1 - 1	136	23	3.375	50	4.05	46.34	44.27	37.70
	1 - 2	135	24	3.125	46	4.08	47.69		
	1 - 3	136	23	2.250	33	4.09	45.88		
	1 - 4	135	23	3.675	44	5.01	37.18		
	2 - 1	136	23	3.750	43	5.23	35.87	34.06	
	2 - 2	136	23	4.500	53	5.09	36.84		
	2 - 3	137	22	4.500	44	6.14	29.47		
	3 - 1	137	23	3.375	44	4.60	41.08	33.87	
	3 - 2	137	23	3.500	35	6.00	31.51		
	3 - 3	135	24	3.000	29	6.21	31.32		
	3 - 4	135	24	2.875	28	6.16	31.55		
D14 - N3A - Water - ~16ml/100gm - Medium heat input	1 - 1	135	24	3.500	66	3.18	61.10	43.71	33.00
	1 - 2	134	25	5.000	60	5.00	40.20		
	1 - 3	135	24	4.125	38	6.51	29.85		
	2 - 1	136	23	7.000	60	7.00	26.81	24.51	
	2 - 2	135	24	5.250	36	8.75	22.22		
	3 - 1	137	22	5.625	55	6.14	29.47	27.93	
	3 - 2	136	23	4.750	52	5.48	34.24		
	3 - 3	136	24	1.625	10	9.75	20.09		

Table 6. Welding parameters for Full-Scale Weldability Trials at DNV (continued)

Weld No./ Description	Pass/Run No.	Welding Parameters					Heat Input (kJ/inch)		
		Amps	Volts	Length (inch)	Time (sec)	Travel Speed (inch/min)	Run	Pass Average	Weld Average
D07 - N3A - Water - ~16ml/100gm - High heat input	1 - 1	136	22	3.250	55	3.55	50.63	52.47	46.30
	1 - 2	135	24	2.625	41	3.84	50.61		
	1 - 3	136	22	2.250	36	3.75	47.87		
	1 - 4	137	21	2.625	56	2.81	61.38		
	1 - 5	135	24	1.875	30	3.75	51.84		
	2 - 1	137	22	3.875	57	4.08	44.33	41.67	
	2 - 2	137	22	4.000	56	4.29	42.20		
	2 - 3	135	24	3.375	53	3.82	50.88		
	2 - 4	132	26	1.875	16	7.03	29.29		
	3 - 1	136	23	3.375	52	3.89	48.19	42.17	
	3 - 2	133	25	4.500	53	5.09	39.16		
	3 - 3	136	24	4.750	57	5.00	39.17		
D13 - N3A - Water - Cellulosic - High heat input	1 - 1	96	31	3.875	53	4.39	40.70	45.53	45.56
	1 - 2	95	30	3.250	53	3.68	46.48		
	1 - 3	97	29	3.250	57	3.42	49.34		
	1 - 4	95	30	3.375	54	3.75	45.60		
	2 - 1	95	31	3.250	53	3.68	48.03	45.02	
	2 - 2	97	28	3.250	53	3.68	44.29		
	2 - 3	97	29	3.000	48	3.75	45.01		
	2 - 4	94	31	3.000	44	4.09	42.74		
	3 - 1	97	29	3.500	52	4.04	41.79	46.14	
	3 - 2	96	30	3.625	56	3.88	44.49		
	3 - 3	98	27	3.000	53	3.40	46.75		
	3 - 4	95	31	2.000	35	3.43	51.54		
D20 - GTN - Water - <4ml/100gm - Low heat input	1 - 1	133	24	4.875	40	7.31	26.19	26.19	24.05
	2 - 1	133	24	5.000	37	8.10	23.62	23.62	
	3 - 1	133	24	5.000	35	8.57	22.34	22.34	
D21 - GTN - Water - <4ml/100gm - Low heat input	1 - 1	132	25	5.00	34	8.82	22.44	22.44	20.68
	2 - 1	133	25	3.250	20	9.75	20.46	19.07	
	2 - 1	133	24	4.875	27	10.83	17.67		
	3 - 1	133	24	4.750	33	8.63	22.17	22.17	

Table 6. Welding parameters for Full-Scale Weldability Trials at DNV (continued)

Weld No./ Description	Pass/Run No.	Welding Parameters					Heat Input (kJ/inch)		
		Amps	Volts	Length (inch)	Time (sec)	Travel Speed (inch/min)	Run	Pass Average	Weld Average
D22 - GTN - Water - <4ml/100gm - Medium heat input	1 - 1	134	25	5.250	52	6.05	33.18	33.18	31.38
	2 - 1	134	25	5.000	46	6.52	30.82	30.82	
	3 - 1	134	25	5.000	45	6.66	30.15	30.15	
D23 - GTN - Water - <4ml/100gm - High heat input	1 - 1	134	25	2.500	55	2.72	73.70	61.81	55.02
	1 - 2	133	24	2.750	43	3.83	49.91		
	2 - 1	134	25	3.125	58	3.23	62.17	50.95	
	2 - 2	133	24	2.250	28	4.82	39.72		
	3 - 1	133	25	3.000	48	3.75	53.20	52.33	
	3 - 2	134	24	2.125	34	3.75	51.45		
D24 - GTN - Water - ~16ml/100gm - Low heat input	1 - 1	134	24	5.125	57	5.39	35.76	35.76	24.17
	2 - 1	133	24	5.125	30	10.25	18.68	18.68	
	3 - 1	133	23	5.250	31	10.16	18.06	18.06	
D25 - GTN - Water - ~16ml/100gm - Medium heat input	1 - 1	132	27	5.000	52	5.76	37.06	37.06	34.24
	2 - 1	134	25	5.000	50	6.00	33.50	33.50	
	3 - 1	134	24	5.000	50	6.00	32.16	32.16	
D26 - GTN - Water - ~16ml/100gm - High heat input	1 - 1	134	25	5.250	74	4.25	47.21	45.94	48.33
	1 - 2	134	25	3.750	50	4.50	44.66		
	2 - 1	134	25	2.000	32	3.75	53.60	53.60	
	3 - 1	134	24	3.250	53	3.67	52.44	48.08	
	3 - 2	134	25	2.375	31	4.59	43.72		
D27 - GTN - Water - Cellulosic - High heat input	1 - 1	99	27	2.000	46	2.60	61.47	49.41	46.81
	1 - 2	99	28	3.562	48	4.45	37.34		
	2 - 1	99	27	3.500	52	4.03	39.71	39.98	
	2 - 2	98	28	2.250	33	4.09	40.24		
	3 - 1	98	28	2.875	54	3.19	51.53	51.04	
	3 - 2	99	27	2.750	52	3.17	50.54		

Table 6. Welding parameters for Full-Scale Weldability Trials at DNV (continued)

Weld No./ Description	Pass/Run No.	Welding Parameters					Heat Input (kJ/inch)		
		Amps	Volts	Length (inch)	Time (sec)	Travel Speed (inch/min)	Run	Pass Average	Weld Average
D30 - EB5 - Water - <4ml/100gm - Low heat input	1 - 1	133	25	5.125	38	8.09	24.65	24.65	22.37
	2 - 1	133	24	3.125	22	8.52	22.47	21.17	
	2 - 2	133	24	2.250	14	9.64	19.86		
	3 - 1	133	24	5.250	37	8.51	22.49	22.49	
D31 - EB5 - Water - <4ml/100gm - Low heat input	1 - 1	133	25	5.000	41	7.31	27.26	27.26	23.86
	2 - 1	133	25	5.125	32	9.60	20.76	20.76	
	3 - 1	133	25	5.500	39	8.46	23.57	23.57	
D32 - EB5 - Water - <4ml/100gm - Medium heat input	1 - 1	132	26	1.750	25	4.20	49.02	44.31	36.71
	1 - 2	132	25	3.250	39	5.00	39.60		
	2 - 1	134	24	5.000	43	6.97	27.65	27.65	
	3 - 1	133	25	5.000	46	6.52	30.59	30.59	
D33- EB5 - Water - <4ml/100gm - High heat input	1 - 1	131	27	3.750	58	3.87	54.70	56.31	59.72
	1 - 2	133	24	1.500	33	2.72	70.22		
	1 - 3	132	25	0.750	10	4.50	44.00		
	2 - 1	132	25	1.500	42	2.14	92.40	72.65	
	2 - 2	133	24	3.500	58	3.62	52.89		
	3 - 1	132	25	3.875	62	3.75	52.80	51.90	
	3 - 2	133	24	1.500	24	3.75	51.00		
D34 - EB5 - Water - ~16ml/100gm - Low heat input	1 - 1	133	25	5.125	38	8.09	24.65	24.65	21.03
	2 - 1	134	24	5.250	30	10.5	18.37	18.37	
	3 - 1	134	23	5.375	35	9.21	20.06	20.06	
D35 - EB5 - Water - ~16ml/100gm - Medium heat input	1 - 1	134	25	5.000	48	6.25	32.16	32.16	30.35
	2 - 1	134	24	4.750	41	6.95	27.75	27.75	
	3 - 1	134	24	4.750	46	6.19	31.14	31.14	

Table 6. Welding parameters for Full-Scale Weldability Trials at DNV (continued)

Weld No./ Description	Pass/Run No.	Welding Parameters					Heat Input (kJ/inch)		
		Amps	Volts	Length (inch)	Time (sec)	Travel Speed (inch/min)	Run	Pass Average	Weld Average
D36 - EB5 - Water - ~16ml/100gm - High heat input	1 - 1	134	25	3.125	47	3.98	50.38	50.24	48.62
	1 - 2	134	24	2.375	37	3.85	50.10		
	2 - 1	133	25	4.000	58	4.13	48.21	48.84	
	2 - 2	134	24	1.625	25	3.90	49.47		
	3 - 1	134	25	2.875	41	4.20	47.77	46.78	
	3 - 2	134	25	3.000	41	4.39	45.78		
D37 - EB5- Water - Cellulosic - High heat input	1 - 1	95	29	2.750	50	3.30	50.09	46.30	49.01
	1 - 2	97	28	2.875	45	3.83	42.51		
	2 - 1	99	27	2.875	54	3.19	50.20	52.94	
	2 - 2	95	29	2.375	48	2.96	55.68		
	3 - 1	96	28	2.500	45	3.33	48.38	47.81	
	3 - 2	97	28	2.875	50	3.45	47.23		
D40 - EB5-S - Water- <4ml/100gm – Low heat input	1-1	133	25	5.625	35	9.64	20.69	20.69	19.87
	2-1	133	25	5.125	28	10.98	18.17	18.17	
	3-1	133	25	5.125	32	9.61	20.76	20.76	
D41 - EB5-S - Water- <4ml/100gm - Medium heat input	1-1	134	25	5.125	53	5.80	34.64	34.64	33.21
	2-1	134	25	5	47	6.38	31.49	31.49	
	3-1	134	25	5	50	6.00	33.50	33.50	
D42 - EB5-S - Water - <4ml/100gm – High heat input	1-1	134	25	3	53	3.40	59.18	54.475	50.37
	1-2	134	25	2.625	39	4.04	49.77		
	2-1	134	23	3.375	51	3.97	46.57	47.225	
	2-2	133	24	2	30	4.00	47.88		
	3-1	134	25	2.75	46	3.59	56.04	49.405	
	3-2	135	24	2.5	33	4.55	42.77		
D43 - EB5-S - Water - ~16ml/100gm – Medium heat input	1-1	134	25	5.25	53	5.94	33.82	33.82	31.52
	2-1	134	24	5.50	47	7.02	27.48	27.48	
	3-1	134	24	5.13	53	5.80	33.26	33.26	

Table 6. Welding parameters for Full-Scale Weldability Trials at DNV (continued)

Weld No./ Description	Pass/Run No.	Welding Parameters					Heat Input (KJ/inch)		
		Amps	Volts	Length (inch)	Time (sec)	Travel Speed (inch/min)	Run	Pass Average	Weld Average
D44 - EB5-S - Water - ~16ml/100gm – High heat input	1-1	134	25	4.50	65	4.15	48.39	48.39	45.84
	2-1	130	26	4.75	62	4.60	44.12	44.12	
	3-1	134	24	4.50	63	4.29	45.02	45.05	
D45 - EB5-S - Water - ~16ml/100gm – High heat input	1-1	120	29	3.50	50	4.20	49.71	37.23	51.51
	1-2	125	33	2.50	15	10.00	24.75		
	2-1	124	26	3.50	48	4.38	44.21	57.59	
	2-2	115	36	1.75	30	3.50	70.97		
	3-1	134	29	3.25	50	3.90	59.78	59.695	
	3-2	127	32	2.25	33	4.09	59.61		
D46- EB5-S - Water- Cellulosic – High heat input	1-1	134	24	4.75	64	4.45	43.33	43.33	50.86
	2-1	134	25	2.50	36	4.17	48.24	54.135	
	2-2	134	24	2.25	42	3.21	60.03		
	3-1	134	23	2.75	43	3.84	48.19	51.36	
	3-2	133	25	2.50	41	3.66	54.53		
D50 –TC2 - Water - <4ml/100gm – Low heat input	1-1	134	25	5	28	10.71	18.76	18.76	20.31
	2-1	133	25	4.75	28	10.18	19.60	19.60	
	3-1	134	25	4.75	32	8.91	22.57	22.57	
D51 - TC2 - Water - <4ml/100gm – Medium heat input	1-1	134	25	4.875	45	6.50	30.92	30.92	30.41
	2-1	134	25	4.75	42	6.79	29.62	29.62	
	3-1	135	24	4.75	45	6.33	30.69	30.69	
D52 - TC2 - Water - <4ml/100gm – Medium heat input	1-1	134	25	2	42	2.86	70.35	56.91	49.84
	1-2	134	24	3.625	49	4.44	43.47		
	2-1	134	25	4.5	57	4.74	42.43	42.655	
	2-2	134	25	1.25	16	4.69	42.88		
	3-1	134	25	2.75	43	3.84	52.38	49.945	
	3-2	134	25	2.75	39	4.23	47.51		

Table 6. Welding parameters for Full-Scale Weldability Trials at DNV (continued)

Weld No./ Description	Pass/Run No.	Welding Parameters					Heat Input (KJ/inch)		
		Amps	Volts	Length (inch)	Time (sec)	Travel Speed (inch/min)	Run	Pass Average	Weld Average
D53 - TC2 - Water - <4ml/100gm – High heat input	1-1	134	25	5.00	52	5.77	34.84	34.84	36.61
	2-1	133	25	4.75	52	5.48	36.40	36.40	
	3-1	134	24	4.75	57	5.00	38.59	38.59	
D54-TC2 - Water- ~16ml/100gm - High heat input	1-1	132	24	5.00	66	4.55	41.82	41.82	33.37
	2-1	134	23	4.75	40	7.13	25.95	25.95	
	3-1	134	24	4.88	49	5.97	32.32	32.32	
D55- TC2 - Water- ~16ml/100gm – High heat input	1-1	125	29	3.50	70	3.00	72.50	57.7	56.87
	1-2	132	25	2.00	26	4.62	42.90		
	2-1	132	26	3.75	68	3.31	62.23	60.89	
	2-2	132	26	1.50	26	3.46	59.49		
	3-1	134	25	4.75	67	4.25	47.25	47.25	
D56 - TC2 - Water - ~16ml/100gm – Cellulosic input	1-1	130	32	4.50	52	5.19	48.07	48.07	46.71
	2-1	130	31	4.25	49	5.20	46.46	46.46	
	3-1	125	31	4.25	50	5.10	45.59	45.59	
D60 –EX1 - Water - <4ml/100gm - Low heat input	1-1	134	26	5.13	45	6.83	30.59	30.59	25.19
	2-1	134	25	5.25	34	9.26	21.70	21.70	
	3-1	134	24	5.25	38	8.29	23.28	23.28	
D61 – EX1- Water - <4ml/100gm - Medium heat input	1-1	132	24	4.50	58	4.66	40.83	42.76	37.63
	1-2	133	24	1.00	14	4.29	44.69		
	2-1	133	24	5.25	45	7.00	27.36	27.36	
	3-1	132	24	5.00	47	6.38	29.78	29.78	
D62- EX1 - Water- <4ml/100gm - High heat input	1-1	133	25	3.75	60	3.75	53.20	54.74	57.13
	1-2	134	24	2.00	35	3.43	56.28		
	2-1	134	24	2.25	38	3.55	54.31	51.625	
	2-2	133	24	3.00	46	3.91	48.94		
	3-1	134	24	2.25	51	2.65	72.90	65.03	
	3-2	134	23	2.75	51	3.24	57.16		

Table 6. Welding parameters for Full-Scale Weldability Trials at DNV (continued)

Weld No./ Description	Pass/Run No.	Welding Parameters					Heat Input (KJ/inch)		
		Amps	Volts	Length (inch)	Time (sec)	Travel Speed (inch/min)	Run	Pass Average	Weld Average
D63- EX1- Water- ~16ml/100gm –Low heat input	1-1	133	22	5.00	31	9.68	18.14	18.14	20.28
	2-1	132	23	5.50	38	8.68	20.98	20.98	
	3-1	133	22.	5.25	39	8.08	21.74	21.74	
D64 - EX1 - Water - ~16ml/100gm –Medium heat input	1-1	131	22	5.13	63	4.88	35.43	35.43	31.68
	2-1	132	22	5.25	51	6.18	28.21	28.21	
	3-1	132	23	5.13	53	5.80	31.40	31.40	
D65 - EX1 - Water - ~16ml/100gm - Medium heat input	1-1	133	24	5.50	60	5.50	34.82	34.82	33.63
	2-1	131	26	5.25	53	5.94	34.38	34.38	
	3-1	131	25	5.38	52	6.20	31.68	31.68	
D66 - EX1 - Water - ~16ml/100gm - High heat input	1-1	133	23	5.13	68	4.52	40.59	40.59	54.76
	2-1	133	24	3.00	60	3.00	63.84	60	
	2-2	134	23	2.25	41	3.29	56.16		
	3-1	131	23	1.75	35	3.00	60.26	56.595	
	3-2	130	25	3.50	57	3.68	52.93		
D67 - EX1 - Water - ~16ml/100gm - High heat input	1-1	132	24	2.75	60	2.75	69.12	59.215	55.79
	1-2	134	23	2.75	44	3.75	49.31		
	2-1	133	23	3.25	52	3.75	48.94	46.645	
	2-2	132	24	2.50	35	4.29	44.35		
	3-1	133	23	2.00	30	4.00	45.89	50.305	
	3-2	133	24	3.50	60	3.50	54.72		
D68- EX1 - Water- Cellulosic – High heat input	1-1	127	30	3.13	51	3.68	62.18	52.77	47.71
	1-2	130	29	2.00	23	5.22	43.36		
	2-1	129	31	5.00	47	6.38	37.59	37.59	
	3-1	130	30	2.25	39	3.46	67.60	62.145	
	3-2	128	29	2.75	42	3.93	56.69		
D70- EX1 – Mineral Oil - <4ml/100gm – Low heat input	1-1	134	22	5.50	42	7.86	22.51	22.51	21.87
	2-1	134	22	5.50	40	8.25	21.44	21.44	
	3-1	133	25	5.38	35	9.21	21.65	21.65	

Table 6. Welding parameters for Full-Scale Weldability Trials at DNV (continued)

Weld No./ Description	Pass/Run No.	Welding Parameters					Heat Input (KJ/inch)		
		Amps	Volts	Length (inch)	Time (sec)	Travel Speed (inch/min)	Run	Pass Average	Weld Average
D71 - EX1 - Mineral oil - <4ml/100gm – Low heat input	1-1	133	24	4.88	48	6.09	31.43	31.43	28.71
	2-1	134	23	4.88	42	6.96	26.55	26.55	
	3-1	133	24	4.88	43	6.80	28.16	28.16	
D72 - EX1 - Mineral oil - <4ml/100gm – Medium heat input	1-1	132	25	5.00	58	5.17	38.28	38.28	33.16
	2-1	132	24	5.00	48	6.25	30.41	30.41	
	3-1	132	24	5.25	51	6.18	30.77	30.77	
D73 - EX1 - Mineral oil - <4ml/100gm - Medium heat input	1-1	134	22	5.25	56	5.63	31.45	31.45	33.76
	2-1	133	24	5.13	53	5.80	33.01	33.01	
	3-1	133	23	5.00	60	5.00	36.71	36.71	
D74 - EX1 - Mineral oil - ~16ml/100gm – Low heat input	1-1	134	23	5.25	42	7.50	24.66	24.66	23.29
	2-1	133	25	5.50	39	8.46	23.58	23.58	
	3-1	133	23	5.38	38	8.49	21.63	21.63	
D75- EX1- Mineral oil - ~16ml/100gm –Medium heat input	1-1	129	26	5.25	60	5.25	38.33	38.33	33.77
	2-1	129	26	5.25	52	6.06	33.22	33.22	
	3-1	134	22	5.25	53	5.94	29.76	29.76	
D76- EX1- Mineral oil - ~16ml/100gm - High heat input	1-1	133	24	2.25	50	2.70	70.93	62.185	60.41
	1-2	134	24	3.25	54	3.61	53.44		
	2-1	131	22	3.25	53	3.68	47.00	54.62	
	2-2	132	23	2	41	2.93	62.24		
	3-1	132	21	2.25	58	2.33	71.46	64.45	
	3-2	132	23	2.75	52	3.17	57.41		

Table 7. Results for Full-Scale Weldability Trials at DNV

Weld No./ Description	Mechanical Testing Results			Metallographic Examination Results		
	Specimen No.	Fracture Test	Face Bend Test	Specimen No.	Average HAZ Hardness, HV-10kg	Crack/ No Crack
D12 - N3A - Water - <4ml/100gm - Low heat input	F1	OK	OK	M1	--	OK
	F2	OK	OK	M2	424	OK
	F3	OK	OK	M3	--	OK
	F4	OK	OK	M4	446	OK
	F5	OK	OK			
	F6	OK	OK			
D11 - N3A - Water - <4ml/100gm - Medium heat input	F1	OK	OK	M1	--	OK
	F2	OK	OK	M2	427	OK
	F3	OK	OK	M3	--	OK
	F4	OK	OK	M4	415	OK
	F5	OK	OK			
	F6	OK	OK			
D06 - N3A - Water - <4ml/100gm - High heat input	F1	OK	OK	M1	--	OK
	F2	OK	OK	M2	406	OK
	F3	OK	OK	M3	--	OK
	F4	OK	OK	M4	405	OK
	F5	OK	OK			
	F6	OK	OK			
D14 - N3A - Water - ~16ml/100gm - Medium heat input	F1	OK*	OK*	M1	--	OK
	F2	OK	OK*	M2	444	OK
	F3	OK*	OK*	M3	--	OK
	F4	OK*	OK*	M4	428	OK
	F5	OK*	OK*	* Includes weld metal cracks but no HAZ cracks		
	F6	OK*	OK*			
D07 - N3A - Water - ~16ml/100gm - High heat input	F1	OK*	OK	M1	--	OK
	F2	OK*	OK	M2	366	OK
	F3	OK	OK	M3	--	OK
	F4	OK*	OK	M4	440	OK
	F5	OK*	Crack	* Includes weld metal cracks but no HAZ cracks		
	F6	OK*	Crack			
D13 - N3A - Water - Cellulosic - High heat input	F1	Crack	OK	M1	--	Crack
	F2	Crack	OK*	M2	443	Crack
	F3	Crack	OK*	M3	--	Crack
	F4	Crack	Crack	M4	437	Crack
	F5	Crack	Crack	* Includes weld metal cracks but no HAZ cracks		
	F6	Crack	OK*			

Table 7. Results for Full-Scale Weldability Trials at DNV (continued)

Weld No./ Description	Mechanical Testing Results			Metallographic Examination Results		
	Specimen No.	Fracture Test	Face Bend Test	Specimen No.	Average HAZ Hardness, HV-10kg	Crack/ No Crack
D20 - GTN - Water - <4ml/100gm - Low heat input	F1	OK	OK	M2	364	OK
	F3	OK	OK	M4	325	OK
	F5	OK	OK			
D21- GTN - Water - <4ml/100gm- Low heat input	F1	OK	OK	M2	361	OK
	F3	OK	OK	M4	426	OK
	F5	OK	OK			
D22 - GTN - Water - <4ml/100gm - Medium heat input	F1	OK	OK	M2	340	OK
	F3	OK	OK	M4	323	OK
	F5	OK	OK			
D23 -GTN - Water - <4ml/100gm - High heat input	F1	OK	OK	M2	268	OK
	F3	OK	OK	M4	353	OK
	F5	OK	OK			
D24 - GTN - Water - ~16ml/100gm - Low heat input	F1	OK	OK	M2	254	OK
	F3	OK	OK	M4	263	OK
	F5	OK	OK			
D25 - GTN - Water - ~16ml/100gm - Medium heat input	F1	OK	OK	M2	285	OK
	F3	OK	OK	M4	309	OK
	F5	OK*	OK	* Includes weld metal cracks but no HAZ cracks		
D26 - GTN - Water - ~16ml/100gm - High heat input	F1	OK	OK	M2	356	OK
	F3	OK	OK	M4	265	OK
	F5	OK	OK			

Table 7. Results for Full-Scale Weldability Trials at DNV (continued)

Weld No./ Description	Mechanical Testing Results			Metallographic Examination Results		
	Specimen No.	Fracture Test	Face Bend Test	Specimen No.	Average HAZ Hardness, HV-10kg	Crack/ No Crack
D27 - GTN - Water - ~Cellulosic - High heat input	F1	Cracks[1,2]	Cracks[1]	M2	345	Cracks[1]
	F3	Cracks[1,2]	Cracks[1]	M4	253	Cracks[3]
	F5	Cracks[1,2]	Cracks[1]	[1] HAZ, [2] Weld Metal, [3] Solidification		
D30 - EB5 - Water - <4ml/100gm - Low heat input	F1	OK	OK	M2	429	OK
	F3	OK	OK	M4	377	OK
	F5	OK	OK			
D31- EB5 - Water - <4ml/100gm- Low heat input	F1	OK	OK	M2	410	OK
	F3	OK	OK	M4	419	OK
	F5	OK	OK			
D32 - EB5 - Water - <4ml/100gm - Medium heat input	F1	OK	OK	M2	440	OK
	F3	OK	OK	M4	443	OK
	F5	OK*	OK	* Porosity		
D33 - EB5 - Water - <4ml/100gm - High heat input	F1	OK	OK	M2	427	OK
	F3	OK	OK	M4	336	OK
	F5	OK	OK			
D34 - EB5 - Water - ~16ml/100gm - Low heat input	F1	Cracks*	Cracks*	M2	353	Cracks*
	F3	Cracks*	Cracks*	M4	396	Cracks*
	F5	OK	Cracks*	* Includes weld metal and HAZ cracks, under cut , and poor weld geometry		
D35 - EB5 - Water - ~16ml/100g- Medium heat input	F1	OK	OK	M2	393	OK
	F3	OK	OK	M4	435	OK
	F5	OK	OK			

Table 7. Results for Full-Scale Weldability Trials at DNV (continued)

Weld No./ Description	Mechanical Testing Results			Metallographic Examination Results		
	Specimen No.	Fracture Test	Face Bend Test	Specimen No.	Average HAZ Hardness, HV-10kg	Crack/ No Crack
D36 - EB5 - Water - ~16ml/100gm- High heat input	F1	OK	OK	M2	443	OK
	F3	OK	OK	M4	358	OK
	F5	OK	OK			
D37 - EB5 - Water - Cellulosic- High heat input	F1	Cracks[1]	Cracks[1,2]	M2	376	Cracks[1,3]
	F3	Cracks[1]	Cracks[1]	M4	445	Cracks[1]
	F5	Cracks[1]	Cracks[2]	[1] HAZ, [2] Weld Metal, [3] Under bead		
D40 - EB5-S - Water- <4ml/100gm – Low heat input	F1	OK	Crack	M2	452	OK
	F3	OK	Crack	M4	451	OK
	F5	OK	Crack			
D41 - EB5-S - Water- <4ml/100gm - Medium heat input	F1	OK	Crack	M2	444	OK
	F3	OK	Crack	M4	424	OK
	F5	OK	Crack			
D42 - EB5-S - Water - <4ml/100gm – High heat input	F1	OK	OK	M2	295	OK
	F3	OK	Crack	M4	396	OK
	F5	OK	OK			
D43 - EB5-S - Water - ~16ml/100gm – Medium heat input	F1	OK	OK	M2	400	OK
	F3	OK	Crack	M4	429	OK
	F5	OK	OK			
D44 - EB5-S - Water - ~16ml/100gm – High heat input	F1	OK	OK	M2	455	OK
	F3	OK	OK	M4	411	OK
	F5	OK	Crack			

Table 7. Results for Full-Scale Weldability Trials at DNV (continued)

Weld No./ Description	Mechanical Testing Results			Metallographic Examination Results		
	Specimen No.	Fracture Test	Face Bend Test	Specimen No.	Average HAZ Hardness, HV-10kg	Crack/ No Crack
D45 - EB5-S - Water - ~16ml/100gm – High heat input	F1	OK	Crack	M2	374	OK
	F3	OK	OK	M4	413	OK
	F5	OK	Crack			
D46- EB5-S - Water- Cellulosic - High heat input	F1	Cracks	Cracks	M2	410	Cracks
	F3	Cracks	Cracks	M4	309	Cracks
	F5	Cracks	Cracks			
D50 –TC2 - Water - <4ml/100gm – Low heat input	F1	Crack	OK	M2	316	Crack
	F3	Crack	OK	M4	333	OK
	F5	Crack	OK			
D51 - TC2 - Water - <4ml/100gm – Medium heat input	F1	Crack	OK	M2	305	Crack
	F3	OK	OK	M4	304	Crack
	F5	Crack	OK			
D52 - TC2 - Water - <4ml/100gm – Medium heat input	F1	Crack	OK	M2	294	OK
	F3	OK	OK	M4	298	OK
	F5	OK	OK			
D53 - TC2 - Water - <4ml/100gm – High heat input	F1	Crack	Crack	M2	324	Crack
	F3	Crack	Crack	M4	315	Crack
	F5	Crack	Crack			
D54-TC2 - Water- ~16ml/100gm - High heat input	F1	Crack	Crack	M2	319	Crack
	F3	Crack	Crack	M4	326	Crack
	F5	Crack	Crack			

Table 7. Results for Full-Scale Weldability Trials at DNV (continued)

Weld No./ Description	Mechanical Testing Results			Metallographic Examination Results		
	Specimen No.	Fracture Test	Face Bend Test	Specimen No.	Average HAZ Hardness, HV-10kg	Crack/ No Crack
D55- TC2 - Water- ~16ml/100gm – High heat input	F1	Crack	Crack	M2	298	OK
	F3	Crack*	Crack*	M4	287	OK*
	F5	Crack*	Crack	* Porosity		
D56 - TC2 - Water - Cellulosic – High heat input	F1	Crack	Crack	M2	309	Crack
	F3	Crack	Crack	M4	304	Crack
	F5	Crack	Crack			
D60 –EX1 - Water - <4ml/100gm - Low heat input	F1	Crack	**	M2	320	Crack
	F3	Crack	**	M4	322	Crack
	F5	Crack	**			
D61 – EX1- Water - <4ml/100gm - Medium heat input	F1	Crack	**	M2	317	Crack
	F3	Crack	**	M4	317	Crack
	F5	Crack	**			
D62- EX1 - Water- <4ml/100gm - High heat input	F1	OK	**	M2	311	OK
	F3	OK	**	M4	312	OK
	F5	OK	**			
D63- EX1- Water- ~16ml/100gm –Low heat input	F1	Crack	**	M2	318	Crack
	F3	Crack	**	M4	320	Crack
	F5	Crack	**			
D64 - EX1 - Water - ~16ml/100gm –Medium heat input	F1	Crack	**	M2	302	Crack
	F3	Crack	**	M4	315	Crack
	F5	Crack	**			

Table 7. Results for Full-Scale Weldability Trials at DNV (continued)

Weld No./ Description	Mechanical Testing Results			Metallographic Examination Results		
	Specimen No.	Fracture Test	Face Bend Test	Specimen No.	Average HAZ Hardness, HV-10kg	Crack/ No Crack
D65 - EX1 - Water - ~16ml/100gm -Medium heat input	F1	Crack	**	M2	315	Crack
	F3	Crack	**	M4	318	Crack
	F5	Crack	**			
D66 - EX1 - Water - ~16ml/100gm -High heat input	F1	Crack	**	M2	311	OK*
	F3	Crack	**	M4	314	Crack
	F5	Crack	**	*Poor root geometry		
D67 - EX1 - Water - ~16ml/100gm -High heat input	F1	Crack	**	M2	307	Crack
	F3	Crack	**	M4	315	Crack
	F5	Crack	**			
D68- EX1 - Water- Cellulosic – High heat input	F1	Crack	**	M2	307	Crack
	F3	Crack	**	M4	308	Crack
	F5	Crack	**			
D70- EX1 – Mineral oil - <4ml/100gm – Low heat input	F1	Crack	**	M2	312	OK
	F3	Crack	**	M4	315	OK
	F5	Crack	**			
D71 - EX1 - Mineral oil - <4ml/100gm – Low heat input	F1	Crack	**	M2	310	OK
	F3	Crack	**	M4	312	OK
	F5	Crack	**			
D72 - EX1 - Mineral oil - <4ml/100gm – Medium heat input	F1	Crack	**	M2	304	OK
	F3	Crack	**	M4	300	OK
	F5	Crack	**			

Table 7. Results for Full-Scale Weldability Trials at DNV (continued)

Weld No./ Description	Mechanical Testing Results			Metallographic Examination Results		
	Specimen No.	Fracture Test	Face Bend Test	Specimen No.	Average HAZ Hardness, HV-10kg	Crack/ No Crack
D73 - EX1 - Mineral oil - <4ml/100gm - Medium heat input	F1	Crack	**	M2	302	OK
	F3	Crack	**	M4	300	OK
	F5	OK	**			
D74 - EX1 - Mineral oil - ~16ml/100gm – Low heat input	F1	Crack	**	M2	315	Crack
	F3	Crack	**	M4	315	Crack
	F5	Crack	**			
D75- EX1- Mineral oil - ~16ml/100gm –Medium heat input	F1	Crack	**	M2	300	Crack
	F3	Crack	**	M4	307	Crack
	F5	Crack	**			
D76- EX1- Mineral oil - ~16ml/100gm -High heat input	F1	Crack	**	M2	306	Crack
	F3	Crack	**	M4	308	Crack
	F5	Crack	**			

** Experimental difficulties produced questionable results..

Table 8. Summary of Results for Full-Scale Weldability Trials

Material	Weld No.	Target Hydrogen Level, ml/100 g	Average HAZ Hardness, HV-10kg*	Crack/ No Crack**
N3A	D12	4	446	Non-Cracked
	D11	4	427	Non-Cracked
	D06	4	406	Non-Cracked
	D14	16	444	Non-Cracked
	D07	16	440	Non-Cracked
	D13	50	315	Cracked
GTN	D20	4	364	Non-Cracked
	D21	4	426	Non-Cracked
	D22	4	340	Non-Cracked
	D23	4	353	Non-Cracked
	D24	16	263	Non-Cracked
	D25	16	309	Non-Cracked
	D26	16	356	Non-Cracked
	D27	50	345	Cracked
EB5	D30	4	429	Non-Cracked
	D31	4	419	Non-Cracked
	D32	4	443	Non-Cracked
	D33	4	427	Non-Cracked
	D34	16	396	Cracked
	D35	16	435	Non-Cracked
	D36	16	443	Non-Cracked
	D37	50	445	Cracked
EB5/EB5-S	D40	4	452	Cracked
	D41	4	444	Cracked
	D42	4	396	Cracked***
	D43	16	429	Cracked
	D44	16	455	Cracked
	D45	16	413	Cracked
	D46	50	444	Cracked

* Highest measured average HAZ hardness from two metallographic sections.
** HAZ cracks only.
*** One face bend test specimens contains a small hydrogen crack

Table 8. Summary of Results for Full-Scale Weldability Trials (continued)

Material	Weld No.	Target Hydrogen Level, ml/100 g	Average HAZ Hardness, HV-10kg*	Crack/ No Crack
TC2	D50	4	333	Cracked
	D51	4	305	Cracked
	D52	4	298	Cracked
	D53	4	324	Cracked
	D54	16	326	Cracked
	D55	16	298	Cracked
	D56	50	309	Cracked
EX1	D60	4	322	Cracked
	D61	4	317	Cracked
	D62	4	312	Non-Cracked
	D63	16	320	Cracked
	D64	16	315	Cracked
	D65	16	318	Cracked
	D66	16	314	Cracked
	D67	16	315	Cracked
	D68	50	308	Cracked
	D70	4	315	Cracked
	D71	4	312	Cracked
	D72	4	304	Cracked
	D73	4	302	Cracked
	D74	16	315	Cracked
	D75	16	307	Cracked
	D76	16	308	Cracked

* Highest measured average HAZ hardness from two metallographic sections.

Table 9. Welding Parameters for Field Validation Trials

Weld No./ Location	Pass/Run No.	Welding Parameters					Heat Input (KJ/inch)	
		Amps	Volts	Length (in)	Time (sec)	Travel Speed (inch/min)	Run	Weld Average
V01 - 10240 - SR	F1	-	-	-	-	-	-	26.25
	F2	92	22	2.06	26	4.76	25.51	
	F3	92	22	2.25	30	4.50	26.99	
V02 - 10240 - LR	F1 - 1	91	21	1.75	39	2.69	42.59	33.10
	F1 - 2	86	22	1.75	30	3.50	32.43	
	F2	66	22	3.50	63	3.33	26.14	
	F3	65	22	3.25	71	2.75	31.24	
V03 - 10240 - LL	F1	85	23	3.50	26	8.08	14.52	15.27
	F2	85	23	3.50	28	7.50	15.64	
	F3	86	22	3.63	30	7.25	15.66	
V04 - 10240 - SL	F1	90	22	2.25	41	3.29	36.08	32.89
	F2	87	22	2.13	35	3.64	31.52	
	F3	87	23	2.13	33	3.86	31.07	
V05 - 1802 - SR	F1	92	22	2.38	25	5.70	21.31	31.41
	F2	91	22	2.25	37	3.65	32.92	
	F3	90	22	2.38	48	2.97	40.02	
V06 - 1802 - LR	F1	89	22	4.13	33	7.50	15.66	16.84
	F2	88	22	4.00	34	7.06	16.46	
	F3	88	22	4.00	38	6.32	18.39	
V07 - 1802 - LL	F1 - 1	87	23	2.75	59	2.80	42.93	41.14
	F1 - 2	86	22	1.25	31	2.42	46.92	
	F2	89	22	3.63	62	3.51	33.49	
	F3 - 1	87	22	2.63	55	2.86	40.10	
	F3 - 2	88	22	1.38	30	2.75	42.24	
V08 - 1802 - SL	F1	89	22	2.25	24	5.63	20.89	17.05
	F2	86	22	2.25	17	7.94	14.30	
	F3	86	22	2.25	19	7.11	15.98	

Table 10. Chemical Composition Results for Field Validation Trial Materials

Element	Composition, Wt. %	
	Sample ID	
	1802 – 20 inch	10240 – 24 inch
C (Carbon)	0.244	0.148
Mn (Manganese)	1.123	1.205
P (Phosphorus)	--	--
S (Sulfur)	0.021	0.025
Si (Silicon)	0.074	0.072
Cu (Copper)	0.064	0.126
Sn (Tin)	--	--
Ni (Nickel)	0.038	0.120
Cr (Chromium)	0.119	0.320
Mo (Molybdenum)	0.034	0.101
Al (Aluminum)	0.022	0.012
V (Vanadium)	0.013	0.033
Nb (Niobium)	0.004	0.008
Zr (Zirconium)	--	--
Ti (Titanium)	0.000	0.000
B (Boron)	0.001	0.000
Ca (Calcium)	--	--
Co (Cobalt)	--	--
CE_{IIW}	0.471	0.456
Pcm	0.320	0.247
CSA Ceq	--	--

Table 11. Results for Field Validation Trials

Weld No./ Location	Specimen No.	Metallographic Examination Results	Average HAZ Hardness, HV-10kg	Crack/ No Crack
V01 - 10240 - SR	M1	OK	279	Non-Cracked
	M2	OK	259	Non-Cracked
V02 - 10240 - LR	M1	OK	249	Non-Cracked
	M2	OK	236	Non-Cracked
V03 - 10240 - LL	M1	OK	306	Non-Cracked
	M2	OK	311	Non-Cracked
V04 - 10240 - SL	M1	OK	275	Non-Cracked
	M2	OK	262	Non-Cracked
V05 - 1802 - SR	M1	OK	209	Non-Cracked
	M2	OK	213	Non-Cracked
V06 - 1802 - LR	M1	OK	294	Non-Cracked
	M2	OK	302	Non-Cracked
V07 - 1802 - LL	M1	OK	228	Non-Cracked
	M2	OK	228	Non-Cracked
V08 - 1802 - SL	M1	OK	306	Non-Cracked
	M2	OK	307	Non-Cracked

Table 12. General Rules of Thumb for Pipe Material Chemical Composition *

Property	Value	Trend
Vintage	Modern	Lower CE
	Older	Higher or lower CE depending on grade
Manufacturing Method	ERW or SAW	Lower CE
	Seamless	Higher CE
Grade	Higher strength (e.g., X70)	Lower CE
	Intermediate strength (e.g., X52)	Higher CE
	Lower strength (e.g., Grade B, X42)	Probably lower CE, but may be down-graded X52

* Note: These are general rules of thumb only. There are many, many exceptions to these rules.

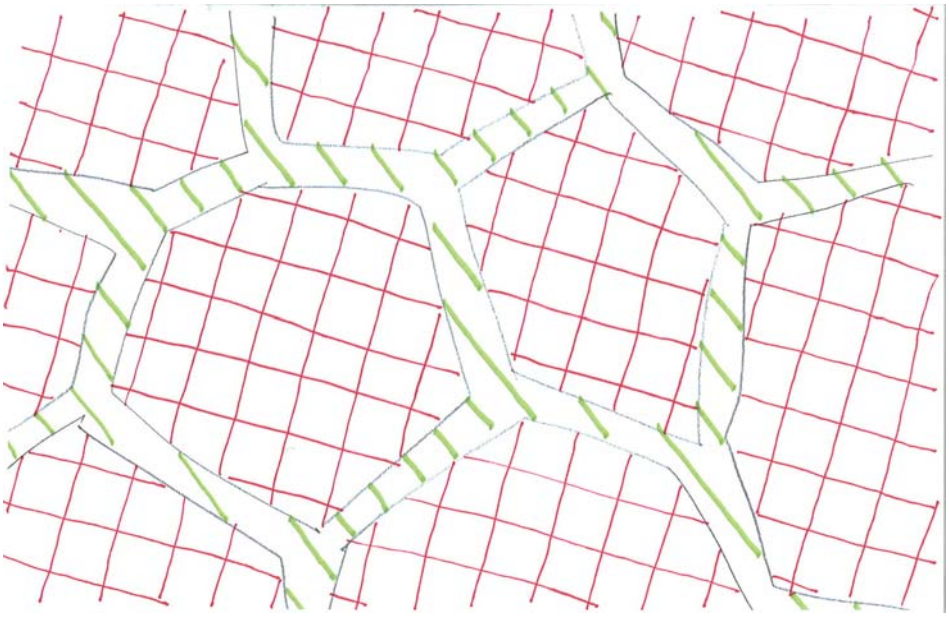

Figure 1. Schematic Illustration of HAZ Microstructure in Low CE Material Consisting of 90% Martensite (%C = 0.06, HV_M = 353, HV = 343).

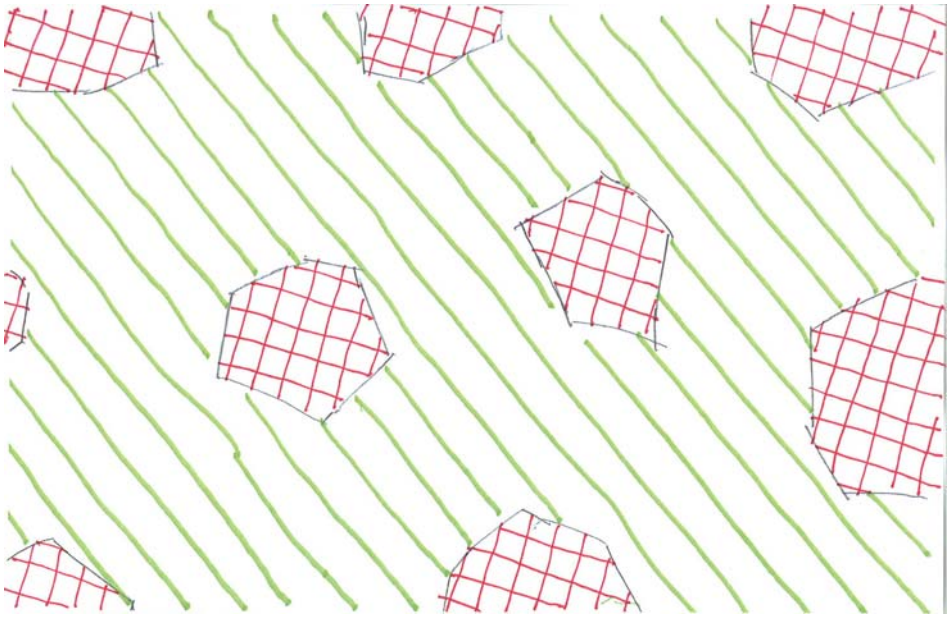

Figure 2. Schematic Illustration of HAZ Microstructure in High CE Material Consisting of 40% Martensite (%C = 0.30, HV_M = 545, HV = 368).

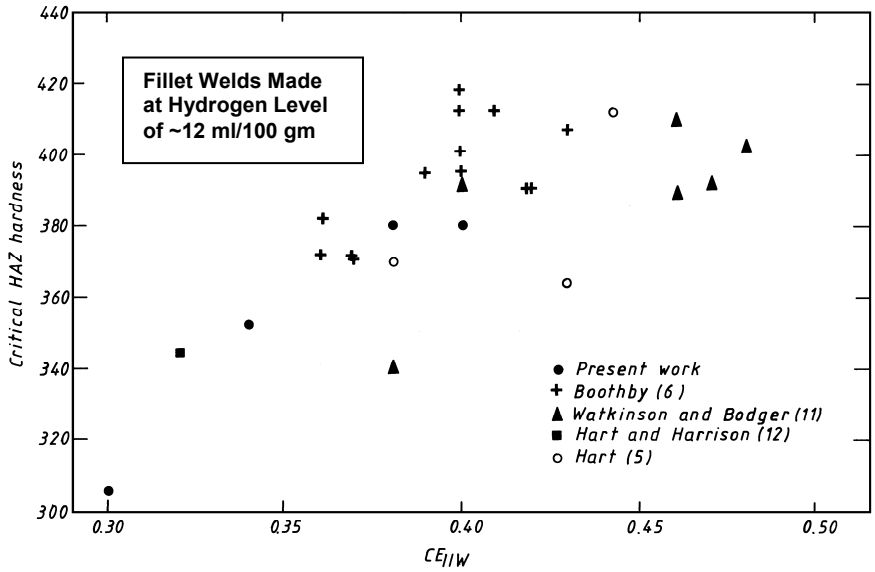

Figure 3. Critical Hardness Level vs. CE_{IIW} Level from Several Previous Programs. [10]

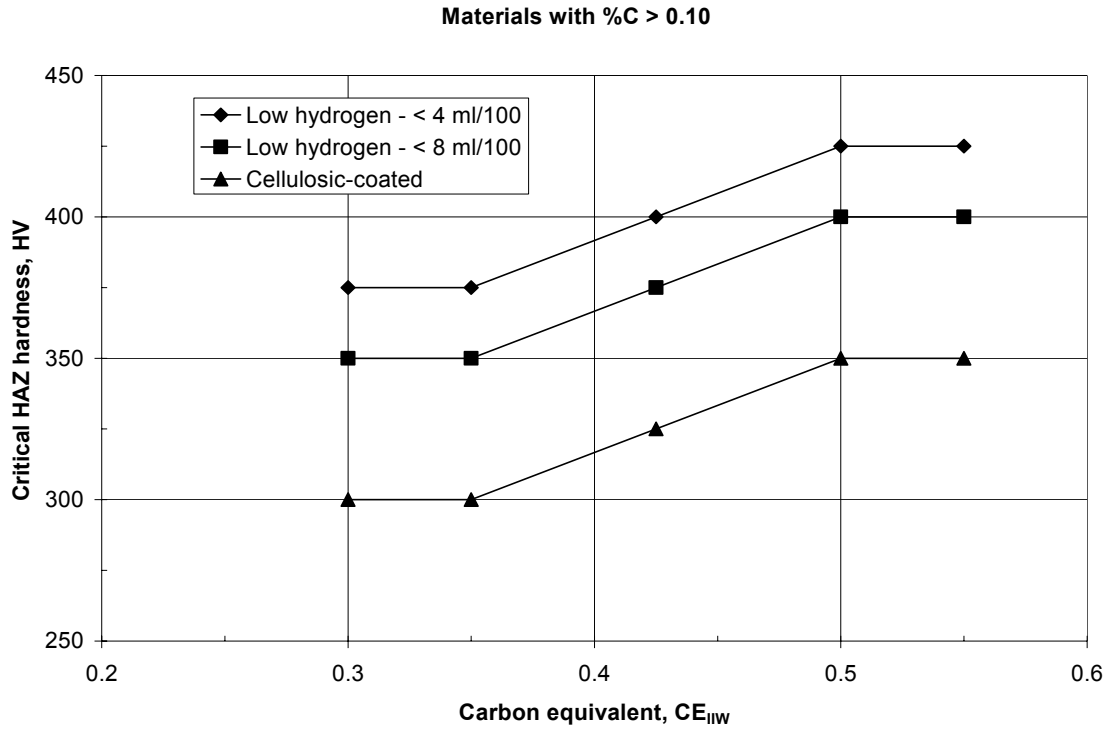

Figure 4. Critical Hardness Level for In-Service Welds vs. CE_{IIW} and Weld Hydrogen Level from Previous Work.

Figure 5. Example of Highly-Restrained Multi-Pass Fillet Weld from Previous Program.

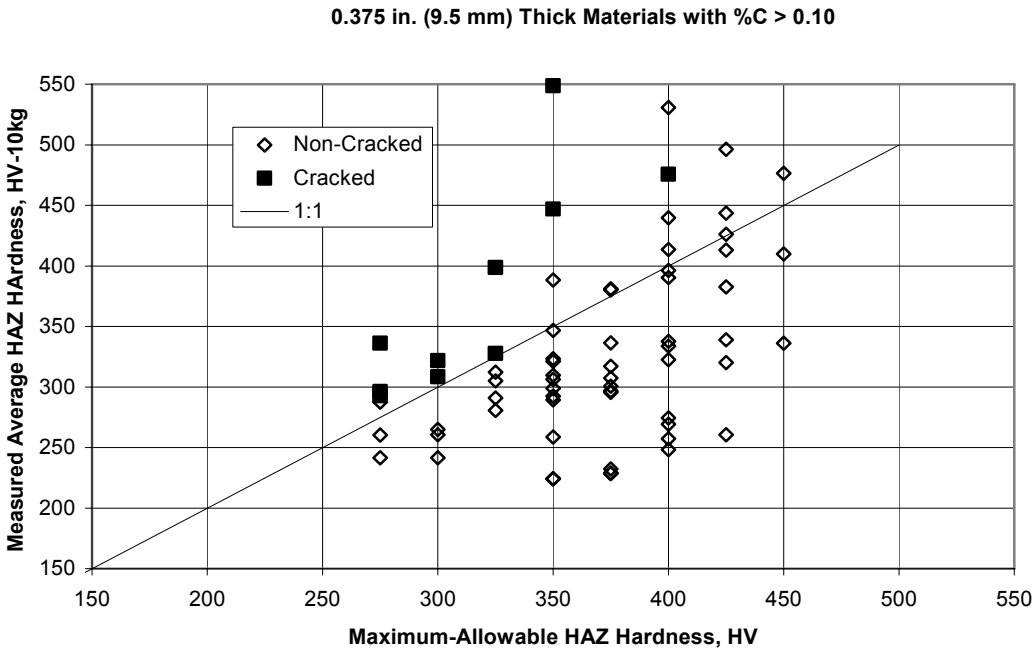

Figure 6. Comparison of Hardness Testing Results with Hardness Evaluation Criterion from Previous Work.

Figure 7. Experimental Setup for Highly-Restrained Multi-Pass Fillet Welds in Current Work.

Figure 8. Setup for Flowing Mineral Oil Condition.

Figure 9. Three-Pass Fillet Weld being made at Target Heat Input Level.

Figure 10. Example of Completed Three-Pass Fillet Weld.

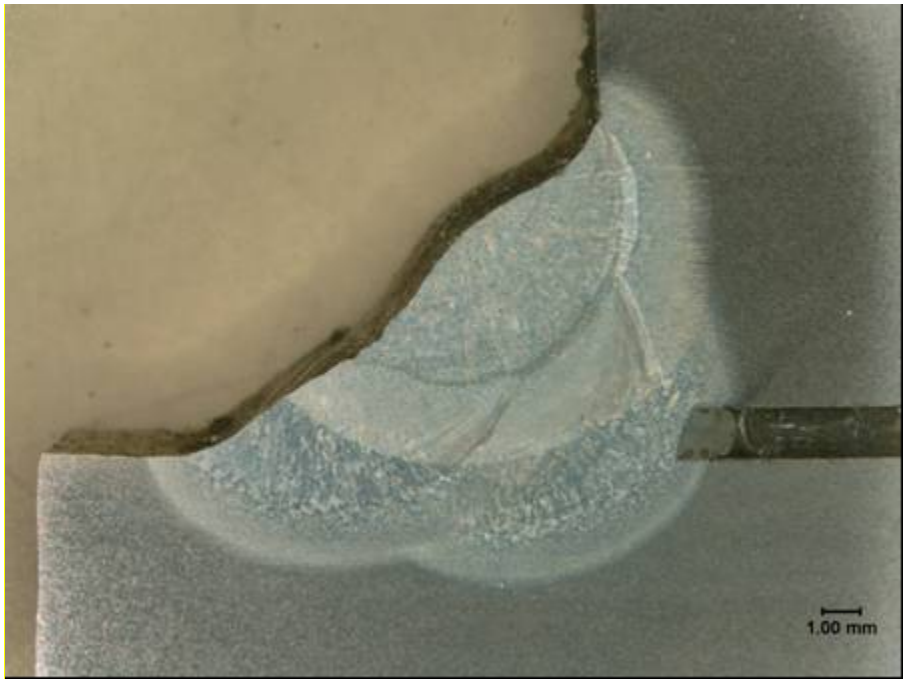

Figure 11. Example of metallographic section completed weld.

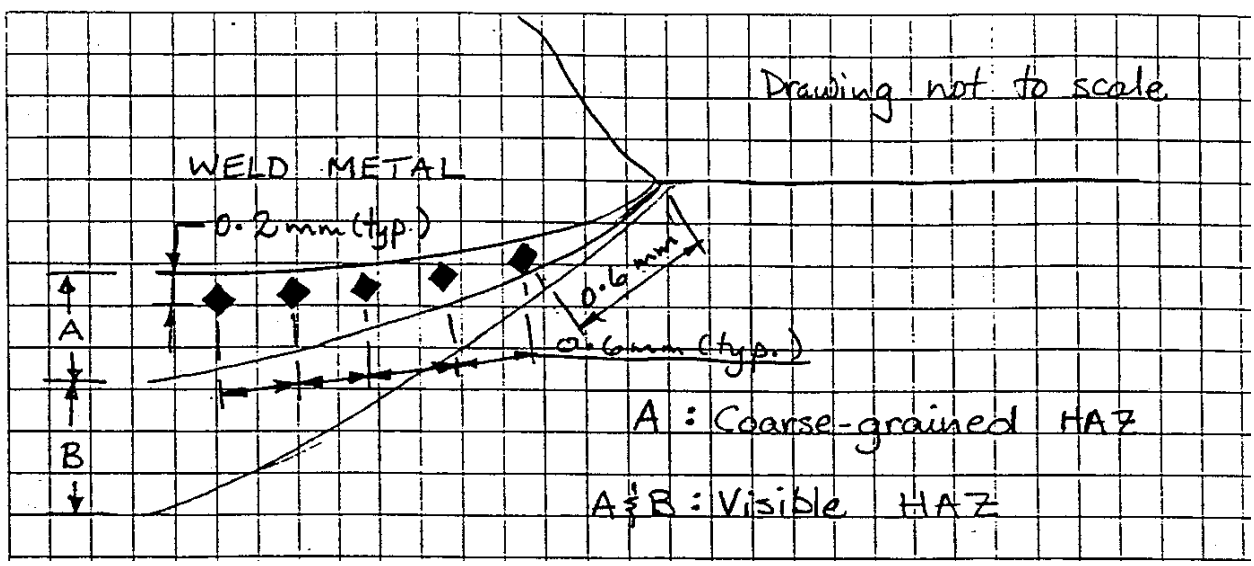

Indents are spaced 0.2 mm (0.008 inch) from fusion line and 0.6 mm (0.024 inch) apart. Initial indent is located 0.6 mm (0.024 inch) from weld toe. Region A is coarse-grain HAZ and Regions A and B are visible HAZ. Figure is not to scale.

Figure 12. HAZ Hardness Indent Locations

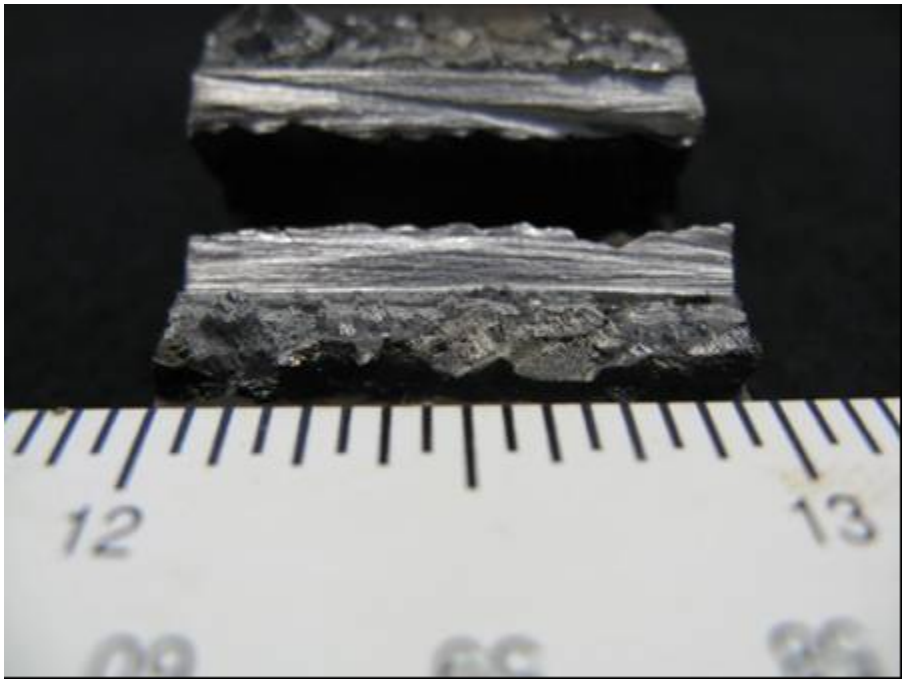

Figure 13. Example of nick-break specimen from completed weld with root crack.

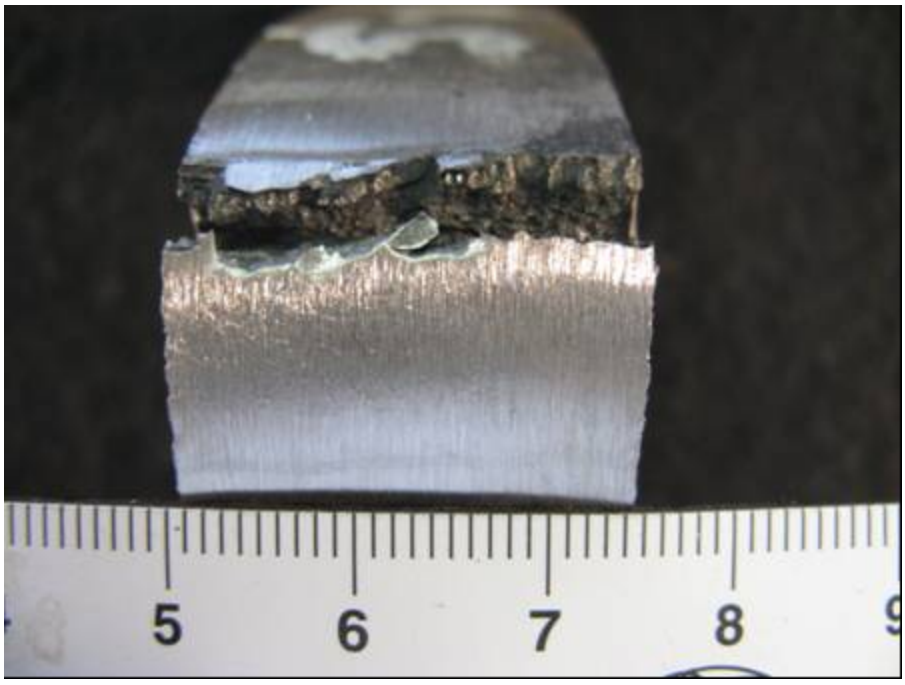

Figure 14. Example of face-bend specimen from completed weld with toe crack.

Figure 15. Preliminary HAZ Hardness Evaluation Criteria based on CEIIW for Thinner Materials with Carbon Contents greater than 0.10%

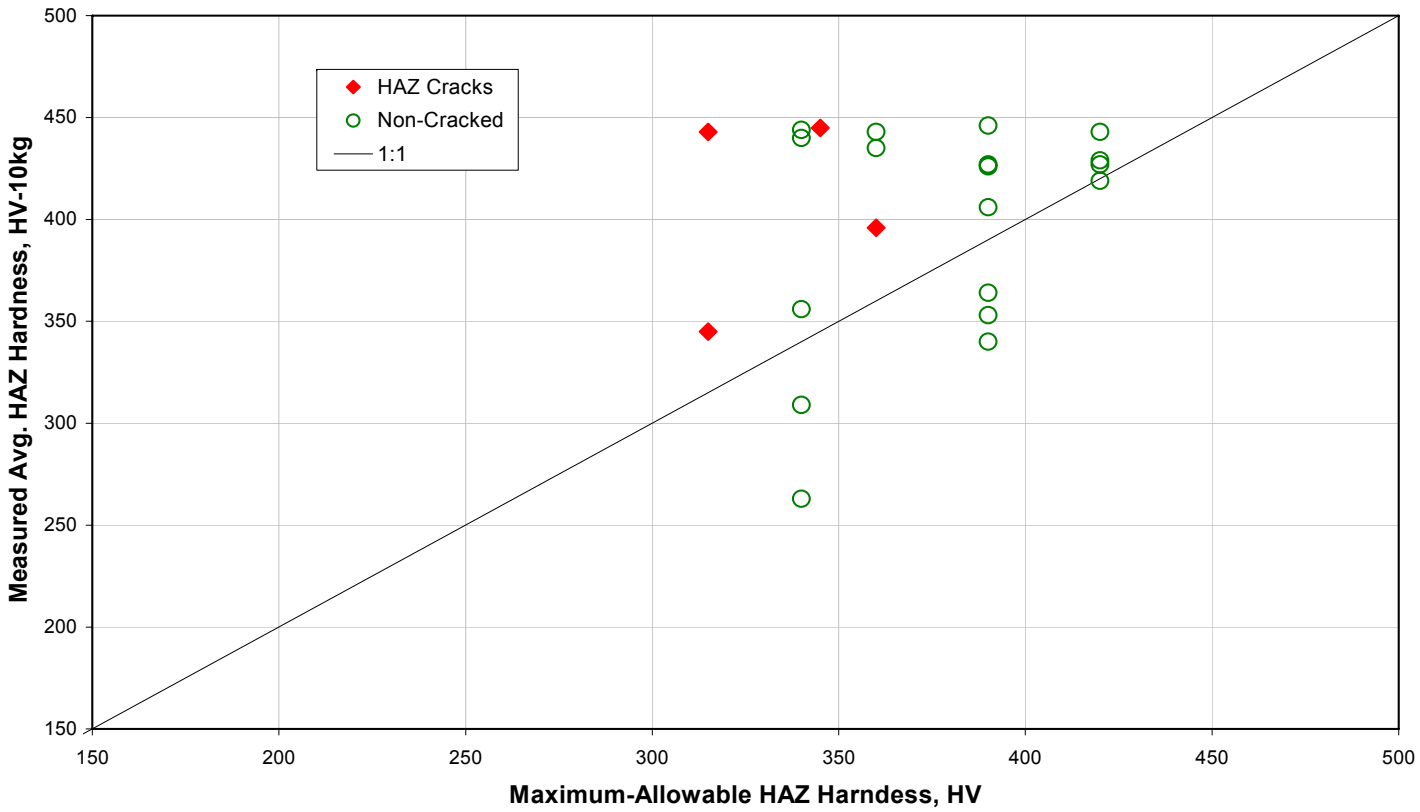

Figure 16. Comparison of HAZ Hardness Testing Results with Preliminary Hardness Evaluation Criterion - Materials with Carbon Contents greater than 0.10%.

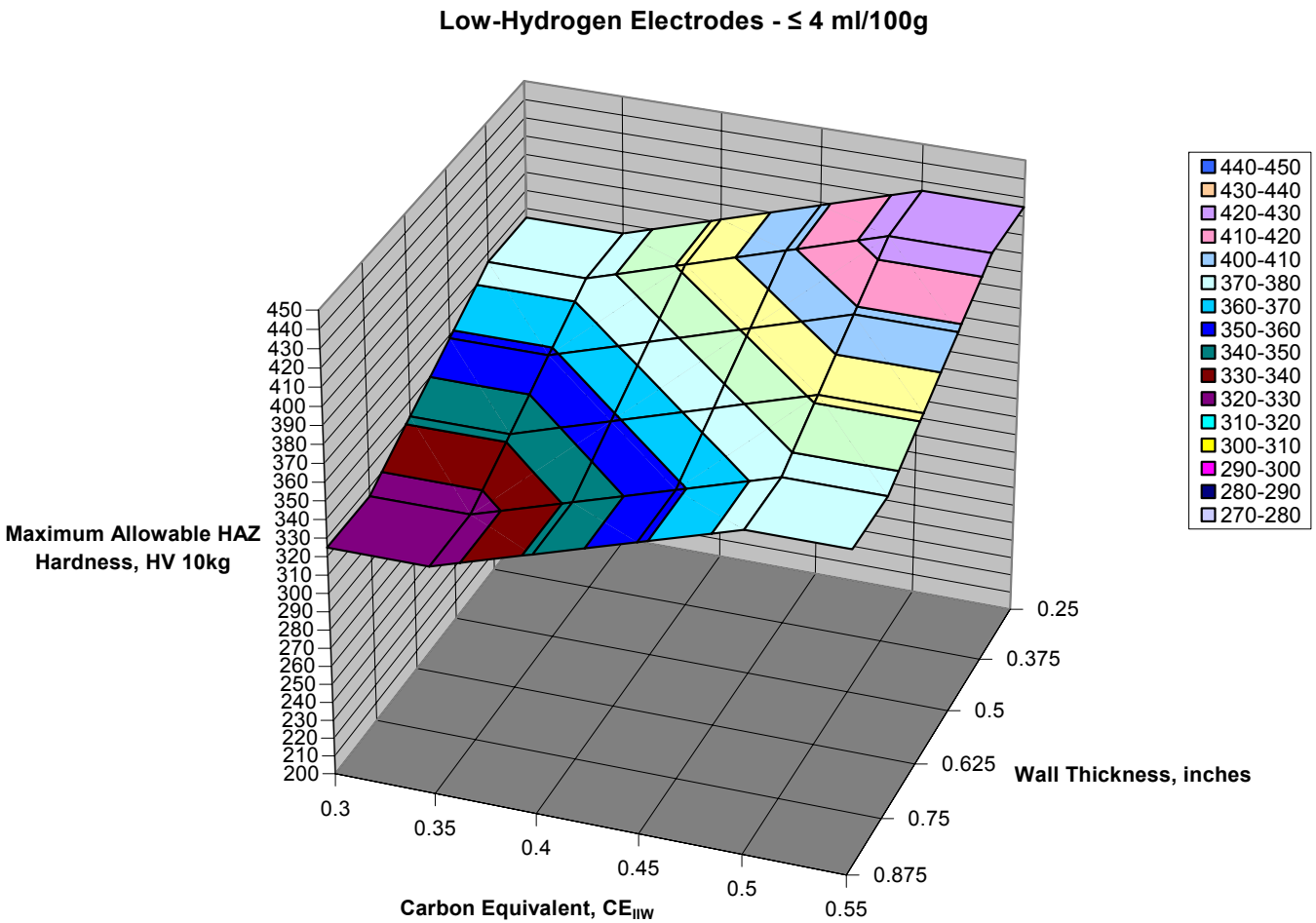

Figure 17. Example of Three-Dimensional HAZ Hardness Evaluation Criteria for In-Service Welds on Materials with Carbon Contents greater than 0.10% – ≤ 4 ml/100g Hydrogen Level

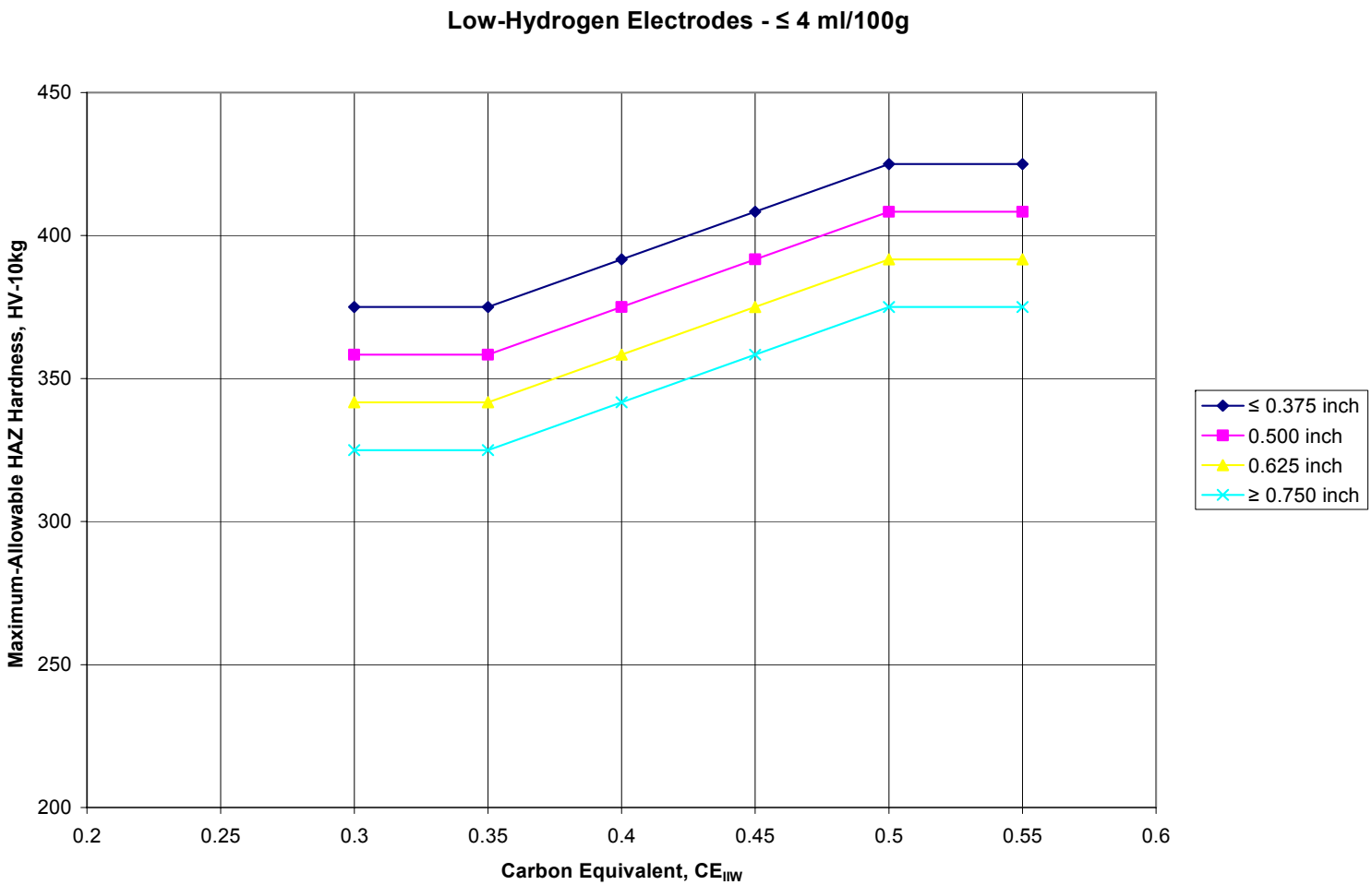

Figure 18. HAZ Hardness Evaluation Criteria for In-Service Welds on Materials with Carbon Contents greater than 0.10% – ≤ 4 ml/100g Hydrogen Level

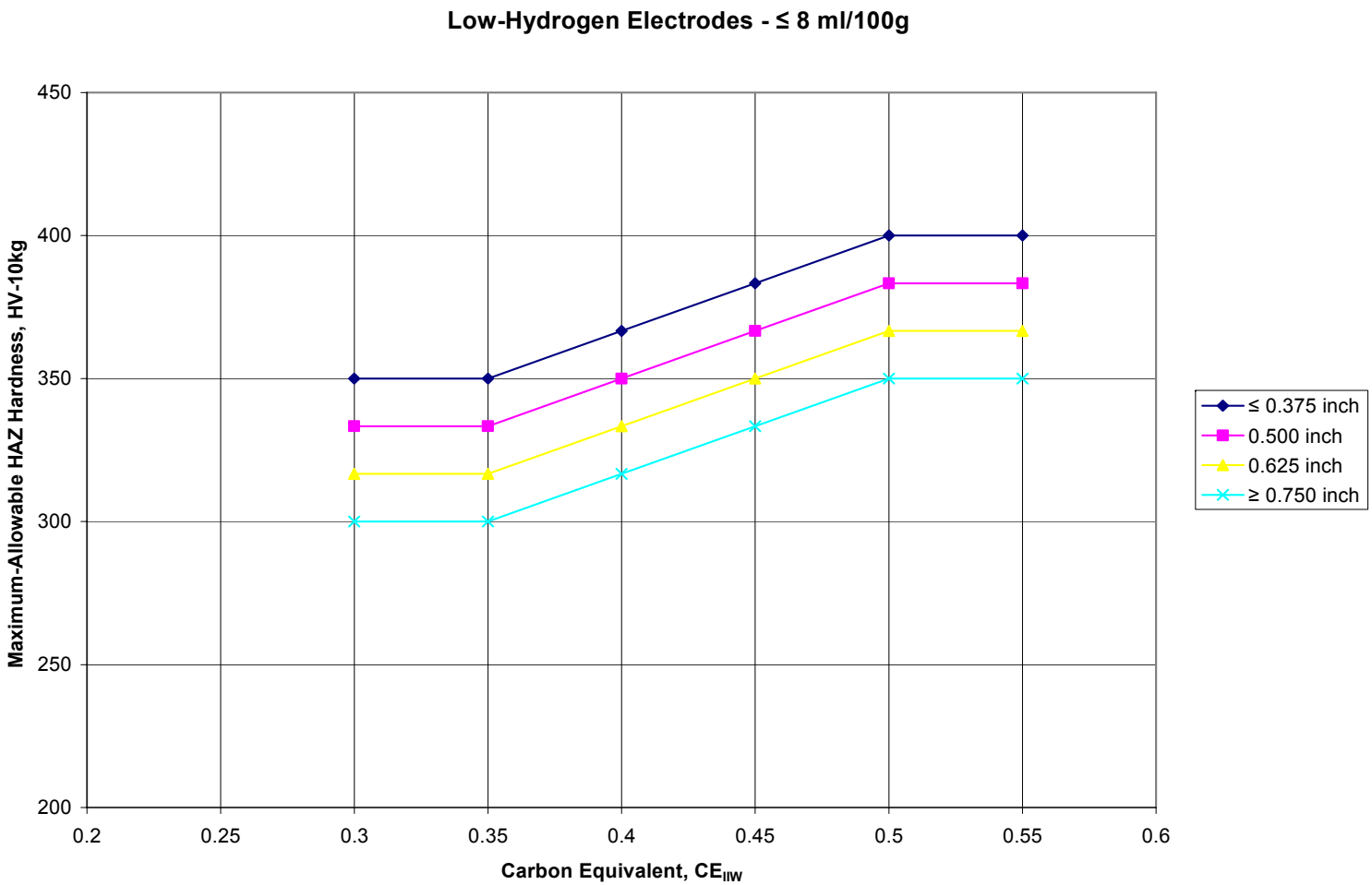

Figure 19. HAZ Hardness Evaluation Criteria for In-Service Welds on Materials with Carbon Contents greater than 0.10% – ≤ 8 ml/100g Hydrogen Level

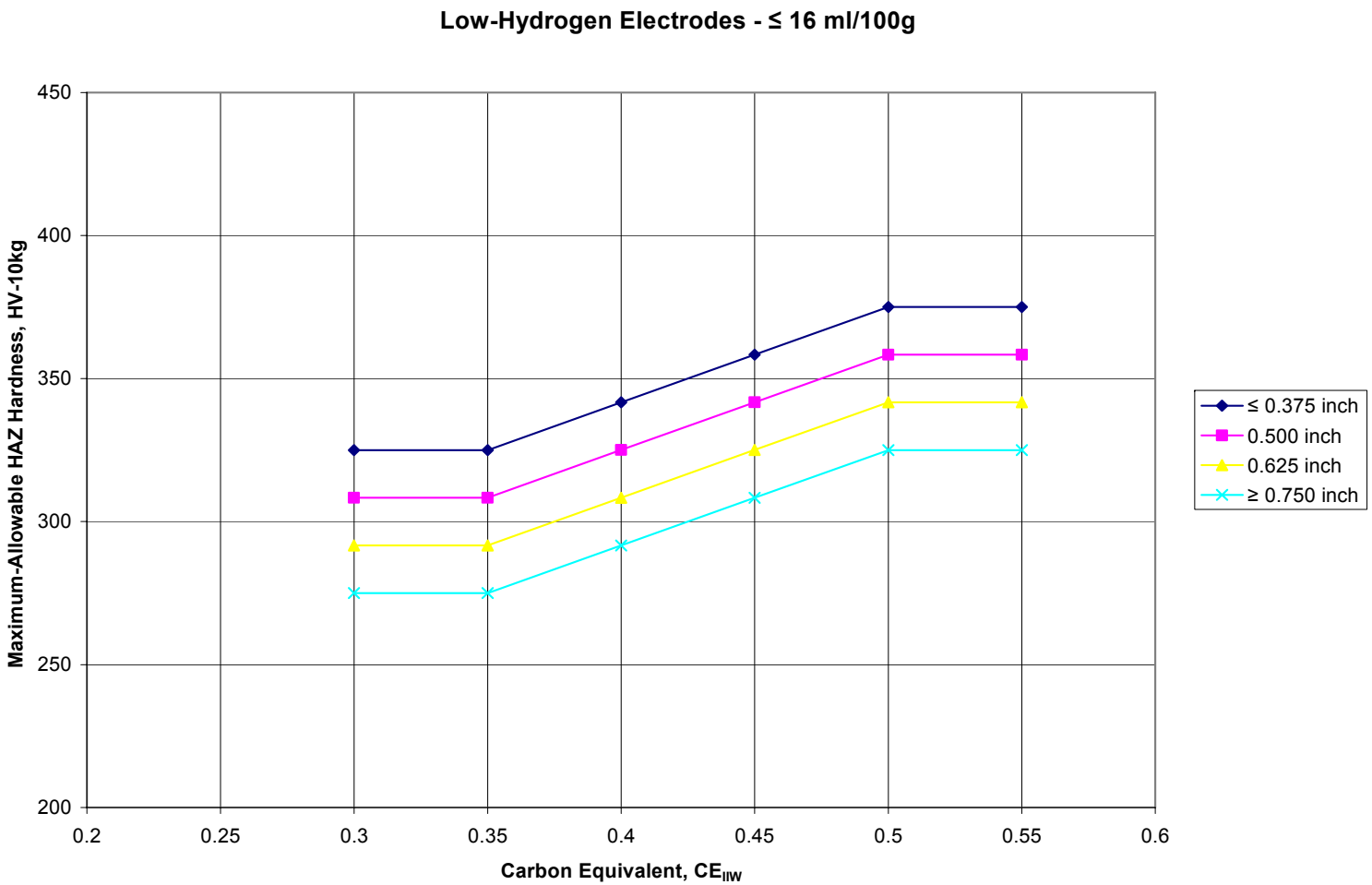

Figure 20. HAZ Hardness Evaluation Criteria for In-Service Weldson Materials with Carbon Contents greater than 0.10% – ≤ 16 ml/100g Hydrogen Level

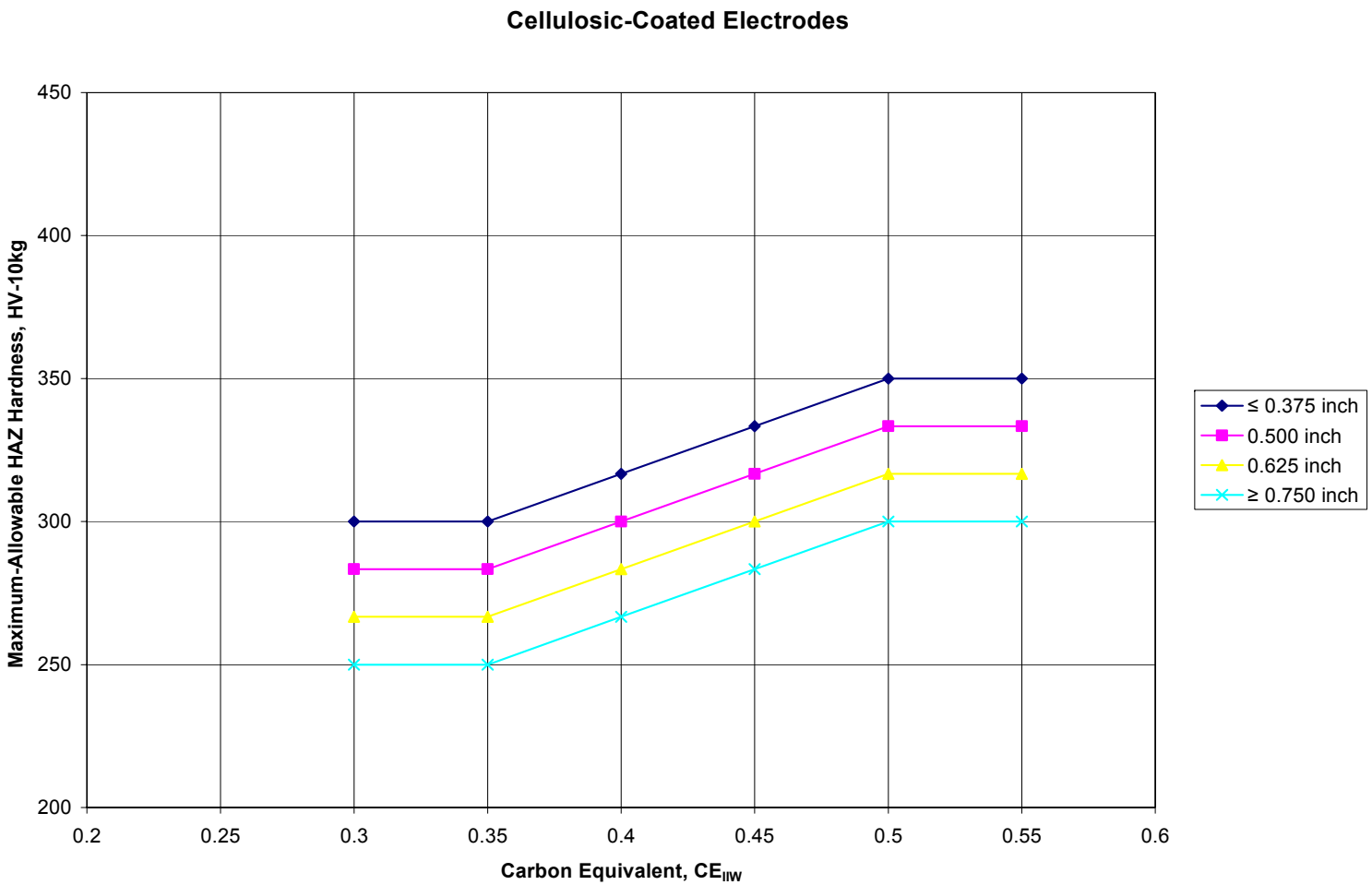

Figure 21. HAZ Hardness Evaluation Criteria for In-Service Welds on Materials with Carbon Contents greater than 0.10% – Cellulosic-Coated Electrodes

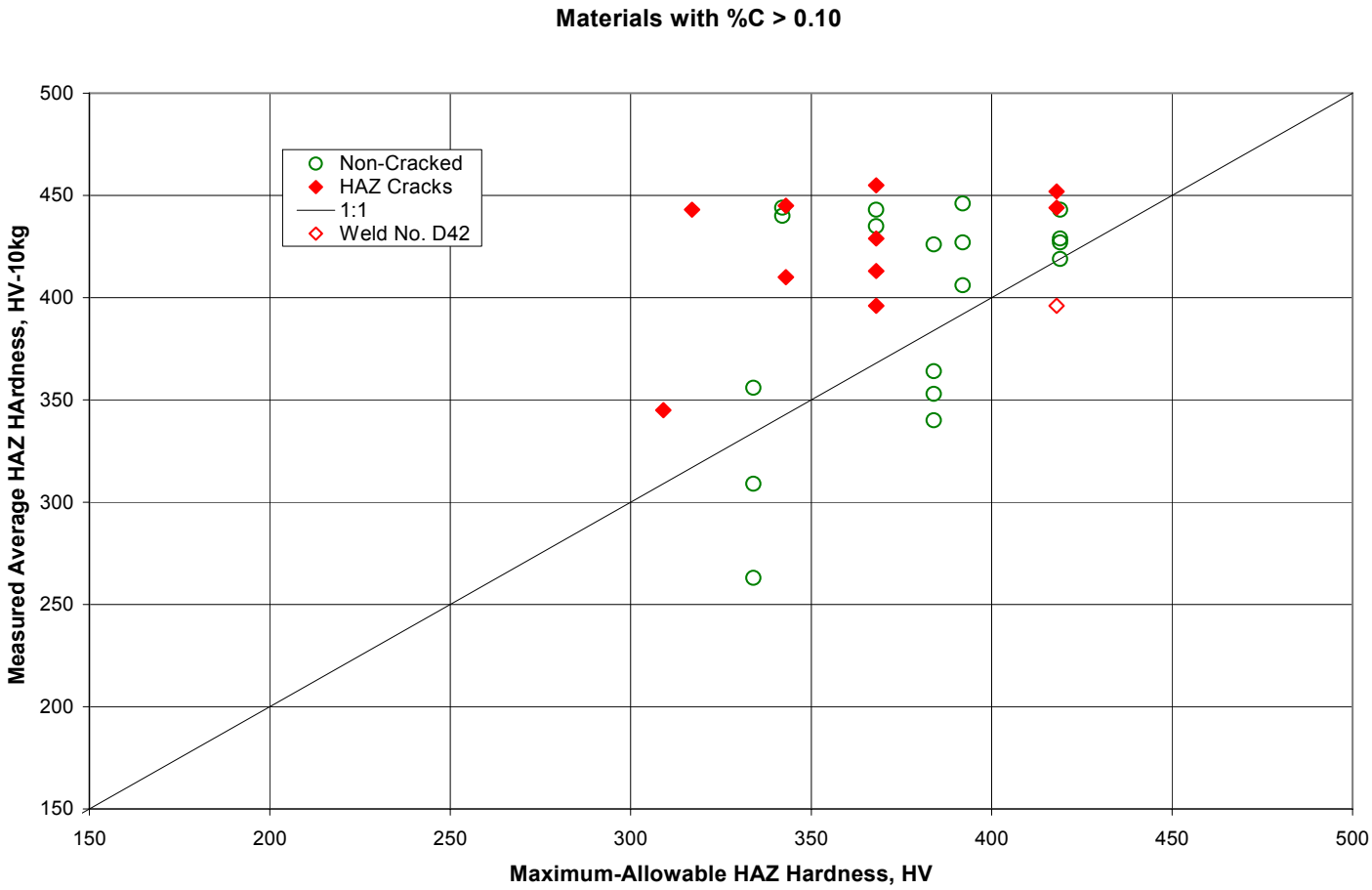

Figure 22. Comparison of HAZ Hardness Testing Results with Hardness Evaluation Criteria shown in Figures 21 through 24 for Materials with Carbon Contents greater than 0.10%.

Figure 23. Columbia Gas Line 1804 with Eventual Hot Tap Location Marked

Figure 24. Completed Confirmation Welds on Line 1804

Figure 25. Hot Tap Branch Welded Over Completed Confirmation Welds

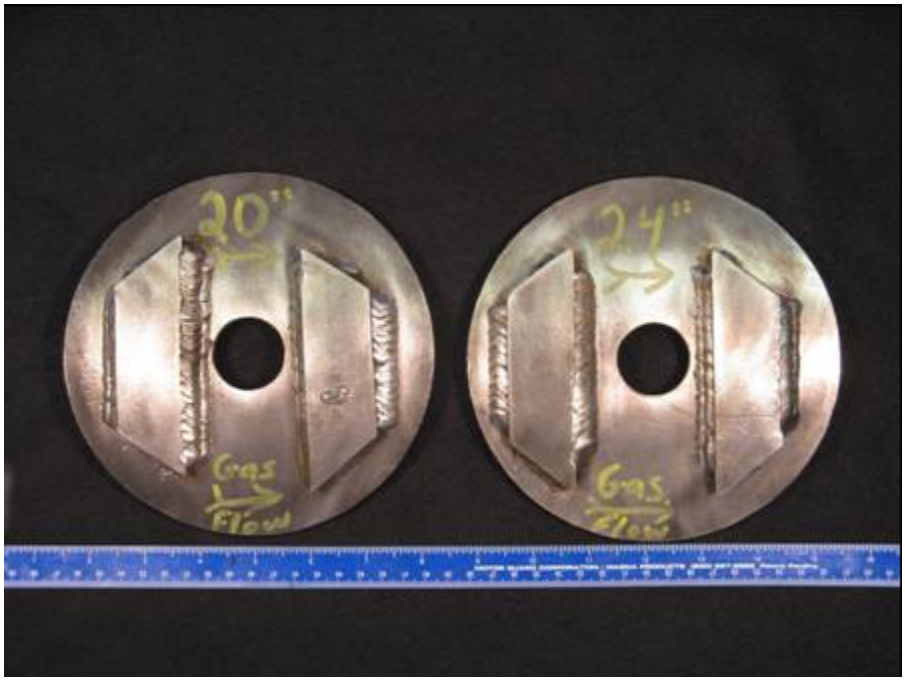

Figure 26. Hot Tap Coupons with Confirmation Welds after Removal

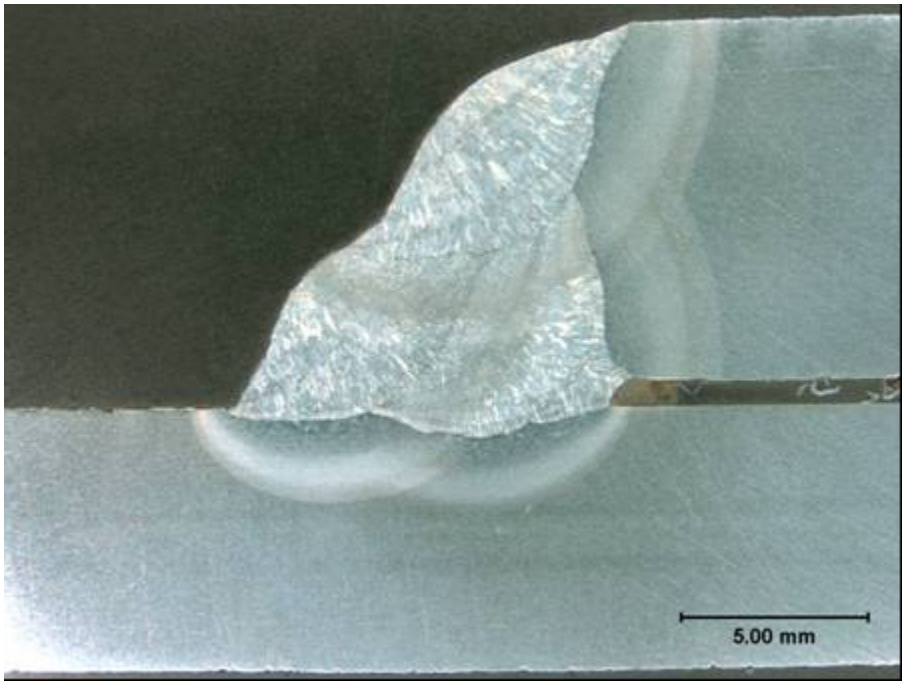

Figure 27. Typical Metallographic Section through Completed Confirmation Welds

Figure 28. E7018-H4R Electrodes in 10-lb (4.5-kg) Hermetically Sealed Can

Appendix A.

Review of Previous Work
Related to the Development of
HAZ Hardness Evaluation Criteria

Review of Previous Work Related to the Development of HAZ Hardness Evaluation Criteria

A1. INTRODUCTION

Heat-affected zone (HAZ) hardness is often used as an indicator of the susceptibility of a microstructure to cracking during the evaluation of procedure qualification welds. A widely used value below which it is generally agreed that hydrogen cracking is not expected to occur is 350 HV. Both API 1104 Appendix B and the Canadian standard CSA Z662 indicate that procedures for in-service welding that produce HAZ hardness greater than 350 HV should be evaluated with regard to the risk of hydrogen cracking. Neither of these codes provides guidance pertaining to how this evaluation should be performed. The Australian standard AS 2885.2 prohibits HAZ hardness greater than 350 HV for in-service welds.

Unfortunately, the hardness level below which hydrogen cracking does not occur is not a fixed value, but varies as a function of hydrogen potential of the welding process, the materials being welded, and the tensile stress levels. For example, closer control of hydrogen level allows higher hardness levels to be tolerated. Also, since the hardness of martensite depends on carbon content, materials with lower carbon content tend to crack at lower hardness levels. Conversely, higher hardness levels can be tolerated when welding materials with higher carbon contents.

The overall objective of a project that is being supported by US Department of Transportation (DOT), Pipeline and Hazardous Materials Safety Administration (PHMSA) is to develop HAZ hardness acceptance criteria that can be used to evaluate welds during the qualification of procedures for welding onto in-service pipelines. In this appendix, previous work related to the development of HAZ hardness evaluation criteria is reviewed. The applicability of previous work related to the development of HAZ hardness evaluation criteria to welds made onto in-service pipelines was assessed and gaps were identified.

A2. BACKGROUND

Welding onto in-service pipelines is frequently required to facilitate a repair or to install a branch connection using the “hot tapping” technique. There are significant economic and environmental incentives for performing pipeline repair and maintenance without removing the pipeline from service. From an economic viewpoint, a shutdown involves revenue loss from the loss of pipeline throughput, in addition to that from the gas lost to the atmosphere. Since methane is a so called “greenhouse gas”, there are also environmental incentives for avoiding the venting of large quantities of gas into the atmosphere.

Welds made in-service cool at an accelerated rate as the result of the ability of the flowing contents to remove heat from the pipe wall. These welds, therefore, are likely to have hard heat-affected zones and a subsequently increased susceptibility to hydrogen cracking.

To prevent hydrogen cracking, at least one of the three conditions necessary for its occurrence must be eliminated or reduced to below a threshold level. Beyond the use of low-hydrogen electrodes to minimize hydrogen levels, it is prudent to develop and use procedures that minimize the formation of crack-susceptible microstructures. However, exactly how crack-susceptible microstructures are defined, and what microstructures and hardness levels will lead to cracking for any given stress level and diffusible hydrogen condition, are matters requiring further investigation.

A3. REVIEW PREVIOUSLY-DEVELOPED CRITERIA

A3.1 History of 350 HV Limit

The generally-regarded notion that 350 HV is a hardness level below which hydrogen cracking is not expected dates back to work by Dearden and O'Neill in the 1940s [1]. This notion was validated by Bailey in the early 1970s for welds with a diffusible hydrogen content of approximately 16 ml/100 g of deposited weld metal [2]. Bailey also noted that for welds with a diffusible hydrogen content of approximately 8 ml/100 g, the critical hardness, or the hardness level below which hydrogen cracking is not expected, is on the order of 400 HV. The 350 HV limit was used in work by Graville and Read in the mid-1970s [3]. This limit was later adopted by Kiefner, et al., during work that resulted in the development of the Battelle thermal analysis computer model for hot tap welding [4]. The Battelle work mentions that this value is especially pertinent to pipelines, as a previous study [5] showed that accidental hard spots (un-tempered martensite) in line pipe will crack during service when exposed to mild hydrogen charging (typical of cathodic protection) if the hardness is in excess of 360 Brinell (equivalent to 380 HV).

A3.2 PRCI-Sponsored work at Edison Welding Institute and APIA-Sponsored work at University of Wollongong

The results of previous work directed specifically at welds made onto in-service pipelines [6-9] indicate that the widely-used limit of 350 HV may be overly conservative for some applications and non-conservative for others. Hardness evaluation criteria were developed that can be used to quantify the trade-offs that can be made between HAZ hardness, hydrogen level, and the chemical composition of the materials being welded for welds made onto in-service pipelines. These criteria were shown to be accurate for predicting the occurrence of cracking for the narrow range of conditions that were investigated [9.5-mm (0.375-inch)-thick materials with a carbon content greater than 0.10%]. The results of this work concluded that, prior to the widespread use of these criteria, further development and validation is required, particularly for modern microalloyed materials and material over a wide range of wall thicknesses.

Recent work at University of Wollongong (UOW) investigated the relationship between heat-affected zone (HAZ) hardness, pipe and fitting material chemical composition, and cooling rate for in-service welding applications. This work has been important in defining the susceptibility of various pipe grades to hardening in the HAZ and to determining the relevance of various hardness predictive methods. Subsequent work at UOW further investigated the relationship between composition, hardness, microstructure, and fracture resistance of the coarse-grained HAZ (CGHAZ) arising from simulated in-service welding procedures.

At Edison Welding Institute (EWI), a series of simulated in-service welding cracking tests have been conducted on pipe steel materials under various simulated in-service conditions using a range of hydrogen levels. UOW developed a small-scale, low-strain rate fracture resistance test in which specific HAZ microstructures were evaluated in terms of mode and level of fracture resistance. The results were cross-referenced with the results from EWI's simulated in-service welding crack tests.

A3.3 HAZ Hardness Limit Work at Edison Welding Institute

The objective of the work undertaken at EWI [9] was to further develop and validate hardness evaluation criteria that can be used to quantify the trade-offs that can be made between HAZ hardness, hydrogen level, and chemical composition for welds made onto in-service pipelines.

A3.3.1 Data from Previous Programs

Critical hardness level is shown as a function of CE_{IIW} level from several previous programs in Figure A1 [10]. The data shown in this figure are for fillet welds made at a hydrogen level of approximately 12 ml/100 g. In previous work at EWI [11], this figure was used as a starting point for the development of a HAZ hardness evaluation criterion for welds made onto in-service pipelines.

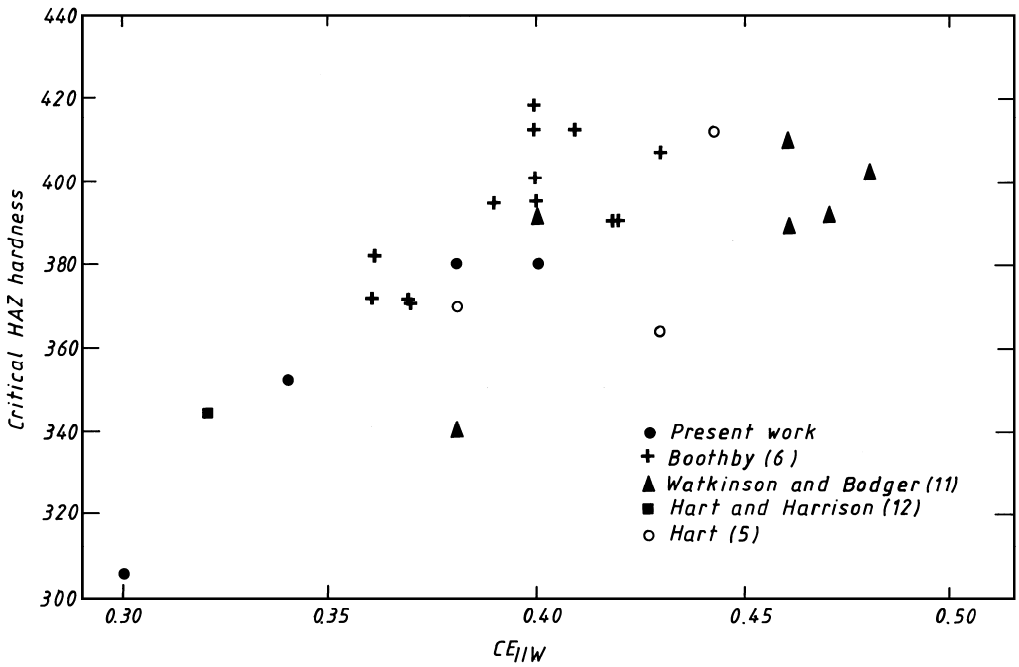

Figure A1. Critical Hardness Level versus CE_{IIW} from previous programs (~12 ml/100 g).

A hardness evaluation criterion for in-service welds that is loosely based on Figure A1 is shown in Figure A2. This figure shows HAZ hardness limits as a function of CE_{IIW} for three different hydrogen levels. For each CE level, the critical hardness level for the 8 ml/100 g hydrogen level is roughly that extrapolated from a lower bound of the data shown in Figure A1 from several previous programs. A 25 HV increase in the critical hardness was allowed for the 4 ml/100 g hydrogen level. A 50 HV decrease was imposed for the welds made using cellulosic-coated electrodes.

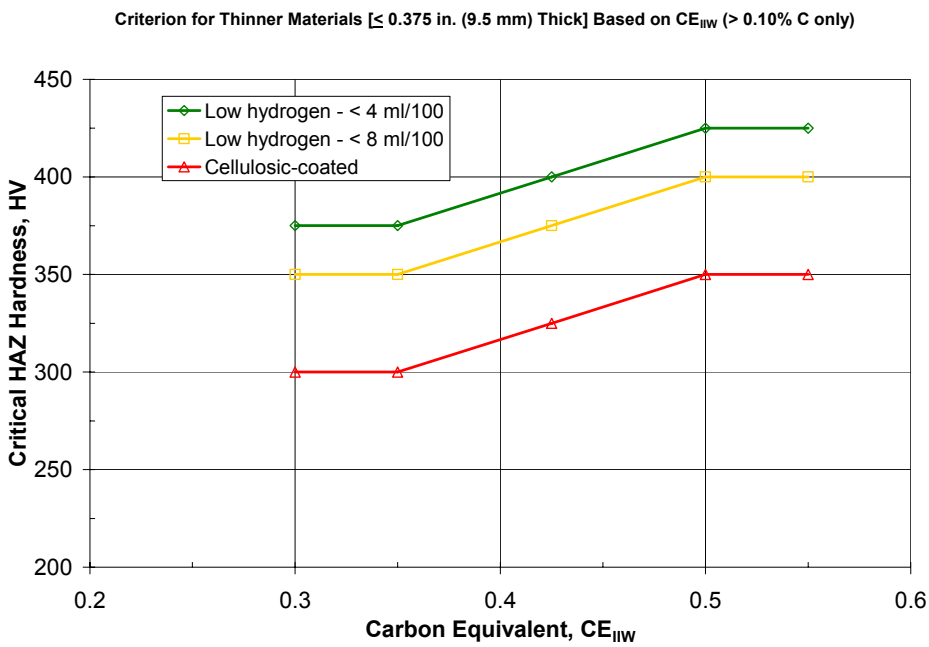

Figure A2. Criterion for thinner materials [≤ 9.5 mm (0.375 inch)] based on CE_{IIW} (> 0.10% C only).

To evaluate this criterion, highly restrained multi-pass fillet welds were made under simulated in-service conditions (Figure A3) on materials with a variety of chemical compositions (Table A1) using a variety of different hydrogen levels, after which they were metallography sectioned to measure hardness at the weld toe and to examine for the presence of cracks. A comparison of the hardness testing results with the evaluation criterion is shown in Figure A4. This figure indicates that the criterion has accurately predicted the occurrence of cracking (i.e., welds that are cracked tend not to meet the criterion).

Table A1. Description of thinner conventional materials from previous program at EWI.

Material	Grade	Thickness mm (inch)	%C	CE_{IIW}	Pcm
N2	ASTM A516-60	9.5 (0.375)	0.14	0.34	0.21
N3	ASTM A516-70	9.5 (0.375)	0.24	0.44	0.31
N4	AISI1035-mod.	9.3 (0.365)	0.38	0.52	0.43

While this criterion has been effective for the conditions investigated [9.5-mm (0.375-inch)-thick materials with a carbon content greater than 0.10%], additional data was required to further validate this criterion and to expand its applicability to a broader range of materials, which is the objective of the recently-completed work at EWI.

Others use or have proposed using HAZ hardness evaluation criteria that are variable depending on the chemical composition of the materials being welded [12]. These criteria may not be suitable for in-service welds, however, as welds made under in-service conditions tend to cool more quickly than other welds. The diffusion rate of hydrogen in steel is strongly influenced by temperature. Hydrogen in welds that are allowed to cool slowly can diffuse away soon after welding. For in-service welds, any hydrogen that enters the weld tends to become trapped there. This is one reason a limit of 350 HV may not be sufficient for in-service welds made using cellulosic-coated (EXX10 type) electrodes.

Figure A3. Highly restrained fillet weld made under simulated in-service conditions.

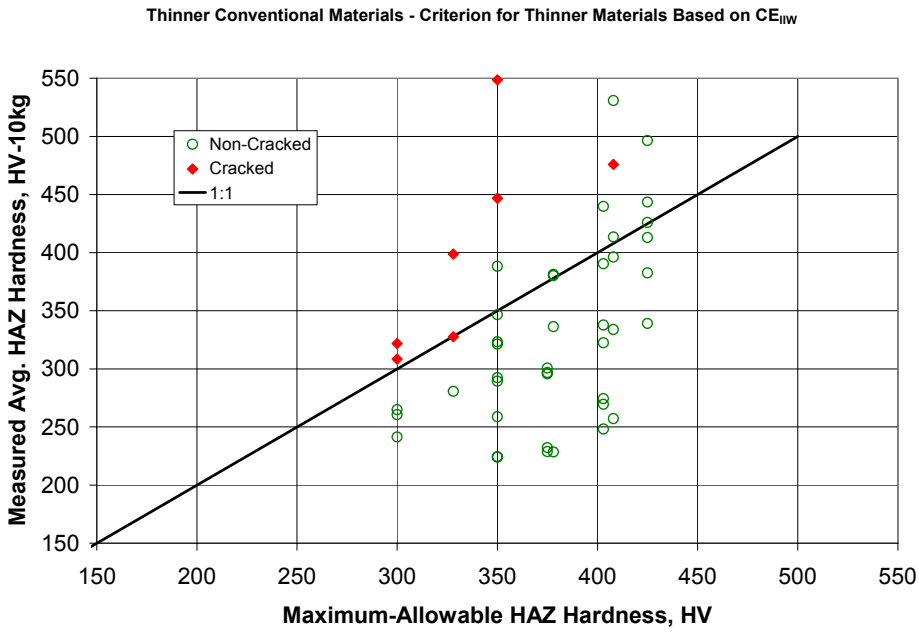

Figure A4. Evaluation of criteria for thinner materials based on CE_{IIW} using data for thinner conventional materials (> 0.10% C).

A3.3.2 Evaluation of Existing Criteria for Wider Range of Conditions

Follow-on work at EWI [9] involved evaluating the criterion shown in Figure A2 for a wider range of conditions using additional data from the previous work at EWI [11]. Five additional materials were included in this phase of the recently-completed work (Table A2).

Table A2. Description of low carbon and thicker conventional materials from previous program at EWI.

Material	Grade	Thickness mm (inch)	%C	CE_{IIW}	Pcm
N1	API 5LX-80 DSAW	9.5 (0.375)	0.068	0.40	0.18
K1	API 5LX-80 DSAW	15.5 (0.610)	0.068	0.40	0.18
K2	ASTM A516-60	19.1 (0.750)	0.11	0.35	0.19
K3	ASTM A516-70	19.1 (0.750)	0.22	0.43	0.29
K4	API 5LX-60 Seamless	15.9 (0.625)	0.24	0.49	0.33

A3.3.2.1 Application for Modern Compositions (<0.10% C)

Data for welds made on Material N1 [9.5-mm (0.375-inch)-thick modern composition with a carbon content less than 0.10%] was used to evaluate the criterion shown in Figure A2. The results indicate that the criterion is non-conservative under some conditions, particularly for welds made at a hydrogen level of 8 ml/100 g. This suggests that a hardness evaluation criteria based on CE_{IIW} may not be appropriate for materials with carbon content of 0.10% and less. It has been suggested that Pcm may be a better carbon equivalent formula on which to base a hardness evaluation criterion, particularly for low carbon steels. CE_{IIW} and Pcm are calculated as:

$$CE_{IIW} = C + Mn/6 + (Cu+Ni)/15 + (Cr+Mo+V)/5 \quad (1)$$

$$Pcm = C + Si/30 + (Mn+Cu+Cr)/20 + Ni/60 + Mo/15 + V/10 + 5B \quad (2)$$

A revised version of the hardness evaluation criterion shown in Figure A2 was developed using Pcm instead of CE_{IIW} (Figure A5). Evaluation of this criterion indicates that Pcm is better for materials with carbon content of 0.10% and less, but that the criterion based on CE_{IIW} works better for conventional steels. It can also be said that the criterion based on Pcm works reasonably well for both types of steels.

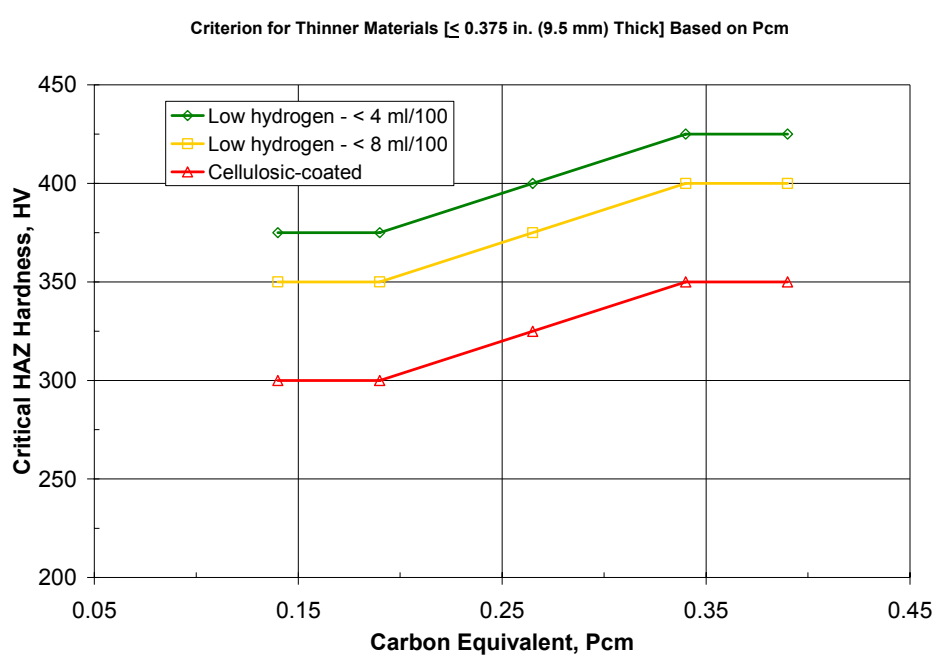

Figure A5. Criterion for thinner materials [≤ 9.5-mm (0.375-inch) thick] based on Pcm.

A3.3.2.2 Application for Thicker Materials

Data for welds made on Materials K2, K3, and K4 [19.1-mm (0.750-inch)-thick conventional steels] was used to evaluate the criterion shown in Figure A2. The results indicate that the criterion is non-conservative under some conditions, indicating the need to further limit HAZ hardness for welds made on thicker materials.

A revised hardness evaluation criterion based on CE_{IIW} was developed for thicker materials by imposing an additional 50 HV reduction (Figure A6). Evaluation of this criterion indicates that imposing an additional 50 HV reduction for thicker materials seems to be appropriate. Application of the hardness evaluation criterion for thicker materials based on CE_{IIW} (Figure A6) to all materials (including those with carbon content less than 0.10%) indicates that, under some condition, the criterion is non-conservative for Material K1 (carbon content less than 0.10%), for which Pcm was found to work better. A revised hardness evaluation criterion based on Pcm was developed for thicker materials by imposing an additional 50 HV reduction (Figure A7). Evaluation of this criterion indicates that imposing an additional 50 HV reduction for thicker materials with carbon content less than 0.10 also seems to be appropriate.

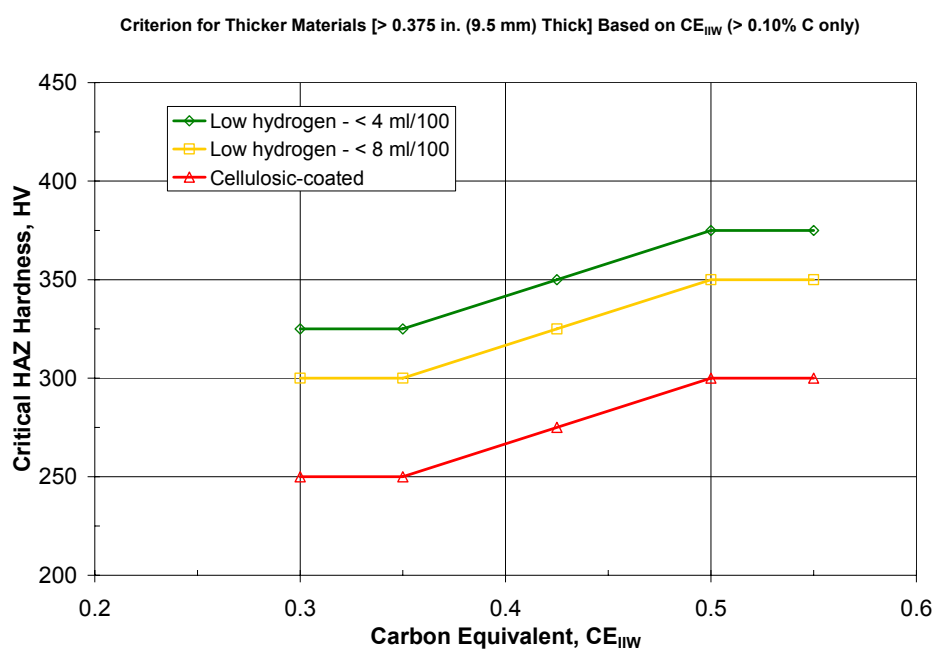

Figure A6. Criterion for thicker materials [> 9.5-mm (0.375-inch) thick] based on CE_{IIW} (> 0.10% C only).

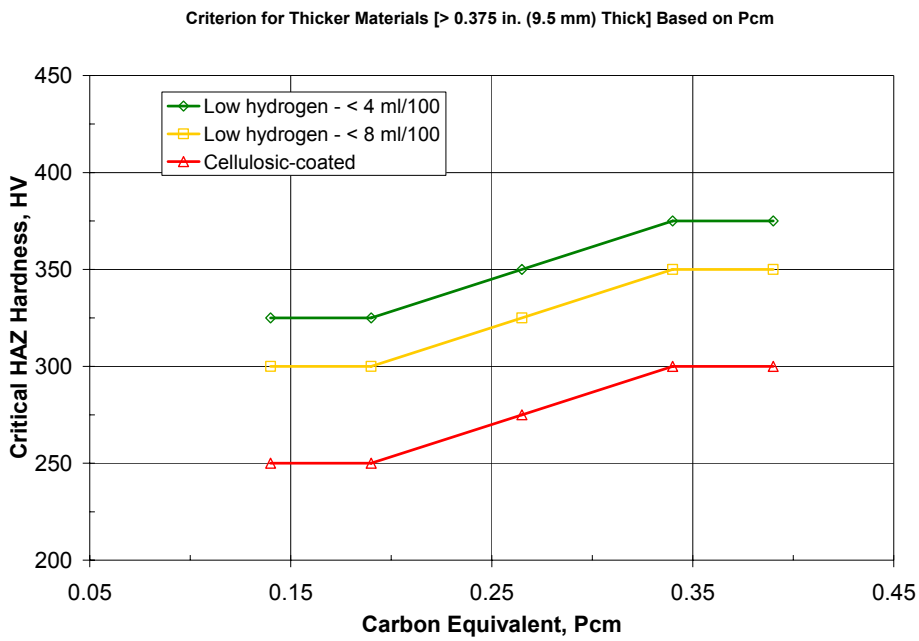

Figure A7. Criterion for thicker materials [> 9.5-mm (0.375-inch) thick] based on Pcm.

For thicker materials [greater than 9.5-mm (0.375-inch) thick], it appears that criterion based on CE_{IIW} works well for conventional steels and Pcm works well for both types of steels, provided that an additional 50 HV reduction is imposed.

A3.3.2.3 Revised Criteria for Wider Range of Conditions

The use of the CE_{IIW} formula is generally considered to be more appropriate for evaluating the weldability of older, conventional types of steel [13], such as those with higher carbon contents (e.g., 0.15-0.30%) that were produced prior to the introduction of thermo-mechanical controlled processing. The use of the Pcm formula treats the effect of carbon as much more significant than that of the remaining alloying elements and is generally considered to be more appropriate for more modern, carbon-reduced or micro-alloyed steels.

Another formula, which was developed by Yurioka et al. [14], as a weldability index for a wide variety of steels, incorporates an interactive term for carbon and alloying elements. The CEN formula approaches the value of CE_{IIW} when applied to higher carbon steels and the value of Pcm when applied to lower carbon steels. CEN is calculated as:

$$CEN = C + A(C) \times [Si/24 + Mn/6 + Cu/15 + Ni/20 + (Cr + Mo + Nb + V)/5 + 5B] \quad (3)$$

$$\text{where } A(C) = 0.75 + 0.25\tanh[20\,(C-0.12)]$$

The development of HAZ hardness evaluation criteria based on the CEN carbon equivalent formula might allow both conventional and low carbon steels to be evaluated together.

The need for an additional 50 HV reduction for thicker materials is based on two factors. The three primary independent conditions that must be satisfied simultaneously in order for hydrogen cracking to occur are (1) hydrogen in the weld, (2) a crack-susceptible weld microstructure, and (3) tensile stresses acting on the weld. As indicated earlier, closer control of hydrogen level allows higher hardness to be tolerated. One of the factors that indirectly affects the amount of hydrogen in the weld is material thickness. After a weld solidifies, it is supersaturated with hydrogen. Hydrogen then diffuses to free surfaces, where it can escape. When the material being welded is thick, diffusion distances are greater, which results in more hydrogen remaining in the weld. Tensile stresses acting on the weld can be either applied or residual. Residual stresses result from the restraint provided by the weld joint and thermal contraction of the weld as it solidifies. Weld joints in thicker materials possess a greater level of restraint, so residual stresses for welds in thicker materials tend to be higher.

A3.3.3 Experimental Validation

The remainder of the work at EWI involved conducting additional experiments to further validate the revised criteria that were developed. Two additional materials were included in this phase of the work (Table A3). Highly restrained multi-pass fillet welds were made under simulated in-service conditions using the apparatus shown in Figure A8.

Table A3. Description of materials from experimental validation.

Material	Grade	Thickness mm (inch)	%C	CE_{IIW}	Pcm
P2	API 5LX-65 DSAW	9.5 (0.375)	0.13	0.40	0.23
P6	API 5LX-52 EFW	7.9 (0.312)	0.32	0.49	0.38

Figure A8. Setup for laboratory experiments.

The results indicate that both criteria for thinner materials (based on CE_{IIW} and Pcm) were fairly accurate, but can be slightly non-conservative for some conditions. The results also indicate that the widely used HAZ hardness limit of 350 HV is very conservative for some applications and non-conservative for others. The use of the criteria that were developed allows the trade-offs that can be made between hardness, hydrogen level, and chemical composition to be quantified.

A3.4. Microstructural Susceptibility Work at UOW

A3.4.1 Background

Recent work conducted at the UOW investigated the relationship between HAZ hardness, pipe and fitting material chemical composition, and cooling rate for in-service welding applications [13,15-17]. This work has been important in defining the susceptibility of various pipe grades to hardening in the HAZ and to determining the relevance of various hardness predictive methods. However, even with greater confidence in predictions of maximum HAZ hardness, there remains a level of uncertainty regarding what hardness levels will result in cracking for a given hydrogen content and stress condition.

The cracking test work at EWI has extended awareness of the crack susceptibility of typical pipe materials during in-service welding, especially in relationship to hardness and common carbon equivalent formulas (as a measure of pipe composition). The weld simulations conducted by EWI are closely representative of the welding conditions experienced by a pipe material during

actual in-service welding. However, these simulations are time consuming and labor intensive and so the number of materials that can be investigated during a short research program is restricted. It was proposed that small-scale fracture testing of simulated CGHAZ specimens might provide a useful augmentation of the weld testing and, further, a method for expanding the range of materials investigated. More specifically, it was suggested that a fundamental study of fracture toughness in CGHAZ would provide valuable insight into the relationship between pipe composition, microstructure, hardness and fracture susceptibility. The opportunity for validation through parallel crack testing on similar materials at EWI was considered to be fortuitous.

In light of this, the work to be described in this section represents an important expansion of our current knowledge regarding the relationship between pipe composition, hardness, microstructure, and fracture behavior arising as a result of in-service welding procedures. However, it should be noted that this was a novel investigation, requiring considerable development in relation to the experimental procedures. The following section will focus on providing a brief theoretical background to small-scale fracture testing, a description of the materials that were investigated and the thermal simulations and fracture test procedures developed, as well as the results.

A3.4.2 Theory of Small-Scale Fracture Testing

In relationship to fracture toughness testing, the requirement for conditions of plane strain and maximum constraint has led to the development of standard test methods that employ a relatively large sample with a wide linear pre-crack, loaded either in uniaxial tension or three point bending modes [18]. In the case of fracture testing of weld HAZs, in particular, specific HAZ regions where the volume of interest may be relatively small, great care and precision is required to locate the pre-crack tip, both in terms of positioning the notch and the actual fatigue crack tip. As a result, the errors associated with fracture testing of CGHAZ microstructures are considerable. This situation can be improved in two ways. First, with reliable data on the yield stress and elastic modulus of the material investigated, it may be possible to reduce the dimensions of the test specimen [19] to the point where it is possible to more reliably position the notch and pre-crack in relation to the region of interest (e.g., CGHAZ). However, there is a lower limit to this reduction in dimension, which is dependent on the requirement for lateral constraint of the material in the vicinity of the crack tip.

Another approach is to manufacture an increased volume of CGHAZ through thermal simulation (e.g., Gleeble) to reduce the error associated with positioning of the fatigue pre-crack tip. It was proposed that combining this simulation method with a reduced scale fracture test will provide a unique way of establishing the fracture toughness of specific CGHAZ microstructures. However, there is a lower limit to the size to which this new method can be applied. As a result of dimensional restrictions arising from material availability, the work aimed to test the validity of the method for small-scale cylindrical specimens down to 5-mm (0.197-inch) diameter. It was also recognized that the microstructures produced by the thermal simulations may have some fundamental differences to actual weld CGHAZ zones, particularly with respect to the overall

prior austenite grain size, which develops without the restriction of adjacent regions in a thermal and grain size gradient in the Gleeble simulations. This effect is likely to result in a conservative over-estimation of hardness and under-estimation of fracture resistance, since an increase in prior austenite grain size will tend to result in higher hardness and lower fracture toughness.

As mentioned above, the current work had a number of dimensional restrictions that mean that standard fracture test methods could not be applied. The pipe wall thickness of available materials and the need to standardize the sample dimensions for uniformity of Gleeble thermal treatments means that the most appropriate sample geometry was a solid cylindrical blank of 6-mm (0.236-inch) diameter. A further 10-mm (0.394-inch) long, central reduced section of 5-mm (0.197-inch) diameter was employed to facilitate more effective thermal control during the thermal cycle. In order to provide a context for the use of the small-scale fracture test methods on such sample geometry, a review of relevant fracture theory is useful.

Where a fracture test specimen retains elastic behavior to fracture, the expression for KI of a notched cylindrical specimen in tension is given by [20,21]:

$$K_I = P/D^{3/2}\,[1.72(D/d)-1.27] \qquad (4)$$

Where P is the load at failure, D is the cylinder outer diameter, and d is the net section diameter. This relationship is valid where $0.5<d/D<0.8$, and the application of this method is restricted to instances where the conditions of plane strain and maximum constraint are met. Shen Wei et al. [22] developed and validated a fracture toughness test method in which a cylindrical specimen with ring-shaped fatigue pre-crack can be used to determine KIc fracture toughness. In relation to the sample size effects and influence on absolute fracture toughness, it was demonstrated that, provided a range of sample diameters were included in the study, conditional validity of the test method down to sample diameters of 10.5 mm (0.413 inch) is possible for a C-Mn steel (0.4%C). Shen Wei et al. [22] also showed that in order for the fracture to be brittle according to the requirements of linear elastic fracture mechanics, then the net section stress, σN, during fracture should be 2.1 times smaller than the uniaxial yielding limit of the material. This condition is met where:

$$D \geq 1.5\,(K_{Ic}/\sigma_{ys})^2 \qquad (5)$$

Where σys is the yield stress, and sample length, L, is at least four times the sample diameter.

Work by Chang [23-25] extended the application of the above test method to samples not meeting the requirement of Equation (5). By applying similarity methods and normalizing against the dimensional parameter, D, Chang proved that it was possible to determine fracture toughness of a material by testing of cylindrical, notched and pre-cracked specimens with diameter down to 20 mm (0.787 inch). Other work has applied the method to fracture toughness evaluation of high-strength pressure vessel steel [26] and rapidly solidified aluminum alloy [27]. More recent work by Ule et al. [28] and Leskovsek et al. [29,30] has extended the application of the method to tool steel specimens of 10-mm (0.394-inch) diameter.

As mentioned above, the most appropriate Gleeble sample geometry is a 6-mm (0.236-inch)-diameter solid cylindrical blank, with a central, 10-mm (0.394-inch)-long reduced section of 5-mm (0.197-inch) diameter. This is considerably less than the 10-mm (0.394-inch) minimum diameter currently being used for steel materials, and below the critical sample dimensions for which previous work has applied. It is recognized that the application of the method to such small samples may prove invalid for absolute measurement of fracture toughness in the strict sense, due to loss of plane strain and maximum constraint requirements, and the fact that it is not possible to produce specimens of larger size from which extrapolations as a function of sample diameter can be derived. Nevertheless, it was proposed that the method can provide a valuable way of testing the comparative resistance to fracture of the simulated CGHAZ microstructures, thereby providing new insight into relationships between composition, hardness, microstructure, and fracture behavior of the CGHAZ in typical in-service welding applications.

A3.4.3 Experimental Procedures

A3.4.3.1 Materials

The materials that were investigated were provided from both Australian and U.S. sources, and represent a broad profile of pipe steel compositions that are commonly subjected to routine in-service welding procedures. The steels range from relatively old high carbon equivalent grades to more modern low carbon, microalloyed grades, with a range of carbon contents from 0.07-0.32%. Table A4 lists the various steels to be investigated, including information on pipe dimensions, grade, composition, and carbon equivalence.

Table A4. Pipe material data, including dimensions, grade, and chemical composition (wt%).

Property	Australian Materials					US Materials		
	A1	A2	A3	A6	A10	P2	P6	P72
OD [mm (inch)]	508 (20)	406 (16)	406 (16)	273 (10.75)	864 (34)	914 (36)	508 (20)	914 (36)
Thick [mm (inch)]	8.6 (0.339)	8.6 (0.339)	7.8 (0.307)	6.6 (0.260)	13.8 (0.543)	9.5 (0.375)	7.9 (0.312)	14.3 (0.562)
Grade	X60	X70	X60	X42	X65	X65	X52	X70
%C	0.17	0.08	0.07	0.24	0.1	0.145	0.32	0.085
%Si	0.25	0.26	0.13	0.05	0.24	0.36	0.01	0.32
%Mn	1.23	1.63	1.35	0.95	1.42	1.41	0.95	1.57
%Cu	0.009	0.001	0.024	0.019	0.021	0.36	0.04	0.007
%Cr	0.026	0.022	0.024	0.02	0.31	0.063	0.03	0.025
%Ni	0.009	0.02	0.02	0.019	0.017	0.033	0.03	0.017
%Mo	0.005	0.005	0.005	0.005	0.005	0.009	0.01	0.001
%V	0.005	0.06	0.005	0.005	0.04	0.002	0.01	0.047
%B	<0.0003	<0.0003	<0.0003	<0.0003	<0.0003	<0.0003	<0.0003	<0.0003
%P	0.008	0.016	0.02	0.009	0.014	0.007	0.016	0.01
%S	0.005	0.005	0.005	0.019	0.005	0.007	0.023	0.001
%Ti	0.005	0.005	0.021	0.005	0.005	0.003	0.01	0.011
%Al	0.021	0.013	0.025	0.005	0.03	0.032	0.01	0.029
%Nb	0.046	0.053	0.04	0.005	0.04	0.031	0.01	0.036
%O	0.0012	0.0007	0.0024	0.0078	0.0019	0.0023	n/a	0.0017
%N	0.0072	0.0018	0.0056	0.0036	0.0077	0.0067	n/a	0.004
CE_{IIW}	0.38	0.37	0.3	0.41	0.41	0.42	0.49	0.36
Pcm	0.25	0.18	0.15	0.29	0.2	0.25	0.37	0.18
CEN	0.39	0.26	0.21	0.41	0.32	0.4	0.49	0.26

A3.4.3.2 HAZ Thermal Cycle Simulation

HAZ thermal cycle simulations were conducted on a Gleeble 1500 thermomechanical test machine. Dimensional requirements arising from both the material availability (pipe wall thickness) and Gleeble test method determined that the sample should be prepared from 6-mm (0.236-inch)-diameter cylindrical specimens, approximately 120-mm (4.72-inch) in length. A 10-mm (0.394-inch)-long reduced section of 5-mm (0.197-inch) diameter was machined in the center of the sample length, to facilitate better thermal control and development of a relatively broad and uniform region of simulated CGHAZ microstructure. A typical thermal cycle profile that was used for all materials is shown in Figure A9. The heating rate was maximized while avoiding overshoot at peak temperature. Residence time at peak T was minimized while allowing temperature to stabilize, and rapid cooling was facilitated by the use of two

high-pressure [600 kPa (87 psi)] argon gas quenching jets, positioned on opposite sides of the sample. The cooling rate was the maximum achievable with the sample and Gleeble configurations, giving a t8/5 cooling time of approximately 3.3 s. This is toward the upper range of cooling rates typical of in-service welding procedures (t8/5 = 2-10 s) [13]. It should also be noted that unlike the previous work by Nolan et al. [13,15-17], the thermal cycle shown in Figure A9 is much more like that associated with actual welding practice, with more rapid heating and exponential cooling. As a result of more realistic dwell times at high austenitizing temperatures, it was expected that such treatments will result in microstructures and hardness levels more similar to actual welds than previously developed in dilatometer studies.

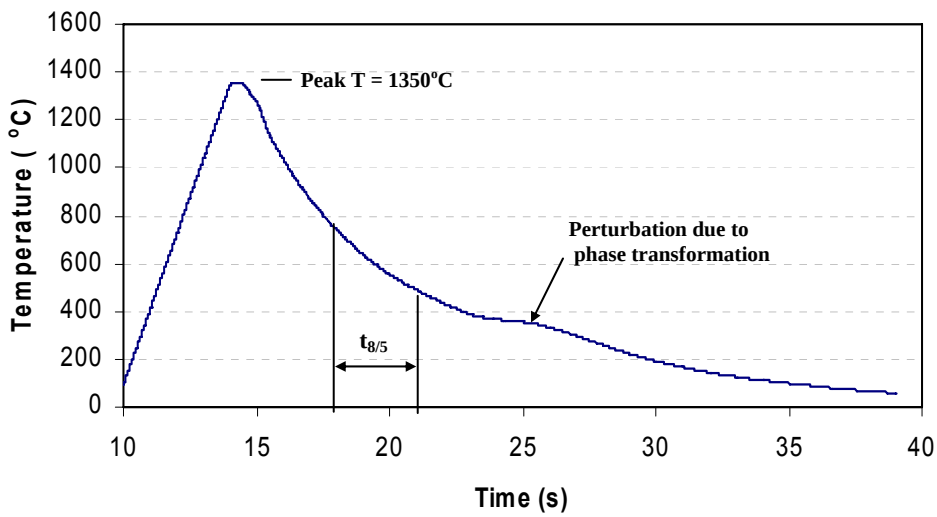

Figure A9. Graph demonstrating a typical Gleeble thermal cycle for CGHAZ simulation.

A3.4.3.3 Fatigue Pre-Cracking and Fracture Testing

Fracture testing requires a ring-shaped fatigue crack be prepared in the cylindrical sample. To facilitate this, a 0.5-mm (0.197-inch)-deep circumferential notch with ~0.05-mm (0.002-inch) root radius and 60-degree included angle was machined in the Gleeble specimen, precisely at the position of the control thermocouple. A rotating three-point bending fatigue pre-cracking method was used to prepare a pre-crack, such that the net section diameter was between 2.5-3.5 mm (0.098-0.138 inch) (thereby satisfying the condition, 0.5<d/D< 0.8).

As the testing used a 6-mm (0.236-inch) blank diameter, and a 5-mm (0.197-inch) test diameter, the sample represents a considerable departure from conventional tensile test specimen designs. Further, the tensile properties of the sample were not uniform, being considerably higher in the central 5-mm (0.197-inch)-diameter section as a result of hardening during thermal cycling.

Fixation of such a small-scale specimen during testing was also experimentally difficult. It was decided that under the circumstances, the best method to ensure fixation would be to produce a long thread at either end of the sample, to which a "head" for the specimen could be affixed. This head could then be clamped into the tensile test machine grips to facilitate transfer of maximum load to the pre-cracked test site. Tensile testing was performed on a 500-kN (56-ton) Instron test machine, and force-displacement data thus obtained.

A3.4.3.4 Hardness, Microstructure, and Fractography

Samples for hardness and metallographic analyses were sectioned both longitudinally and transversely through the volume of simulated CGHAZ to be subjected to fracture testing, mounted in bakelite and polished according to standard metallographic methods for C-Mn steels. Vickers hardness (10 kg) and microstructure profiles were determined in both sections of heat-treated materials to ensure sufficient uniformity of mechanical properties were produced in the volume of material subjected to fracture testing. Digital images were taken on a Nikon optical microscope and scanning electron microscopy of cross sections and fracture surfaces were performed on a JEOL JSM-6500F field emission microscope.

A3.4.4 Results

A3.4.4.1 Microstructure and Hardness

The microstructure and hardness of the simulated CGHAZ microstructures for each of the materials are presented in Figure A10. A1 appears to be composed entirely of martensite, with hardness of 418 HV10. The microstructure of the A2 material is characterized by a mixed structure of predominantly bainitic ferrite and a minor proportion of martensite, with hardness of 303 HV10. The A3 material indicates a mixture of polygonal and bainitic ferrite, with a hardness of only 222 HV10. The A6 material shows a more complex structure. With the high carbon content, it was expected that the structure would be exclusively martensitic. While martensite does represent a major proportion of the phases present, there is also an unexpected dark-etching transformation product apparent at the locations of prior austenite boundaries (indicated by the arrow in Figure A10(d)). On closer examination, this appears to be a pearlitic product. This dual phase effect produces a composite material, with a mean hardness of 384 HV10, but the hardness of the martensitic and pearlitic structural components is 491 HV and 253, respectively (as measured by microhardness testing at an indentation load of 100g).

The A10 material is predominantly martensitic, with some polygonal ferrite apparent at the prior austenite grain boundaries, and a mean hardness of 350HV10. P2 is fully martensitic with a hardness of 446 HV10. P6 has the highest carbon content (0.32%) of all the steels investigated, and so the structure was expected to be fully martensitic. However, a dual phase structure was again evident, similar to that occurring for material A6 (see arrow in Figure A10(g)). The result is a mean hardness of 393 HV10, but microhardness of 572 and 267 for the martensitic and pearlitic constituents, respectively. Material P72 is a low carbon material with a mixed structure of polygonal and bainitic ferrite, and a hardness of only 242 HV10.

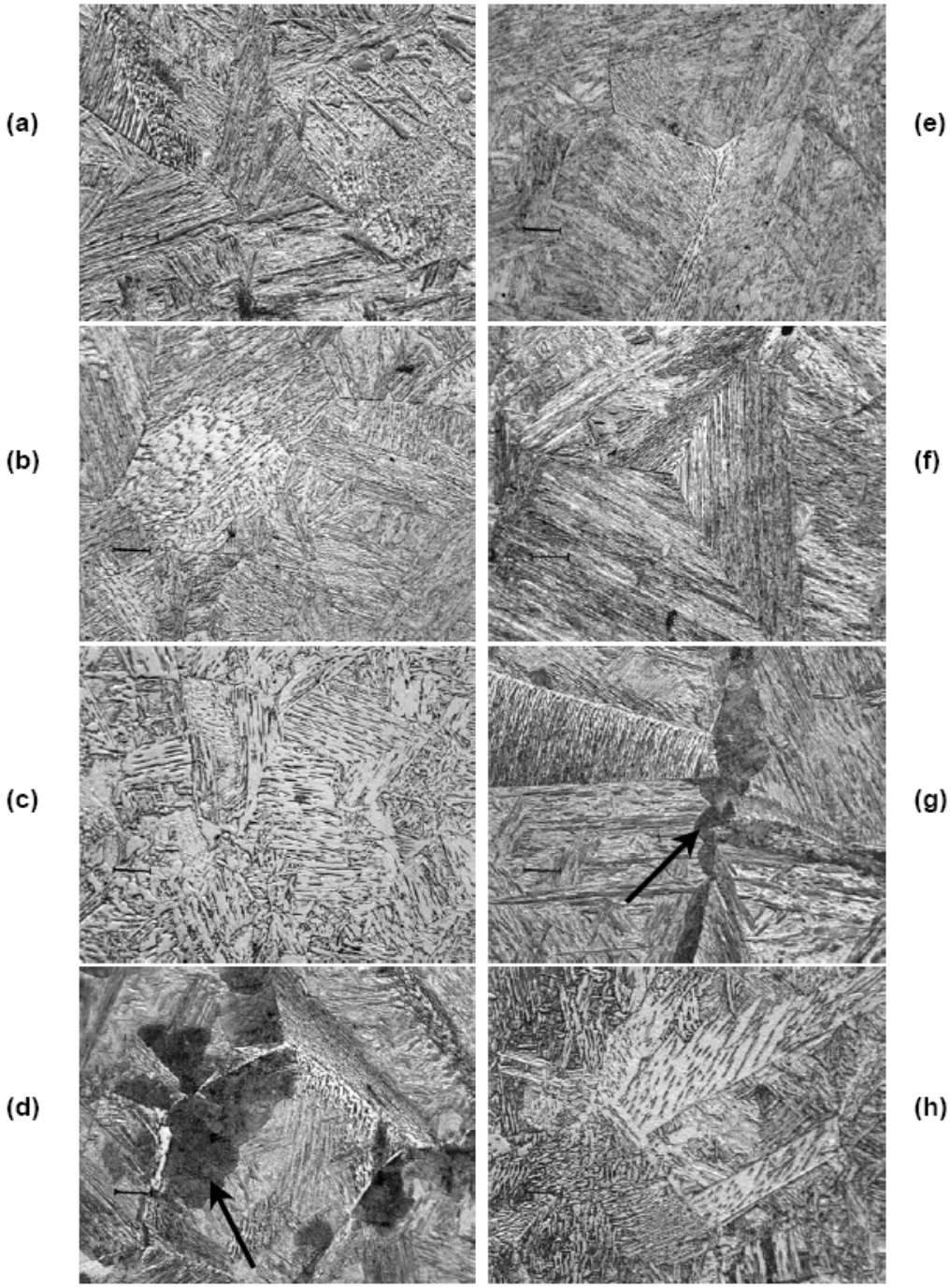

Figure A10. Optical Micrographs showing typical simulated CGHAZ microstructures for the 8 different steels. (a) Material A1, 418 HV10, (b) Material A2, 303 HV10, (c) Material A3, 222 HV10, (d) Material A6, 384 HV10, (e) Material A10, 350 HV10, (f) Material P2, 446 HV10, (g) Material P6, 393 HV10 and (h) Material P72, 242 HV10. Micron bar represents 15 um.

A3.4.4.2 Fracture Testing

Fracture testing of Gleeble heat-treated specimens was difficult on a number of levels. Firstly, minor misalignment of the samples associated with the high temperature thermal cycling created variability in the material's response to the fatigue pre-cracking procedure. At times, this resulted in unpredictable eccentricity of the net section for some samples. Theoretically, this eccentricity could influence the axiality of the test procedure, and therefore the existence of the plane strain condition as a result of uneven distribution of stresses around the ring-shaped pre-crack. Further, many samples failed prematurely during tensile testing by yielding of the relatively low strength base material in the region of the thread that fixed the sample to the sample "head", and thence to the Instron grips. This was particularly problematic in the case of lower carbon equivalent steels, where the strength of the heat-treated microstructure was much greater that of the base material. Despite these experimental difficulties, the method was successfully applied to at least three samples of each material, providing an indication of reproducibility of test results.

The force displacement curves for the different materials tested in the pre-cracked condition showed two distinct types of behavior relating to the extent of plastic deformation prior to failure. This behavior could be simply correlated to the carbon content of the steel and the hardness of the CGHAZ. Figure A11 shows typical force-displacement curves for materials A1, A3 and P72, all with carbon contents <0.09% and CGHAZ hardness levels <310 HV10. These materials show significant plastic deformation at the crack tip, followed by work hardening and finally fracture. Such extensive plastic behavior means that it is not possible to apply the KI calculations to these materials. It is suffice to say that for these materials, the low alloy content results in low hardness and high toughness in the CGHAZ, and so these materials are not expected to be susceptible to HACC, even at high diffusible hydrogen contents (e.g., associated with cellulosic-coated consumables).

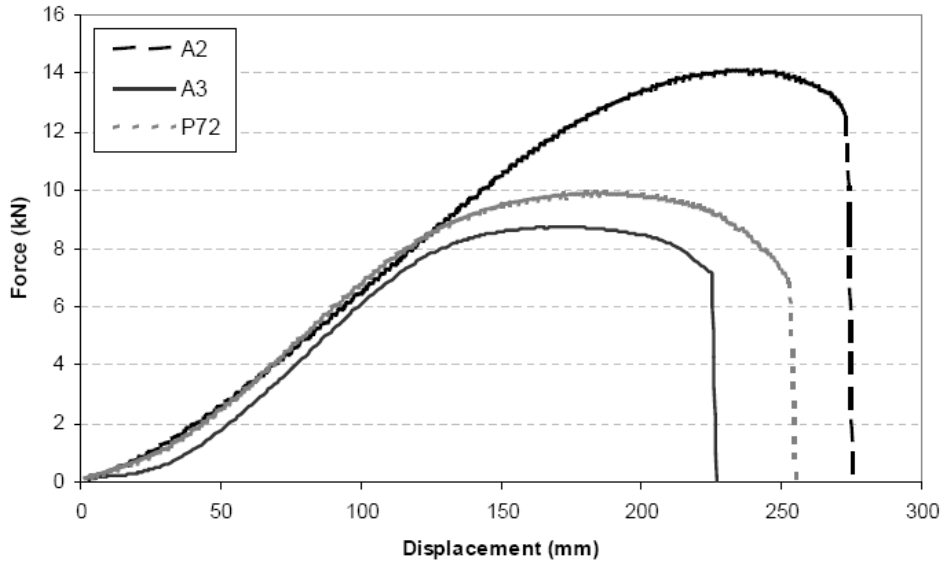

Figure A11. Force-displacement curves for materials A2, A3 and P72, with carbon contents <0.09%.

For the second group of materials with carbon >0.09% and mean hardness > 340 HV10, tensile behavior in the pre-cracked condition was essentially elastic to fracture. The minor departures from linearity observed in the typical load-displacement curves shown in Figure A12 are expected, initially due to slippage and load accommodation in the non-standard sample grips, and later due to unavoidable minor geometric eccentricities in the circumferential fatigue pre-cracks. Since the conditions for 0.5<d/D<0.8 were met for at least three specimens for each material, values for KI were then calculated according to Equation (4) above.

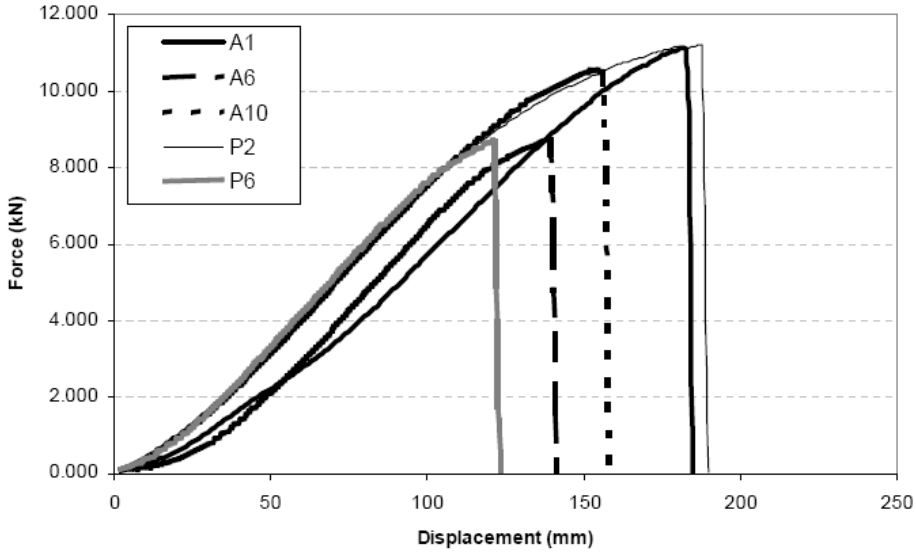

Figure A12. Force-displacement curves for A1, A6, A10, P2 and P6, with carbon contents >0.09%.

In relation to fractography of fracture surfaces, the results illustrate behavior consistent with the microstructures observed, and the tensile testing and hardness data obtained. Fracture mode varies from predominantly ductile in the lower carbon materials (<0.09%C), to a mixture of predominantly brittle cleavage with regions of microvoid coalescence in the intermediate-level carbon material (0.09%<C<0.2%C), to a predominantly brittle cleavage mode in the high carbon materials (>0.2%C), as illustrated in Figure A13.

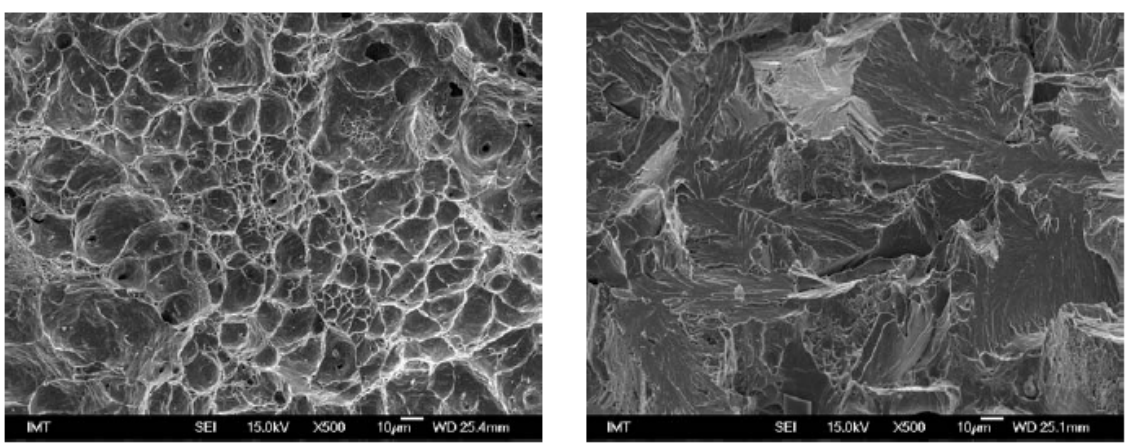

(a) (b)

Figure A13. Fractography of materials (a) A2 and (b) P6 showing progression from ductile microvoid coalescence to brittle cleavage fracture with an increase in carbon content from 0.07% to 0.32%.

A3.4.5 Discussion

Where materials show elastic behavior to failure, it is possible to calculate fracture toughness, KIc, according to the relationship given in Equation (4) above. However, it must be noted that as a result of the small specimen size and errors associated with the non-standard testing procedures, the results obtained in this work are considered to be qualitative only and not indicative of true fracture toughness. Despite this, it is considered that the results are still useful as comparative analysis of fracture resistance in weld HAZ regions, as a function of compositional and microstructural differences. Figure A14 presents a graphical correlation of fracture toughness and compositional parameters, including carbon content and the three common hardenability measures, CE_{IIW}, Pcm and CEN. It can be seen that for these materials, there is a sharp transition from higher to lower fracture toughness at a carbon content of ~0.2%, corresponding to carbon equivalent values of approximately 0.26 Pcm and 0.41 CEN (in that order of reliability). The correlation for the CE_{IIW} carbon equivalent is not as reliable, with some overlap of data points indicating both high and low fracture toughness in the range 0.40-0.42 CE_{IIW}. From this analysis, it is considered that carbon content is perhaps the most robust indicator of fracture toughness in the CGHAZ of weld zones in the C-Mn pipeline steels investigated. Interestingly, while the Pcm measure is typically considered to be most useful for prediction of hardenability in low carbon steels (<0.11%C), it appears to provide the most accurate correlation with fracture toughness of the three formulas considered.

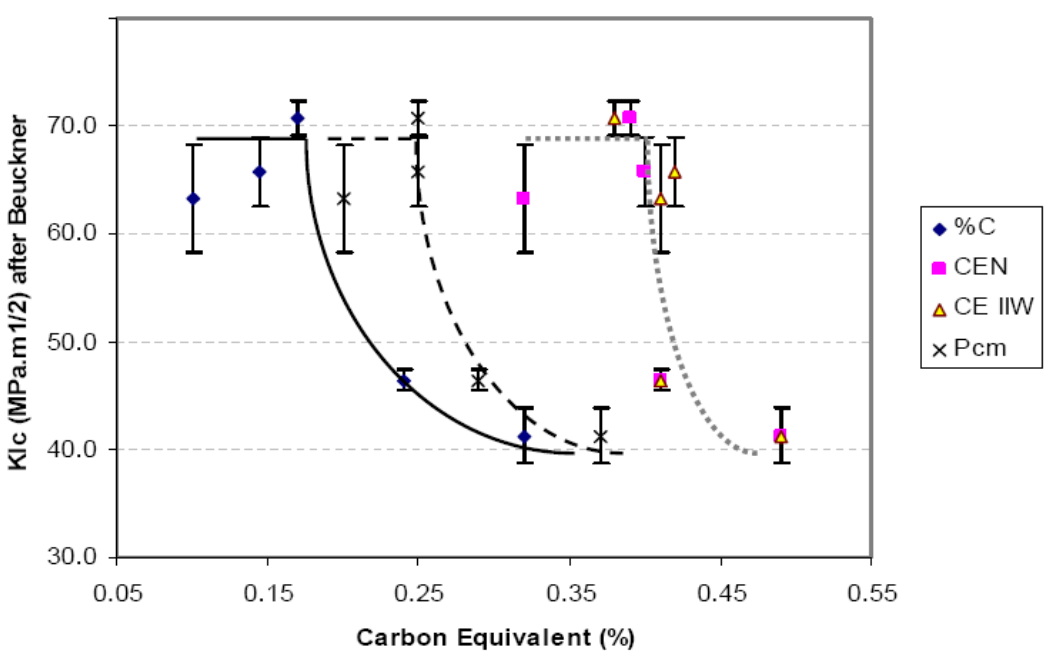

Figure A14. Graph showing the relationship between fracture toughness and composition (%C and carbon equivalent).

From an applied perspective, there are great potential benefits that can arise from this work. A better appreciation of the relationship between composition, microstructure, hardness and fracture resistance can lead to more economical weld procedures by removal of unnecessary conservatism. It was previously suggested that relaxation of the widely-used hardness limit of 350 HV may be feasible for some materials, resulting in an increased use of in-service welding and the realization of significant economic and environmental benefits. However, it was also noted that for other applications (e.g., welds made on low carbon materials at high hydrogen levels), it may be prudent to further restrict allowable hardness levels to reduce the risk of cracking. This would result in increased safety and reliability of completed welds. In any case, there is a level of uncertainty remaining in the welding community about how we define the critical hardness level for cracking as a function of pipe composition, welding parameters and diffusible hydrogen content. For example, it has been suggested [27] that the volume fraction of martensite in the HAZ may be a better indicator of cracking susceptibility than HAZ hardness, and while the results of this work lend some support to this idea, there are still many unknowns, such as standardization of methods to quantify martensite content in steels of varying carbon content, and subjected to various thermal cycles. For example, while previous work [8] has succeeded in confirming the validity of current hardness evaluation criteria, it is clear that a better appreciation of the relationship between composition, microstructure, and hardness is necessary before any significant changes to industrial practices are recommended.

This work has made a significant contribution to the body of knowledge in this field, confirming that the relationship between carbon content, martensite, and hardness has an important influence on fracture resistance in the CGHAZ. It would appear that, all else being equal, fracture resistance is most closely related to carbon content. In general, steels with <0.09%C have a very high resistance to brittle fracture in the CGHAZ, steels with between 0.09-0.2%C have a moderate resistance to brittle fracture, and steels with >0.2%C are likely to be highly susceptible to brittle fracture propagation.

From an experimental perspective, the work was successful in developing the heat-treatment cycles and the methods for fatigue precracking and tensile testing of small-scale cylindrical fracture specimens with a test diameter of only 5mm. This enables the testing of pipe steels with wall thickness of down to 6mm. While the method may not be reliable enough for quantification of absolute fracture toughness (as measured by KIc), it has been shown to offer great potential as a cost effective method for comparing the fracture resistance of specific HAZ microstructures.

Further work is required to investigate the effect of diffusible hydrogen on fracture toughness and mode of failure [31].

A3.5 Work at ConocoPhillips

In the early 1990s, Conoco (now ConocoPhillips) developed and adopted the use of a sliding scale for HAZ hardness limits during qualification of procedures [12]. This was the result of recognizing that steels with lower carbon equivalent levels tend to crack at lower hardness levels. The scale considers chemical composition of the steel only. Hydrogen level of the welding process being used is not considered. The scale restricts HAZ hardness to less than 350 HV when carbon equivalent levels are low. The development of the scale was based on the same experimental data that were generated at TWI [10] and used by EWI in the development of a hardness evaluation criterion for in-service welds. The scale used by ConocoPhillips is based on the Pcm formula since the weldability of steels with low carbon contents tends to be better predicted using this formula. An equivalent scale that uses the CE_{IIW} formula was developed as well, however. These two scales are shown in Figures A15 and A16.

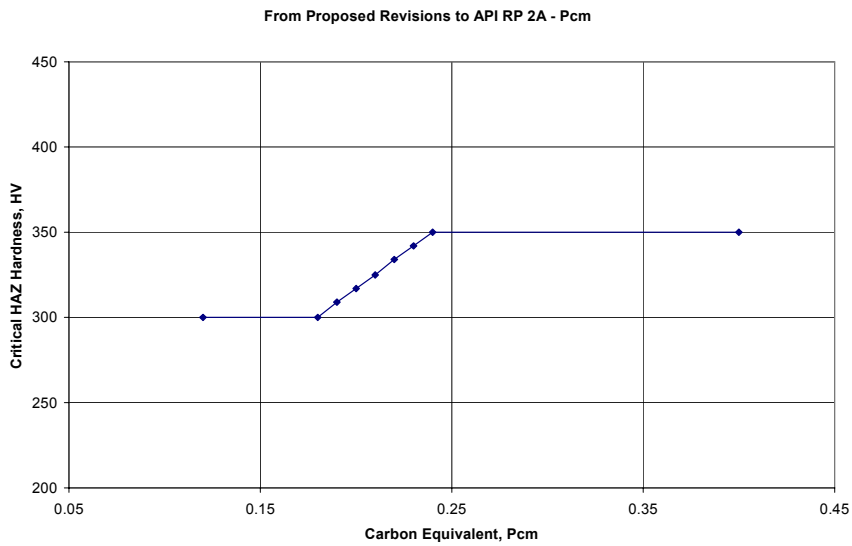

Figure A15. Criteria from proposed revisions to API RP 2A – Pcm.

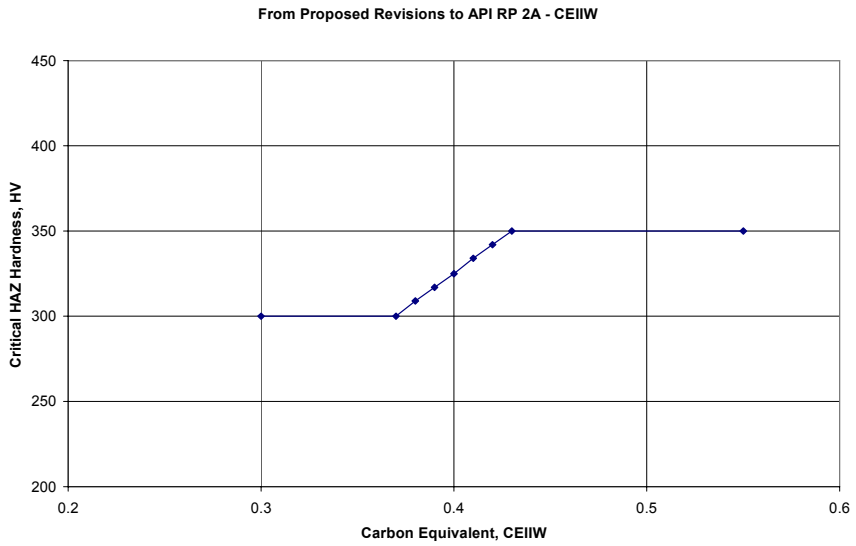

Figure A16. Criteria from proposed revisions to API RP 2A – CE_{IIW}.

There was some effort expended to later incorporate the Conoco sliding scale into API RP 2A – Recommended Practice for Planning, Designing and Constructing Fixed Offshore Platforms. There is also evidence that there was a movement to incorporate a slightly more conservative version of the Conoco sliding scale (Figure A17) into ISO DIS 19902 – Fixed Steel Structures. Neither of these documents currently contain a sliding scale for HAZ hardness limits during qualification of procedures.

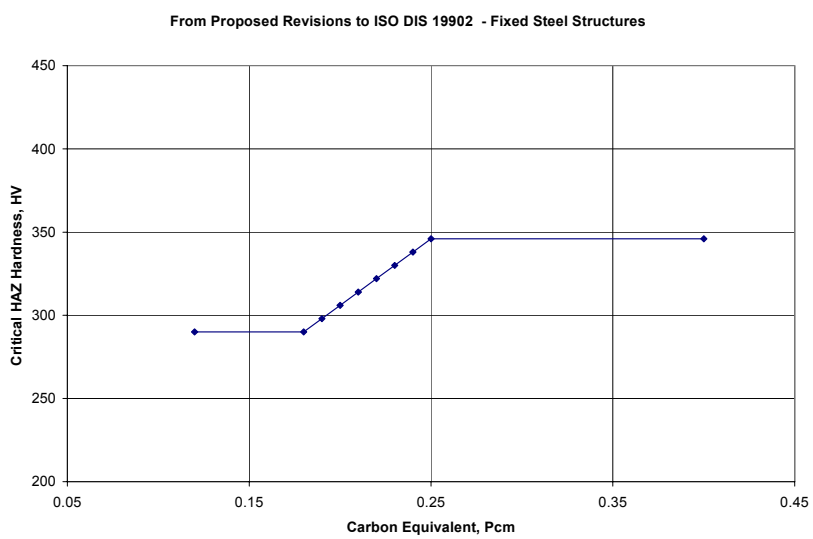

Figure A17. Criteria from proposed revisions to ISO DIS 19902 – fixed steel structures.

A4. GAP ANALYSIS

The aim of the PRCI and APIA-sponsored work at EWI and UOW was to contribute toward a more complete understanding of the relationship between maximum HAZ hardness, diffusible hydrogen content, and cracking behavior for in-service welding applications. Relaxation of the widely used hardness limit of 350 HV may be feasible for some materials, resulting in an increased use of in-service welding and the realization of significant economic and environmental benefits. However, for other applications (e.g., welds made on low carbon materials at high hydrogen levels), it may be prudent to further restrict allowable hardness levels to reduce the risk of cracking. This would result in increased safety and reliability of completed welds. In any case, the work is contributing to a greater level of confidence in our definition of critical hardness level for cracking as a function of pipe composition, welding parameters and diffusible hydrogen content.

The work at EWI has succeeded in confirming the validity of the hardness evaluation criteria investigated. However, the work has also identified several issues that remain to be addressed and opportunities for additional work in this area. One of these is the suitability of high HAZ hardness from an environmental cracking perspective. A previous study showed that accidental hard spots in line pipe will crack in service when exposed to mild hydrogen charging (typical of cathodic protection) if the hardness is in excess of 360 Brinell (equivalent to 380 HV) [5]. The current fracture test methodology under development at UOW would be a valuable tool for studying such hydrogen embrittlement phenomena. Other opportunities for further work include the development of HAZ hardness evaluation criteria based on the CEN carbon equivalent formula, which might allow for both conventional and low carbon steels to be evaluated together, and the development of criteria for intermediate thicknesses (i.e., a sliding scale for thickness as opposed to a stepwise increase from thinner to thicker materials). Previous work at UOW has shown CEN can be used effectively as a basis for hardness prediction across a range of pipe compositions, and so its application to hardness evaluation criteria would seem to be appropriate. As indicated earlier, volume fraction of martensite in the HAZ may be a better indicator of cracking susceptibility than HAZ hardness. The work at UOW has shown such a study would need to properly account for the hardness and composition of the martensite, as well as the fracture behavior expected for a given microstructure. However, it is anticipated that HAZ hardness testing will remain a useful tool for procedure qualification, as it is much easier to perform than determining the volume fraction of martensite, particularly in a procedure qualification setting.

The work to date at UOW has been successful in developing the heat-treatment cycles and the methods for fatigue pre-cracking and tensile testing of small-scale cylindrical fracture specimens with a test diameter of only 5 mm (0.197 inch). This enables the testing of pipe steels with wall thickness of down to 6 mm (0.236 inch). Early indications are that, on this scale, the method may not be reliable enough for quantification of absolute fracture toughness (as measured by KIc). However, it has been shown to offer great potential as a cost-effective method for

comparing the fracture resistance of specific HAZ microstructures. In the case of CGHAZ microstructures arising from in-service welding applications, it is anticipated that the results will contribute to a significant expansion of our understanding of the relationships between pipe composition, hardness, microstructure, and fracture behavior. Further work is required to investigate the effect of diffusible hydrogen on fracture toughness and mode of failure.

A5. SUMMARY AND CONCLUSIONS

The applicability of previous work related to the development of HAZ hardness evaluation criteria to welds made onto in-service pipelines was assessed and gaps were identified. The work has shown that a sliding scale for HAZ hardness limits during qualification of procedure is an effective and efficient way of insuring that qualified procedures are resistant to hydrogen cracking over a wide range of conditions. Small-scale fracture testing of simulated CGHAZ specimens provides a useful augmentation of full-scale weldability testing and provides a method for expanding the range of materials investigated, although further work is required to investigate the effect of diffusible hydrogen on fracture toughness and mode of failure. The gaps that were identified include applicability of previously-developed criteria to modern microalloyed materials and material over a wide range of wall thicknesses.

A6. REFERENCES

[1]. Dearden, J. and O'Neill, H., "A Guide to the Selection and Welding of Low Alloy Structural Steels," Institute of Welding Transactions, Vol. 3, October 1940.

[2]. Bailey, N., "Welding Procedures for Alloy Steels," The Welding Institute, Abington Hall, Cambridge, July 1970.

[3]. Graville, B. A. and Read, J. A., "Optimization of Fillet Weld Sizes," Welding Research Supplement, Welding Journal, April 1974.

[4]. Kiefner, J. F., Fischer, R. D., and Mishler, H. W., "Development of Guidelines for Repair and Hot Tap Welding on Pressurized Pipelines," Final Report, Phase 1, to Repair and Hot Tap Welding Group, Battelle Columbus Division, Columbus, OH, September 1981.

[5]. Groeneveld, T. P., "Hydrogen Stress Cracking," 5th Symposium on Line Pipe Research, American Gas Association, Catalog No. L30174, November 1974.

[6]. Bruce, W. A., "Qualification of Procedures for Welding Onto In-Service Pipelines," International Pipeline Conference – IPC 2002 (Calgary), 2002.

[7]. Bruce, W. A., Nolan, D., and Dunne, D., "Weldability Issues for In-Service Pipeline Welding," International Conference on Pipeline Repairs and In-Service Welding (Wollongong, Australia), Welding Technology Institute of Australia, 2003.

[8]. Bruce, W. A., Nolan, D., Sterjovski, Z., and Dunne, D., "Effect of Steel Composition and Cooling Rate on Microstructure and Hardness of the HAZ for In-Service Welding of Pipelines," International Pipeline Integrity and Repairs Conference (Sydney), Welding Technology Institute of Australia, 2004.

[9]. W. A. Bruce, and M. A. Boring, "Realistic Hardness Limits for In-Service Welding," Draft Final Report to PRCI for Contract No. GRI-8758, Edison Welding Institute, Columbus, OH, January 2005.

[10]. S. Matharu and P.H.M. Hart, "Heat Affected Zone (HAZ) Hydrogen Cracking Behavior of Low Carbon Equivalent C-Mn Structural Steels," The Welding Institute, Report No. 29/1985, Abington Hall, Cambridge, November 1985.

[11]. W. A. Bruce, "Qualification and Selection of Procedures for Welding onto In-Service Pipelines and Piping Systems," Final Report to a Group of Sponsors, Edison Welding Institute, Columbus, OH, January 1996.

[12]. J. Kiefer, Private Communication, ConocoPhillips, July 2004.

[13]. Z. Sterjovski and D. Nolan, "Material Composition Effects in Relation to In-Service Welding of Gas Pipelines," CRC Project 2002-320 Final Report, University of Wollongong, Wollongong, Australia, December 2004.

A6. REFERENCES (continued)

[14]. N. Yurioka, H. Suzuki, and S. Ohshita, Welding Research Supplement, Welding Journal, Vol. 62, No. 6, 1983.

[15]. D. Nolan and Z. Sterjovski, "Prediction of Heat-Affected Zone Hardness during Welding of In-Service Pipelines", International Pipeline Integrity Conference, Sydney, March 2005.

[16]. Z. Sterjovski, D. Nolan, D. Dunne and J. Norrish, "Predicting the HAZ Hardness of Pipeline and Tap Fitting Steels with Artificial Neural Networks", 4th International Conference on Pipeline Technology, Ostend, Belgium, May 2004.

[17]. D. Nolan, Z. Sterjovski, P.Grace and W. Bruce, "Effect of Steel Composition on Microstructure and Hardness of the Heat-Affected Zone for In-Service Welding of Pipelines", International Pipeline Integrity and Repairs Conference, Sydney, March 2004, Paper 11.

[18]. ASTM E399-90. Standard test method for plane strain fracture toughness of metallic materials.

[19]. M. Janssen, J. Zuidema and R. Wanhill, Fracture Mechanics, Delft University press, The Netherlands, 2002, p. 111.

[20]. P.G. Parish and G.C Sih, Stress analysis of cracks. ASTM-STP 318, 1965, p. 30.

[21]. H.F. Beuckner, Discussion of stress analysis of cracks. ASTM-STP 318, 1965, p. 82.

[22]. S. Wei, Z. Tingshi, G. Daxing, L. Dunkang, L. Poliang and Q. Xiaoyun, "Fracture Toughness Measurement by Cylindrical Specimen with Ring-Shaped Crack", Engineering Fracture Mechanics, Vol. 16, No. 1, 1982, pp. 69-82.

[23]. W. Chang, "Measurement of Fracture Toughness KIc by Single Small-Scale Cylindrical Specimen with Ring-Shaped Crack", Engineering Fracture Mechanics, Vol.28, No.3, 1987, pp. 241-250.

[24]. W. Chang, "Applying Similarity Methods to Fracture Mechanics - Measurement of Fracture Toughness KIc, KQ Values by Small-Scale Single Specimen", Engineering Fracture Mechanics, Vol. 31, No. 5, 1988, pp. 807-816.

[25]. W. Chang, "An Improvement of Applying Similarity Methods to Fracture Mechanics - Measurement of Fracture Toughness KIc, KQ Values by Small-Scale Single Specimen", Engineering Fracture Mechanics, Vol. 36, No. 2, 1990, pp. 313-320.

[26]. J. Giovanola and T. Kobayashi, "Mechanics of Deformation and Ductile Tearing in Cracked Round Bar Specimens", Engineering Fracture Mechanics, Vol. 59, No. 2, 1998, pp. 117-136.

A6. REFERENCES (continued)

[27]. D. Li and A. Bakker, "Fracture Toughness Evaluation using Circumferentially-Cracked Cylindrical Bar Specimens", Engineering Fracture Mechanics, Vol. 57, No. 1, 1997, pp. 1-11.

[28]. B. Ule, V. Leskovsek and B. Tuma, "Estimation of Plain Strain Fracture Toughness of AISI M2 Steel from Precracked Round Bar Specimens", Engineering Fracture Mechanics, 65, 2000, pp. 559-572.

[29]. V. Leskovsek and B. Ule, "Fracture Toughness as a Criterion for Optimising the Heat Treatment of High Speed Steel", Heat Treatment of Metals, 2, 2001, pp. 39-45.

[30]. V. Leskovsek, B. Ule and B. Liscic, "Relations between Fracture Toughness, Hardness and Microstructure of Vacuum Heat-Treated High Speed Steel", Journal of Materials Processing Technology, 127, 2002, pp. 298-308.

[31]. D. Nolan, B. Šuštaršič, B. Bruce, P. Grace and Z. Sterjovski, "Fracture Resistance of Heat-Affected Zones arising from In-Service Welding of Pipeline Steels", In Proc. of the 5th Asian Pacific IIW Congress, Sydney, Australia, March, 2007.

Appendix B.

Results of Small-Scale Experimental Simulations at University of Wollongong

Development of HAZ Hardness Limits for In-Service Welding

Small-Scale Experimental Simulations at the University of Wollongong

B1. BACKGROUND

Fracture toughness testing is most commonly performed using relatively large samples so as to maintain conditions of plane strain and maximum constraint.[1] In the study of the mechanical property of welds, the particular region of interest, such as the heat affected zone (HAZ), may be quite small and its exact location may be unknown. In addition, the microstructures found in welded samples are very heterogeneous. This makes preparing bulk samples from weld material very difficult, in that the notch and pre-crack must be directed at the region of interest and the subsequent crack growth must penetrate that region of interest during the test. This can be overcome by reducing the size of the sample to ensure that the entire region being tested is the desired microstructure. However, reducing the size of the sample runs the risk of no longer satisfying the conditions of plane strain and maximum constraint.

As the sample dimensions are reduced, it is difficult to maintain predominantly elastic conditions during fracture testing in metals. In large samples, the plastic zone at the crack tip is relatively small compared to the specimen dimensions and its effect on the elastic conditions of loading is negligible. However, in small samples, this plastic zone at the crack tip becomes significant and the loading conditions are considered plastic-elastic in nature. Therefore, it may be necessary to measure the crack tip energy release rate (J_I) under elastic-plastic conditions.[2] This can be achieved by calculating the critical crack tip energy release rate (J_{IC}) using the J-integral method.[3] This method involves determining the J-integral as a function of crack extension (Δa). The J-integral is calculated from the area under the load-displacement curve and the crack extension can be measured by either multiple specimen techniques (where different samples are tested to different loads and broken open to measure the crack length) or single sample in-situ techniques (where the crack length is determined by compliance measurements or electric potential drops during progressive loading/unloading of the sample).

The relationship between the J-integral and the crack extension is given by the J-resistance curve (illustrated in Figure B1), which is extrapolated back to a line corresponding to crack blunting, thereby giving a value of J corresponding to crack initiation (J_{IC}). Since the J-integral is path independent,[4] it can be related to the fracture toughness (K_{IC}) in a large specimen by:[5]

$$K_{IC} = \sqrt{\frac{J_{IC} E}{1 - \nu^2}} \qquad (1)$$

where E is the Young's Modulus and ν is the Poisson's Ratio.

Such methods have been used to determine the fracture toughness of a number of sub-sized specimens down to thicknesses as small as 1.02mm with very little effect on the J_{IC} values obtained.[5-8]

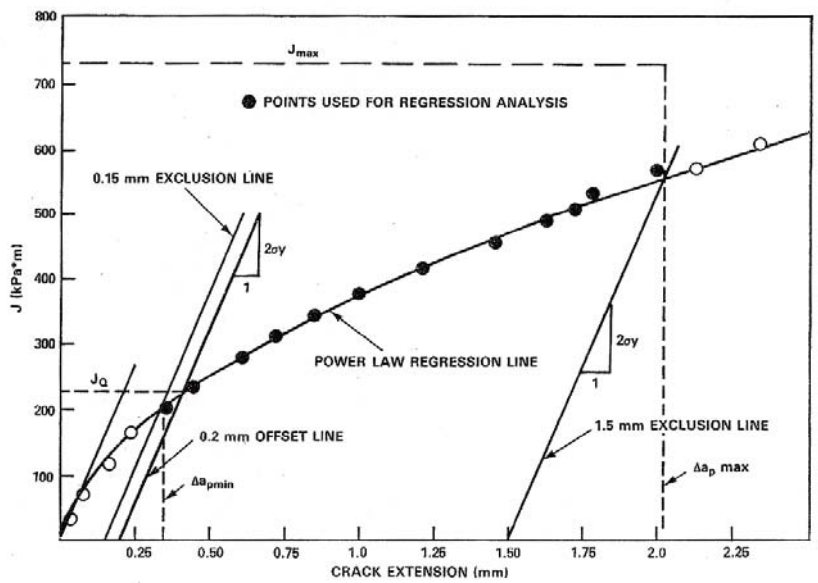

Figure B1. J-resistance curve used to determine J_{IC}.[3].

B2. EXPERIMENTAL

B2.1 Materials

The five steels investigated were selected from Australian, Canadian and American sources so as to provide a representative range of pipeline steels that are commonly subjected to in-service welding procedures. The steels ranged from relatively old, high carbon grades to more modern, low carbon, microalloyed grades, with carbon contents between 0.06-0.29%. Table B1 details the steels used in this study, including the pipe dimensions, grade, composition and carbon equivalents.

Table B1. Pipeline steel details, including pipe dimension and composition.

	Australian Steel	American Steels		Canadian Steels	
	A1	**P2**	**P6**	**GTN**	**TC2**
Pipe OD (mm)	508	N/A	508	914	914
Thickness (mm)	8.6	9.5	7.9	11.1	13.8
Grade	X60	X65	X52	X52	X80
%C	0.17	0.13	0.29	0.218	0.056
%Mn	1.23	1.41	0.96	1.03	1.69
%Cr	0.026	0.05	0.03	0.011	0.106
%Ni	0.009	0.03	0.038	0.073	0.131
%Mo	0.005	0.01	0.005	0.004	0.275
%Si	0.25	0.35	0.005	0.035	0.245
%Cu	0.009	0.37	0.04	0.086	0.241
%Al	0.021	0.032	0.008	0.001	0.034
%P	0.008	0.009	0.011	0.011	0.010
%S	0.005	0.008	0.024	0.022	0.004
%O	0.0012	N/A	0.0033	N/A	N/A
%N	0.0072	N/A	0.0079	N/A	N/A
%B	<0.0003	<0.0003	<0.0003	N/A	0.0001
%Ti	0.005	0.003	0.005	N/A	0.012
%Nb	0.046	0.023	0.005	0.001	0.088
%V	0.005	0.002	0.005	0.001	0.008
CE_{IIW}	0.38	0.40	0.46	0.40	0.44
P_{CM}	0.24	0.24	0.34	0.28	0.19
CE_N	0.39	0.36	0.46	0.40	0.28

B2.2 HAZ Thermal Cycle Simulation

Simulation of the HAZ thermal cycle during in-service welding was achieved on a Gleeble 3500 thermomechanical testing machine. Samples were machined to a rectangular bar with a cross-section of 9×5mm and a length of 80mm. A small neck 10mm long with a reduced width of 5mm was machined in the center of the bar to achieve a more uniform temperature profile along the sample and obtain a more uniform HAZ microstructure. These dimensions were dictated by the amount of material available and the thicknesses of the pipeline steels studied, as well as the need to achieve rapid heating and cooling for the thermal cycle simulations. The sample geometry and dimensions are shown in Figure B2.

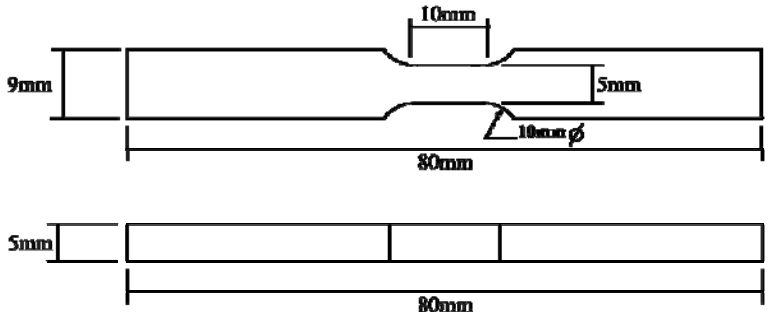

Figure B2. Gleeble sample geometry and dimensions for HAZ thermal cycle simulations.

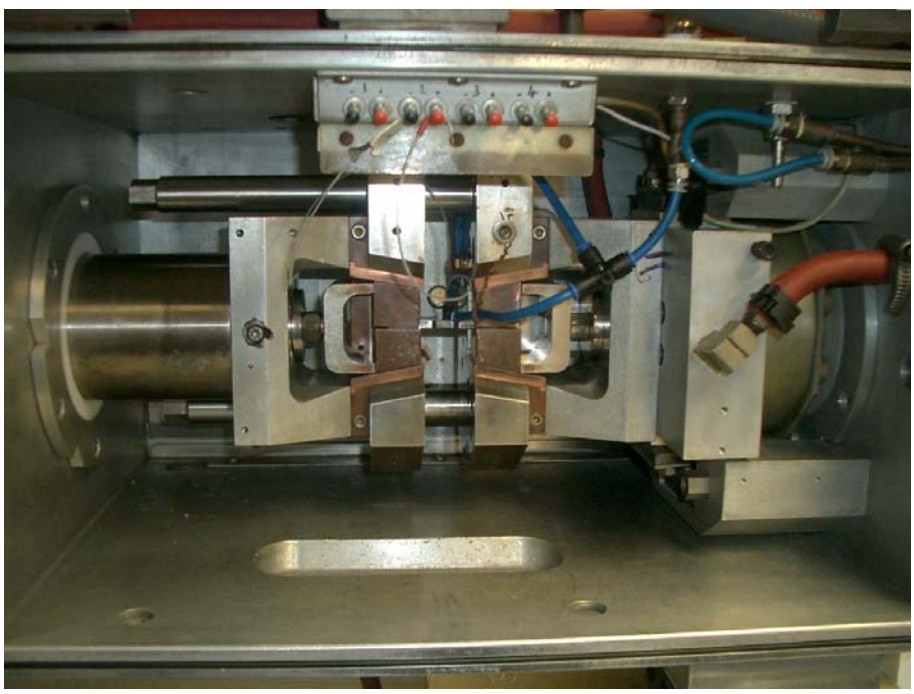

Figure B3. Experimental set up for HAZ welding simulation in Gleeble.

The Gleeble sample was clamped in between copper contacts (Figure B3) and a current was applied to resistively heat the sample according to the required temperature cycle. The thermal cycle was designed to simulate that experienced by the HAZ during in-service welding by replicating the thermal cycle of Nolan et al.[9] The heating rate was maximized whilst maintaining adequate control to avoid overshooting the peak temperature of 1350°C. The hold time at the peak temperature was minimized whilst allowing the temperature to stabilize and the sample was cooled rapidly through the use of two high-pressure argon gas quenching jets on opposite sides of the neck of the Gleeble samples. Through the use of the argon jets, a high cooling rate was obtained, such that the time to cool from 800°C to 500°C ($t_{8/5}$) was approximately 3 seconds.

This is at the lower end of the range of cooling times typically observed during in-service welding procedures (with a $t_{8/5}$ of 2-10 seconds).[10] A typical thermal cycle achieved during the HAZ simulation is shown in Figure B4.

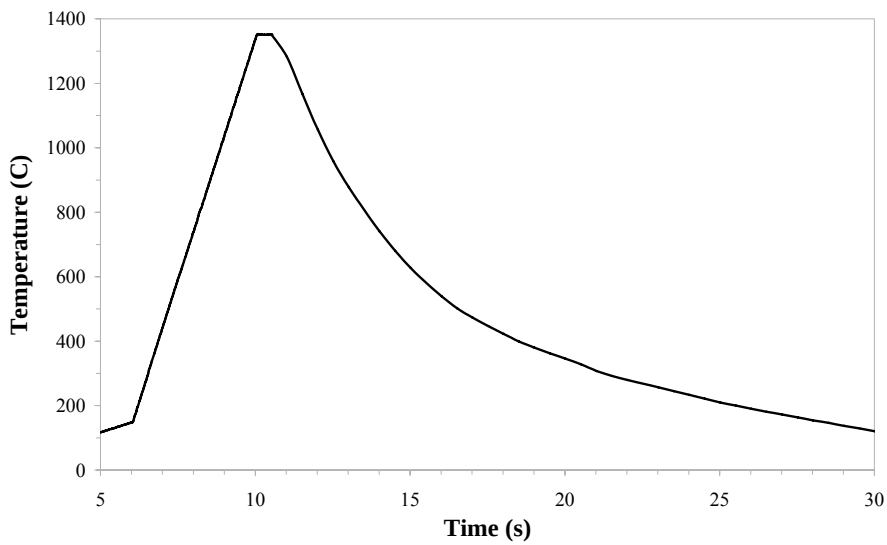

Figure B4. Typical HAZ thermal cycle simulation.

Once the HAZ microstructure was produced by the HAZ thermal cycle simulation, the Gleeble sample was machined into a small three-point bend (3PB) test bar 5×5×25mm in size. The 3PB bar utilized the neck of the Gleeble sample and was centered along its length so that the HAZ microstructure was situated in the center of the bar. A notch 300µm wide and 2.5mm deep was machined in the center of the 3PB bar and the notch had a root radius of 300µm.

B2.3 Hydrogen Charging

Once the 3PB bar was machined, the surface was ground on SiC paper to a 600 grit finish using ethanol as a lubricant, so as to minimize oxidation of the surface of the steel samples. The 3PB bar was then charged with hydrogen using electrolytic hydrogen charging. The sample was suspended in the center of a platinum mesh anode in an electrolyte inside a glass beaker (see Figure B5), and a current was passed through the circuit. The electrolyte consisted of a solution of 0.1M H_2SO_4 with the addition of 2.5mg/l of As_2O_3 as a hydrogen recombination inhibitor. A constant current density of 50mA/cm^2 was used for hydrogen charging.

In order to obtain the desired hydrogen levels of 2 and 4ml/100g, calibration curves were established so as to determine the times required to reach 2 and 4ml/100g for each steel. This was achieved by charging notched 3PB bars for different times and measuring the hydrogen content on a ELTRA ONH-2000 Oxygen/Nitrogen/Hydrogen Determinator at BlueScope Steel.

The hydrogen is measured through a fusion process, whereby the sample is melted and the released gases are analyzed. The hydrogen charging rate over time was then extrapolated to estimate the times needed for 2 and 4ml/100g. These charging times were then verified experimentally with notched 3PB bars.

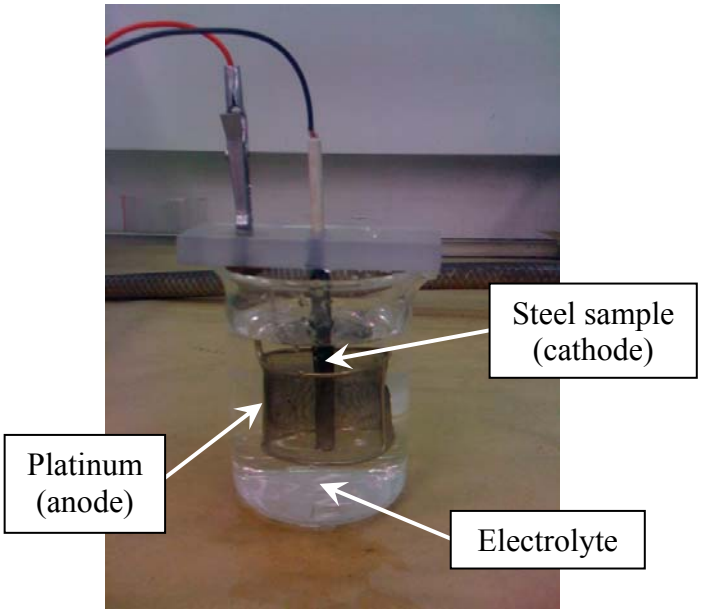

Figure B5. Electrolytic hydrogen charging experimental set up.

B2.4 Mechanical Testing

The fracture toughness of the steel samples was determined by three-point bending, using the J_{IC} method for sub-sized samples.[3 Samples were notched, as previously described, but were not pre-cracked. This was due to experimental simplicity in light of previous work that found the toughness values from pre-cracked samples were only slightly smaller (5-10%) than those from notched-only samples.

B5. REFERENCES (continued)

[11

Immediately after hydrogen charging, the samples were washed in ethanol and placed in liquid nitrogen for transportation to the 10kN Instron 5566 mechanical tester. Before testing, the samples were again washed in ethanol to bring the samples to room temperature and then quickly dried and placed in the three-point bend rig for testing. The samples were loaded and unloaded

according to ASTM E813 at a speed of 0.2mm/min. Given the small size of the 3PB bars and the absence of an optical system, the crack opening displacement (COD) could not be measured. Instead, the crack extension was determined from the load-line displacement using the compliance coefficients developed by Haggag and Underwood[12] in place of the COD compliance factors specified in the ASTM standard.

B2.5 Hardness, Microstructure and Fractography

Samples for hardness and metallographic analyses were sectioned along the cross-section of the 3PB bar in the center of the HAZ, mounted in bakelite and polished according to standard metallographic methods for C-Mn steels. Optical microscopy was performed on a Leica DMR optical microscope fitted with a DFC280 digital camera. Scanning electron microscopy of the fracture surfaces was performed on a JEOL LV6490 SEM operating at 15kV. The hardness values were determined through Vickers indentation hardness testing with a 10kg load, using 8 measurements to give an average value.

B3. RESULTS AND DISCUSSION

B3.1 Microstructure and Hardness

The micrographs of the simulated HAZ microstructures are shown in Figure B6, indicating the four older, higher-carbon steels (A1, P2, P6 and GTN) have martensitic microstructures, resulting in quite high hardness (see

Table **B2**). Samples P6 and GTN, in Figures B5(c) and B 5(d) respectively, also appear to contain some polygonal ferrite on the prior austenite grain boundaries. This was unexpected, as both steels have high carbon contents (0.29wt% for P6 and 0.218wt% for GTN) and the resulting microstructures were expected to be entirely martensitic. The more modern low-carbon steel (TC2) appears to have a predominantly bainitic microstructure with some minor amount of martensite, giving the sample a reasonable hardness for the low carbon content (0.056wt%).

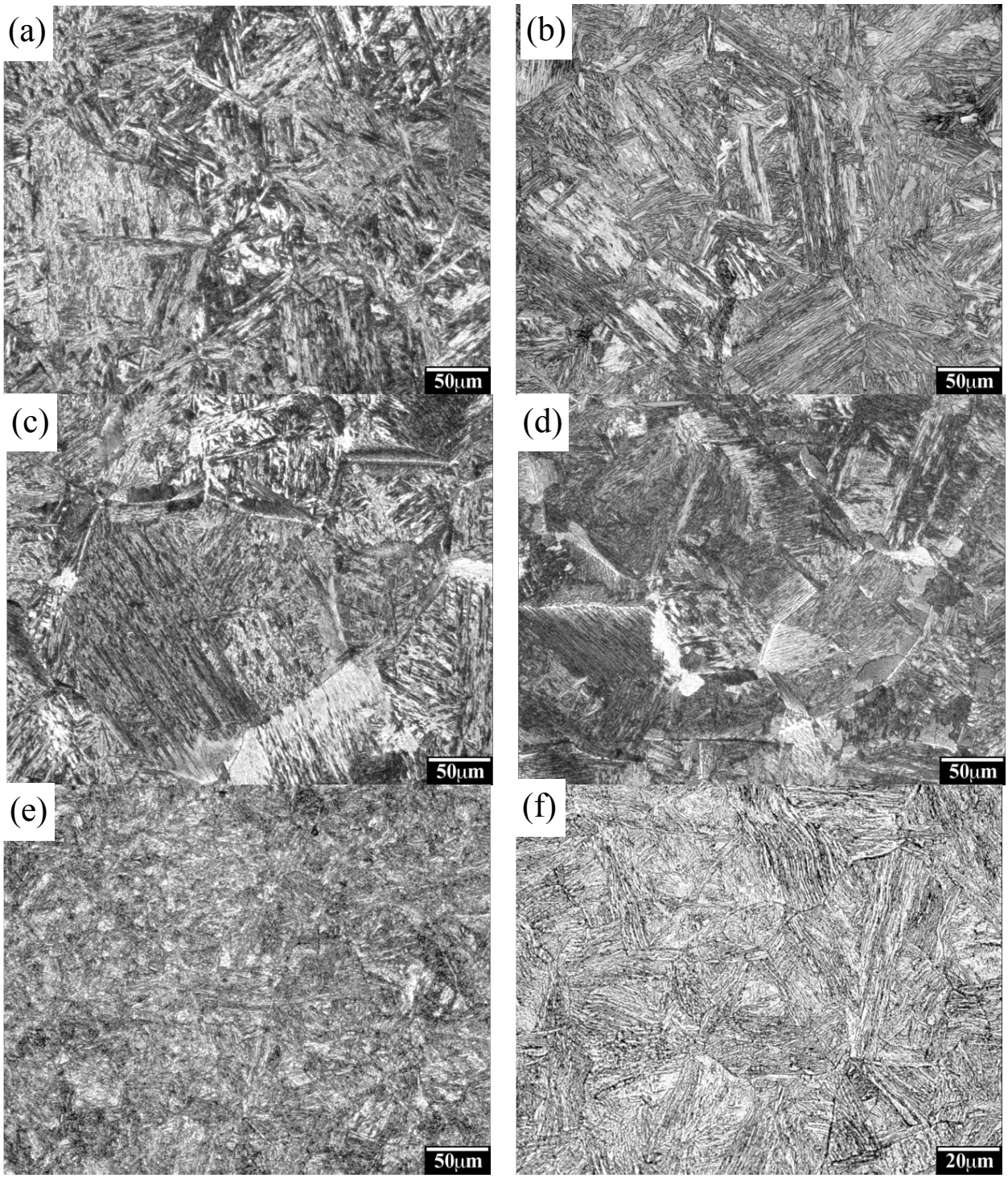

Figure B6. Optical micrographs of simulated HAZ microstructures (a) A1, (b) P2, (c) P6, (d) GTN and (e-f) TC2.

Table B2. Vickers hardnesses of simulated HAZ microstructures.

Sample	H_{V10} (MPa)
A1	435 ± 7
P2	410 ± 6
P6	474 ± 14
GTN	395 ± 14
TC2	331 ± 6

B3.2 Hydrogen Charging

The calibration curves for the electrolytic hydrogen charging were obtained for samples P2, GTN and TC2 to study the effect of different compositions (particularly carbon content), different hardnesses and different microstructures. The hydrogen charging rates were found to behave the same for the two martensitic microstructures (P2 and GTN) while the bainitic microstructure (TC2) charged at a slower rate. The calibration curves for the different microstructures are shown in Figure B7. All four martensitic microstructures were then charged at the estimated times of 15 minutes (2ml/100g) and 80 minutes (4ml/100g) to confirm the correct hydrogen contents were obtained. Likewise, the TC2 steel was charged to confirm 2ml/100g and 4ml/100g were achieved after 20 and 100 minutes, respectively.

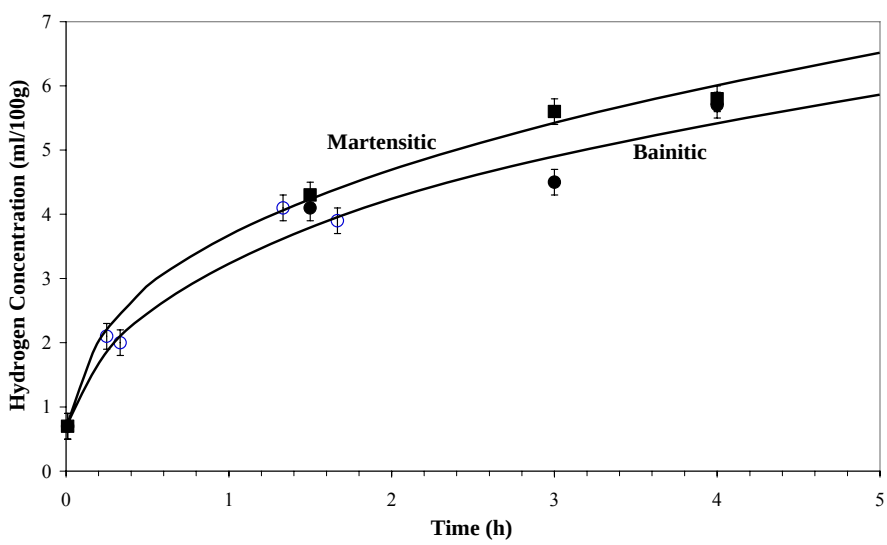

Figure B7. Electrolytic hydrogen charging calibration curves (open circles indicate confirmation samples).

B3.3 Fracture Testing

The loading/unloading procedure used in ASTM E813 is shown in Figure B8 for an uncharged A1 steel sample. The crack-tip energy (J) was calculated from the area under the load-displacement curve at successive unloading points, and plotted against the crack extension (Δa) at those points. The resulting J-resistance curve in Figure B9 was then extrapolated back to the 0.2mm offset line to give the critical crack-tip energy (J_{IC}), from which the fracture toughness K_{IC} was then calculated using equation 1.

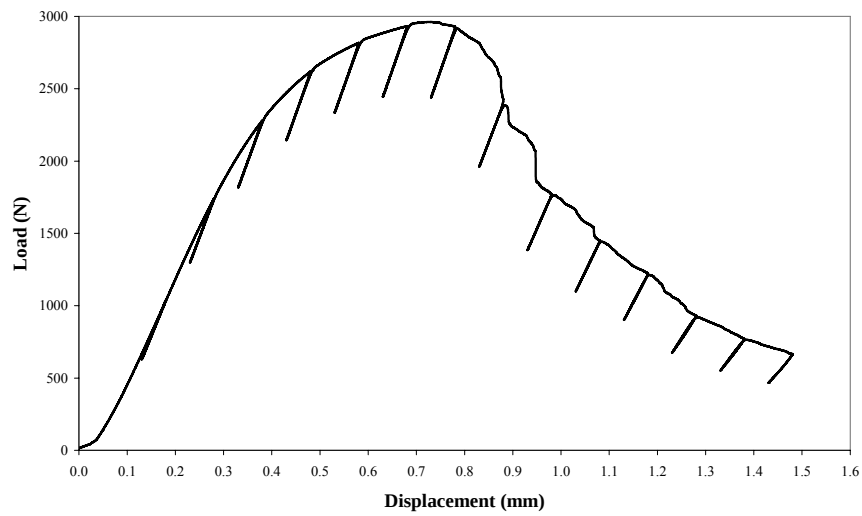

Figure B8. Fracture testing of uncharged A1 steel using JIC method.

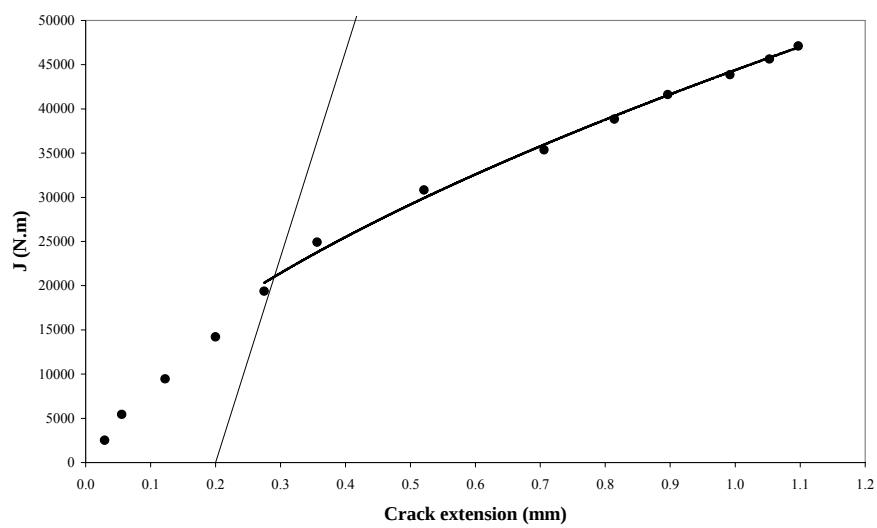

Figure B9. J-resistance curve of uncharged A1 steel.

Three samples were tested for each hydrogen content for each steel so as to obtain average values, and the results are given in Table B3. These values are in good agreement with results for the Australian and American steels previously reported.[9] The average toughness values for the three hydrogen levels were plotted against carbon equivalent for the three different carbon equivalent equations, as shown in Figure B10. It is clear in Figures B9(a) and (c) that there is a clear trend in the uncharged steels for decreasing toughness with increasing carbon equivalent. However, this is less apparent in Figure B10(b). This is due to the predominance of older higher-carbon steels in this study, such that the CE_{IIW} carbon equivalent, which is considered to be more relevant to older steels, is more appropriate to use. The CE_N carbon equivalent was developed to approximate both CE_{IIW} for older higher-carbon steels, as well as P_{CM} for newer lower-carbon microalloyed steels.[13] Thus, it will also show a similar trend to that seen using the CE_{IIW} carbon equivalent. It should be noted, however, that the uncharged samples that do not fit the trends in Figures B9(a) and (c) are GTN and TC2, respectively. This is unfortunate, as GTN is an older higher-carbon steel for which CE_{IIW} should give good agreement, while CE_N was developed to also account for newer lower-carbon steels, such as TC2.

Table B3. Fracture toughness values for steels.

Sample	K_{IC} uncharged ($MPa{\cdot}m^{1/2}$)	K_{IC} @ 2ml/100g ($MPa{\cdot}m^{1/2}$)	K_{IC} @ 4ml/100g ($MPa{\cdot}m^{1/2}$)
A1	70 ± 3	25 ± 4	12 ± 3
P2	55 ± 6	25 ± 2	13 ± 3
P6	24 ± 3	19 ± 1	12 ± 1
GTN	31 ± 5	20 ± 1	21 ± 3
TC2	35 ± 4	27 ± 2	12 ± 3

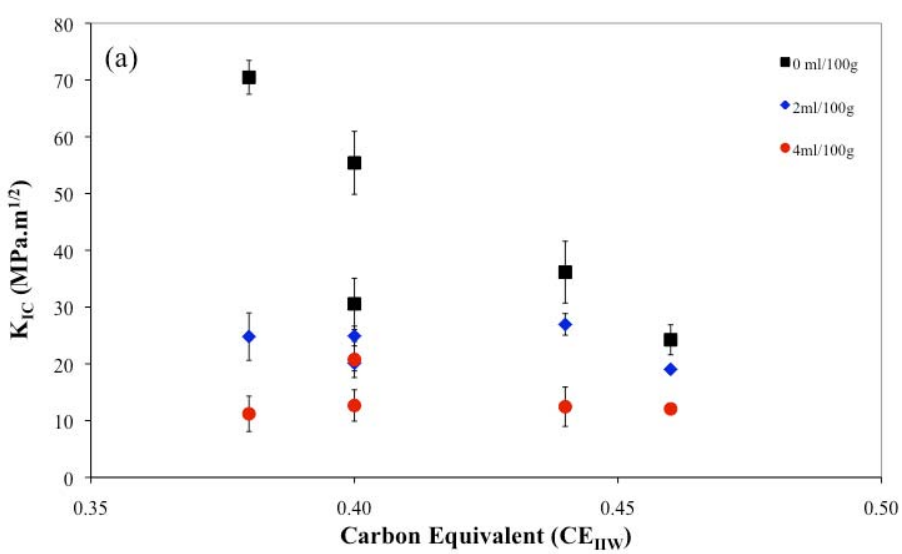

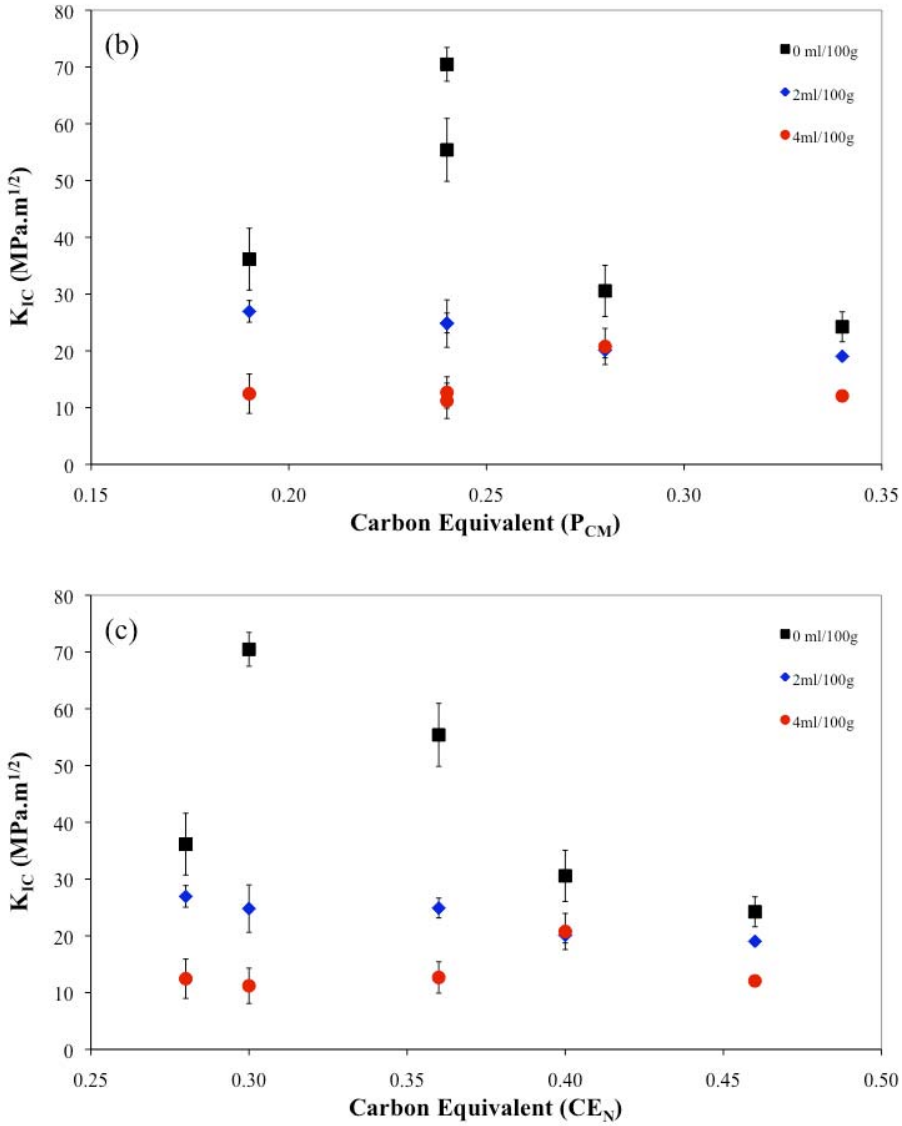

Figure B10. Fracture toughness as a function of carbon equivalent for (a) CE_{IIW}, (b) P_{CM} and (c) CE_N.

The fracture toughness trends, however, disappear after hydrogen charging. It seems the toughness values for the steels studied are all close to being the same, within error, for both hydrogen levels of 2 and 4ml/100g. This may be a result of the nature of hydrogen charging. Introducing hydrogen through electrolytic charging after simulating the welding thermal cycle will likely result in enrichment of hydrogen along the most favorable diffusion paths, namely the grain boundaries. This differs from actual welds in that the hydrogen is introduced at high temperature when the steel is austenitic and the microstructure transforms during cooling,

resulting in a more homogenous distribution of hydrogen in the microstructure. More importantly, the hydrogen will also be distributed within the grains of the final microstructure. Therefore, the composition of the steel and, hence, its hardness, may play a smaller role when using post-weld simulation hydrogen charging, compared to the effect of the morphological features of the microstructure on the hydrogen embrittlement of the steel.

Although the fracture toughnesses of the steels are similar after hydrogen charging, this does indicate different degrees of embrittlement from the original uncharged steel. A comparison of the charged toughness to the uncharged toughness for each steel indicates that the order of decreasing embrittlement follows:

2ml/100g: A1 > P2 > GTN > TC2 > P6 *(2)*

4ml/100g: A1 > P2 > TC2 > P6 > GTN *(3)*

These trends are at odds with expectations, as the TC2 steel should have a reasonable toughness and suffer the least amount of embrittlement as a result of its low carbon content and moderate hardness. Similarly, the P6 steel would be expected to suffer more severe hydrogen embrittlement due to its high carbon content and high hardness. However, its uncharged toughness is already quite low, limiting the degree to which it can be embrittled, as seen after charging to 2ml/100g. Of particular note is that at both hydrogen levels, the A1 and P2 steels suffer the greatest embrittlement, which is unexpected as they have the two lowest carbon contents of the older steels studied.

B3.4 Fractography

The fracture surfaces of the uncharged steels are shown in Figure B11, showing a reasonable relationship between fracture surface morphology and fracture toughness. The trend of decreasing fracture toughness in the uncharged samples in Table B3 correlates well with the proportion of decreasing microvoid coalescence and increasing brittle cleavage. This is highlighted by a comparison of the fractographs of A1 and P6 in Figures B11(a) and (c), respectively. Sample A1, with the highest toughness of 70 MPa.m^{½}, demonstrates failure by microvoid coalescence only, whereas sample P6, with the lowest toughness of 24 MPa.m^{½} shows a significant fraction of brittle cleavage on the fracture surface in addition to some microvoid coalescence.

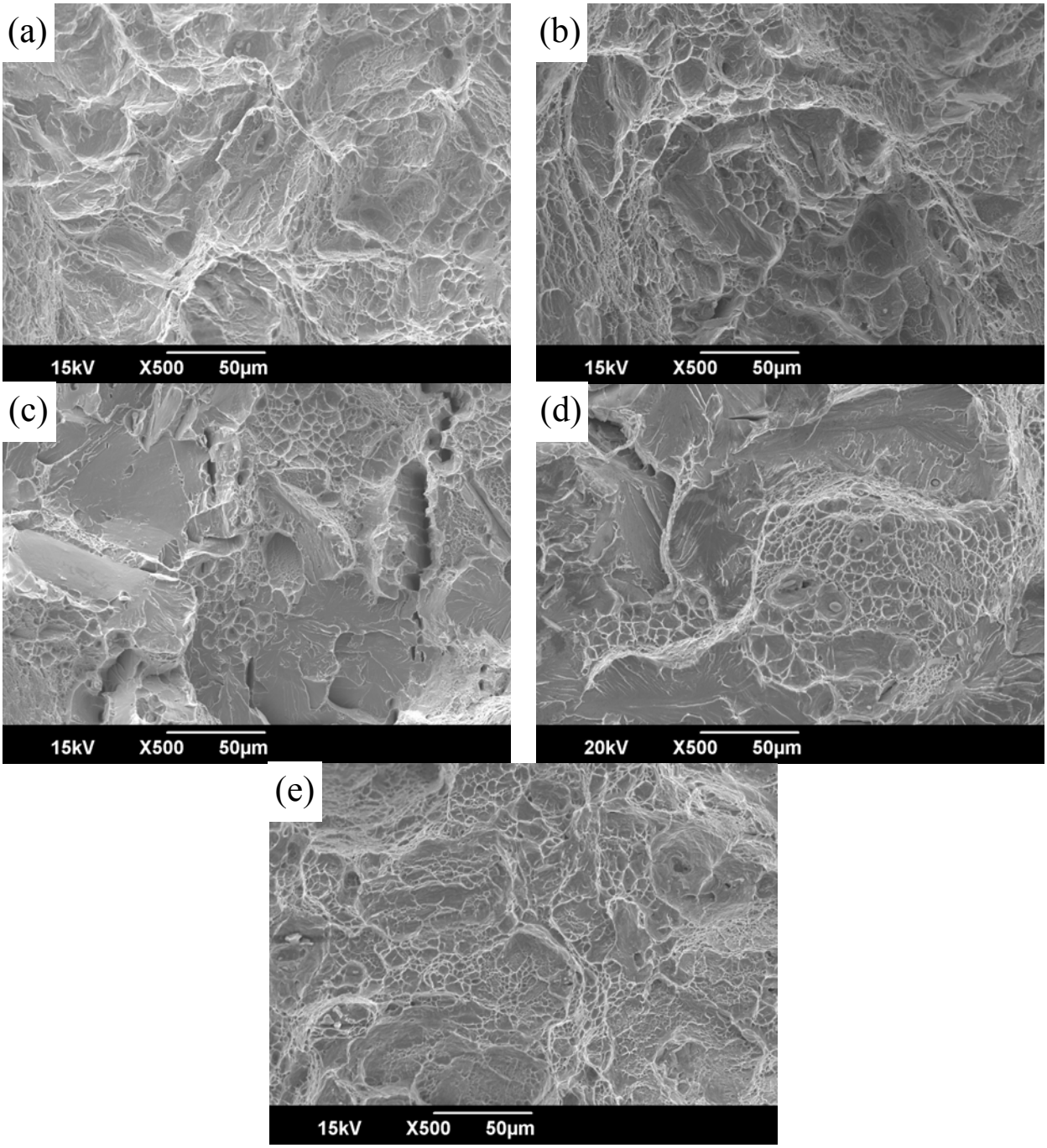

Figure B11. Fractographs of uncharged samples (a) A1, (b) P2, (c) P6, (d) GTN and (e) TC2.

The relationship between toughness and fracture surface morphology is further highlighted when the fractographs of the uncharged samples in Figure B11 are compared with those of the hydrogen charged samples. The fractographs of the hydrogen charged samples are shown in Figures B12 and B13 for hydrogen levels of 2 and 4 ml/100g, respectively. It is clear from the fracture surfaces that hydrogen charging results in a decrease in ductile microvoid coalescence failure and an increase in brittle intergranular cleavage failure. This is consistent with the decreases in toughness observed in all steels for both hydrogen levels. In addition, the degree to which microvoid coalescence changes to intergranular cleavage is consistent with the degree of embrittlement, except in the case of TC2, where there does not appear to be a great deal of intergranular fracture expected after hydrogen charging to 4 ml/100g. For example, sample A1 underwent the greatest embrittlement and appears to show the greatest change in fracture surface morphology when comparing Figures B11 − B13. Likewise, the P6 steel, which had a much smaller decrease in toughness, showed the least change in fracture surface morphology, predominantly due to the presence of a significant degree of brittle cleavage in the original uncharged material.

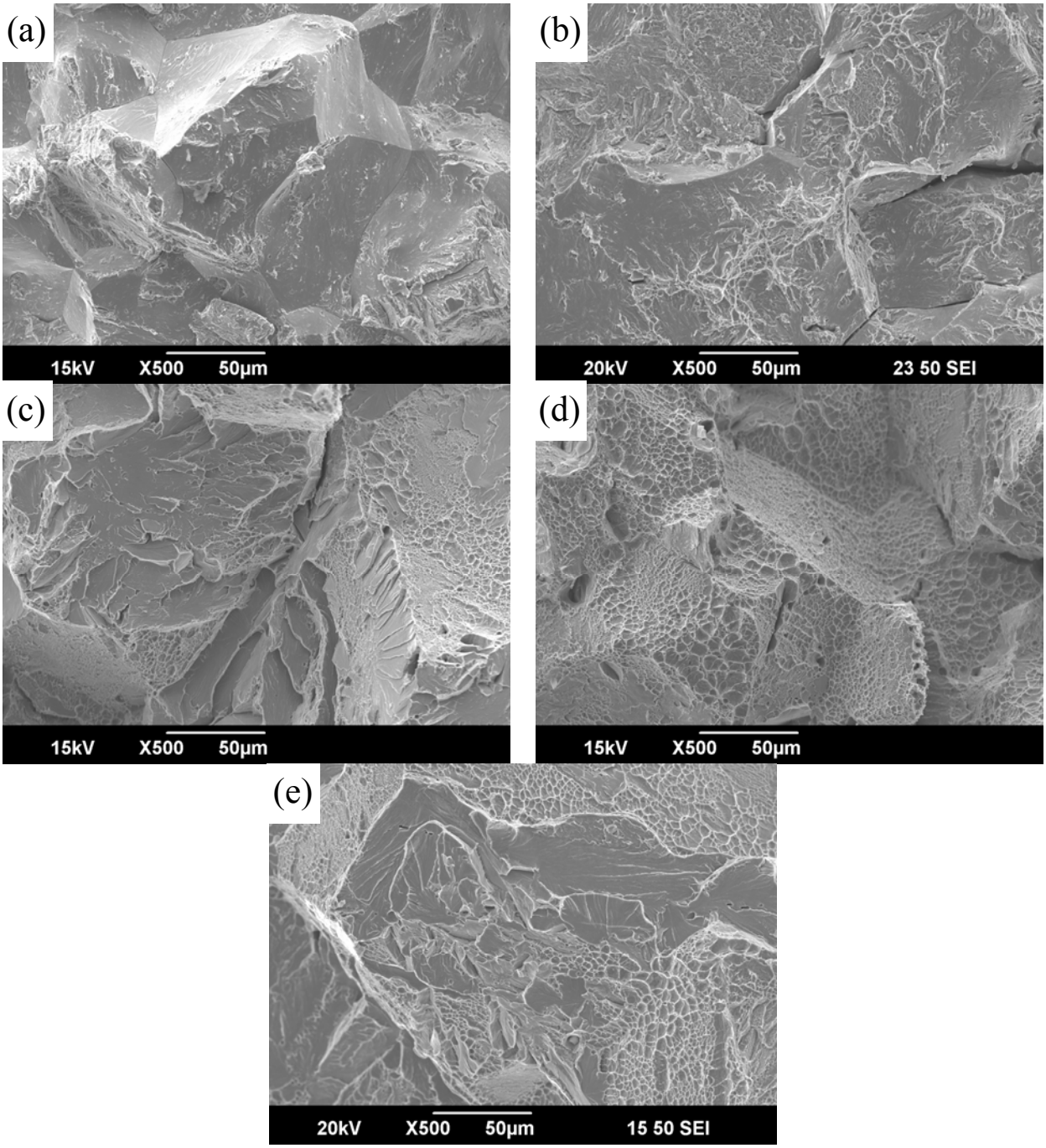

Figure B12. Fractographs of samples hydrogen charged to 2ml/100g (a) A1, (b) P2, (c) P6, (d) GTN and (e) TC2.

Of particular interest is the dramatic difference between the uncharged fractographs in Figure **B11** and those of the samples charged to 2 ml/100g in Figure B12. In comparison, the difference between the two charging levels in Figures B12 and B13 show a much smaller change in fracture surface morphology. This is consistent with the large drop in toughness for all steels when the uncharged samples are charged to 2 ml/100g, followed by a more moderate drop when the hydrogen level in increased from 2 to 4 ml/100g, as shown in Table B3. Thus, this highlights the dangers of introducing hydrogen into steels, even at low levels.

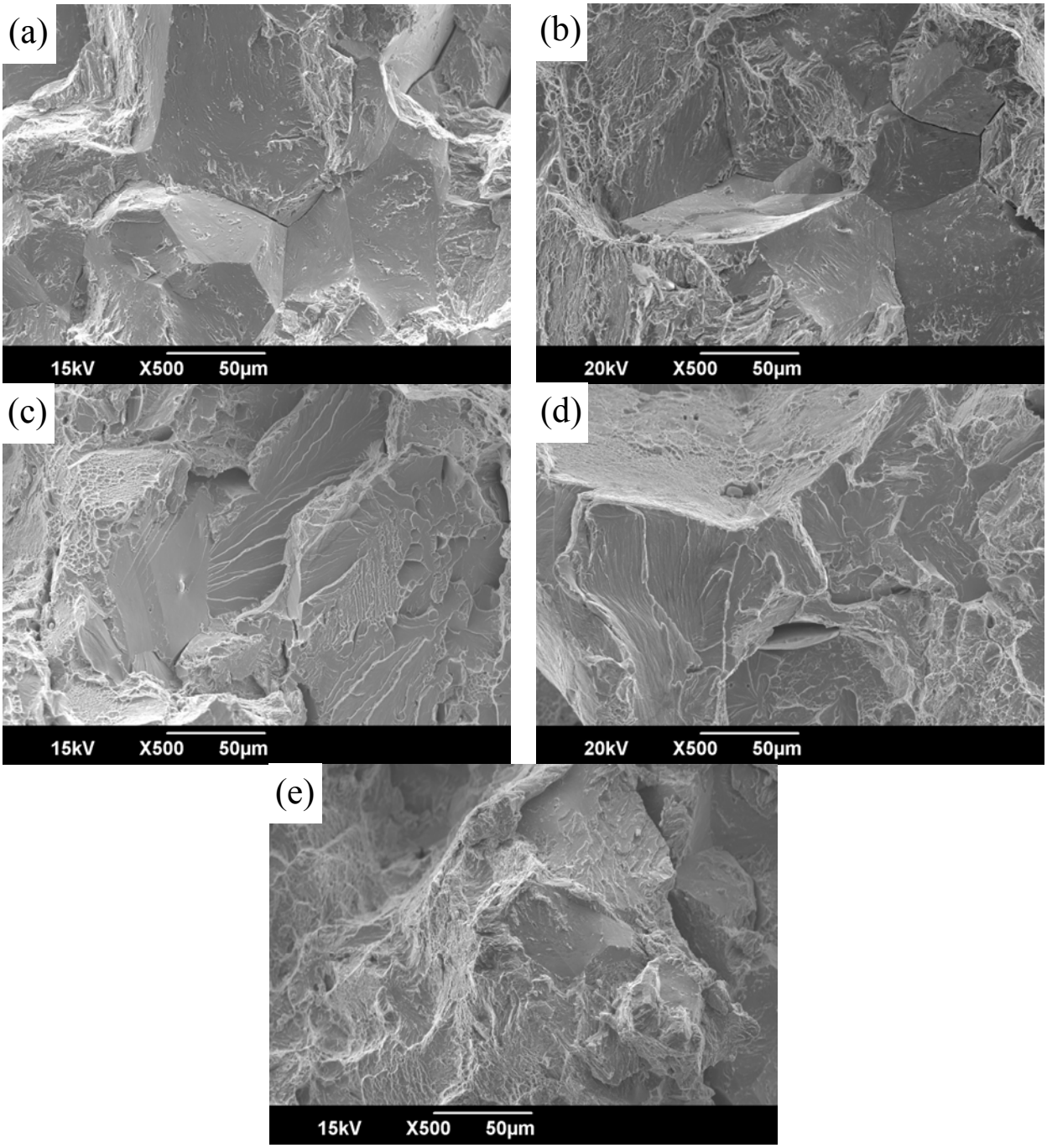

Figure B13. Fractographs of samples hydrogen charged to 4ml/100g (a) A1, (b) P2, (c) P6, (d) GTN and (e) TC2.

B4. CONCLUSIONS

Based on the small-scale experimental simulations performed at the University of Wollongong, the following conclusions can be made:

- Hydrogen embrittlement was observed in all five steels after electrolytic hydrogen charging of simulated HAZ microstructures. The fracture roughness was found decrease dramatically at the relatively low hydrogen level of 2 ml/100g, with toughness values decreasing by up to 65%. Increasing the hydrogen level to 4 ml/100g resulted in further decreases in toughness. However, the decreases in toughness from 2 to 4 ml/100g of hydrogen were much smaller than those from uncharged steel to 2 ml/100g of hydrogen. These decreases in toughness are consistent with the changes in the fracture surfaces from ductile microvoid coalescence failure to brittle intergranular cleavage failure.

- Electrolytic hydrogen charging to higher levels, such as 8 ml/100g, was unsuccessful, due to the inability of the steel microstructures to accommodate hydrogen. This is consistent with the phenomenon of hydrogen embrittlement, where the level of hydrogen that dissolves in the austenite at the welding temperature cannot be accommodated in the HAZ microstructure after cooling, such that the HAZ becomes supersaturated in hydrogen. In addition, given the embrittlement observed at 4 ml/100g, higher levels of hydrogen may not be representative of the true in-service weld HAZ hydrogen contents expected.

- Introducing hydrogen into the steel microstructures at room temperature by electrolytic hydrogen charging after the weld thermal cycle simulation is performed may lead to a hydrogen distribution that is not entirely representative of in-service welds. The hydrogen will be enriched at the grain boundaries, rather than within the grains themselves. This may be resolved by introducing the hydrogen during the weld thermal cycle simulation so as to more closely reproduce true in-service welding conditions.

B5. REFERENCES

[1.] ASTM E399-90, "Standard Test Method for Plane-Strain Fracture Toughness of Metallic Materials", Annual Book of ASTM Standards 3.01, American Society for Testing and Materials, West Conshohocken, PA (1997).

[2.] P. Jung, A. Hishinuma, G. E. Lucas and H. Ullmaier, "Recommendation of miniaturized techniques for mechanical testing of fusion materials in an intense neutron source", *Journal of Nuclear Materials*, 232(2-3), 186-205 (1996).

[3.] ASTM E813-89, "Standard Test Method for J_{IC}, A Measure of Fracture Toughness", Annual Book of ASTM Standards 3.01, American Society for Testing and Materials, West Conshohocken, PA (1997).

[4.] J. R. Rice, "A Path Independent Integral and the Approximate Analysis of Strain Concentration by Notches and Cracks", *Journal of Applied Mechanics*, 35, 379-386 (1968).

[5.] G. E. Lucas, "Review of small specimen test techniques for irradiation testing", *Metallurgical Transactions A*, 21A(5), 1105-1119 (1990).

[6.] E. Wakai, H. Ohtsuka, S. Matsukawa, K. Furuya, H. Tanigawa, K. Oka, S. Ohnuki, T. Yamamoto, F. Takada and S. Jitsukawa, "Mechanical properties of small size specimens of F82H steel", *Fusion Engineering and Design*, 81(8-14), 1077-1084 (2006).

[7.] Xinyuan Mao, Tetsuo Shoji and Hideaki Takahashi, "Development of a Miniaturized Specimen Technique for Fracture Toughness J_{IC} Measurement", *Journal of Testing and Evaluation*, 16(2), 229-241 (1988).

[8.] G. R. Odette, M. He, D. Gragg, D. Klingensmith and G. E. Lucas, "Some recent innovations in small specimen testing", *Journal of Nuclear Materials*, 307-311(2), 1643-1648 (2002).

[9.] D. Nolan, B. Šuštaršič, W. Bruce and P. Grace, "Small-scale fracture testing of heat-affected zones of in-service welds of pipeline steels", *Australasian Welding Journal*, **52**(3rd Q), 41-48 (2007).

[10.] Z. Sterjovski and D. Nolan, "Material Composition Effects in Relation o In-Service Welding of Gas Pipelines", *CRC Project 2002-320 Final Report*, University of Wollongong, Wollongong, Australia, December 2004.

B5. REFERENCES (continued)

[11.] Shiro Jitsukawa, Akira Naito and Jun Segawa, "Effect of size and configuration of 3-point bend bar specimens on J-R curves", *Journal of Nuclear Materials*, 271-272**,** 87-91 (1999).

[12.] Fahmy M. Haggag and John H. Underwood, "Compliance of a Three-Point Bend Specimen at Load Line", *International Journal of Fracture*, 26(2), R63-65 (1984).

[13.] N. Yurioka, H. Suzuki, S. Ohshita and S. Saito, "Determination of necessary preheating temperature in steel welding", *Welding Journal*, 62(6), 147-153 (1983).

Appendix C.

Control of Weld Hydrogen Levels for Welds Made onto In-Service Pipelines

Control of Weld Hydrogen Levels for Welds Made onto In-Service Pipelines

C1. INTRODUCTION

The main objective of this project is to develop heat-affected zone (HAZ) hardness acceptance criteria that can be used to evaluate welds during the qualification of procedures for welding onto in-service pipelines. Guidance pertaining to issues related to the application of these limits was also developed. This appendix focuses on control of weld hydrogen levels for welds made onto in-service pipelines.

C2. BACKGROUND

The ability to tolerate HAZ hardness levels that are higher than the limits that have been traditionally imposed (e.g., 350 HV) depends strongly on the ability to closely control weld hydrogen levels. The importance of controlling hydrogen levels for welds made onto in-service pipelines is well established. Some pipeline operating companies simply specify the use of low hydrogen electrodes without providing additional guidance. Storage and handling of low-hydrogen electrodes is an in-exact science at best, even though general guidelines for their use are available.[1-4] The hydrogen level of welds made using low-hydrogen electrodes can vary widely depending on a range of factors. These include the manufacturer, classification/supplemental designation, packaging, storage conditions, handling, atmospheric exposure, and drying/re-conditioning practices. Guidance related to the various aspects of weld hydrogen level control for welds made onto in-service pipelines was developed previously[5] and is discussed below.

C3. ELECTRODE PROCUREMENT

C3.1 Electrode Classification/Supplemental Designations

AWS A5.1[6] (Specification for Carbon Steel Electrodes for Shielded Metal Arc Welding) lists several classifications of "low hydrogen" electrode. These include EXX15, EXX16, and EXX18, where “XX” refers to the specified-minimum ultimate tensile strength in ksi. Although EXX16-type electrodes are used for welding onto in-service pipelines to some extent, EXX18-type electrodes are by far the most common. AWS A5.1 requires that E7018 electrodes must have a coating moisture level of less than 0.6%. This moisture level corresponds to a weld hydrogen level that is typically in the range of 16 ml/100 g, which is extremely high for in-service welding applications where the pipe material has an unfavorable chemical composition (i.e., high CE) and the flow rate and pressure are high. AWS A5.5[7] (Specification for Low-Alloy Steel Electrodes for Shielded Metal Arc Welding) requires that E7018 electrodes must have a coating moisture level of less than 0.4%. For E8018 and E9018 electrodes, the limits are 0.2 and 0.15%, respectively.

Many modern E7018-type electrodes have actual coating moisture content levels much lower than 0.6% in the as-received condition and produce weld hydrogen levels that are much less than 16 ml/100 g. AWS has introduced optional supplementary designators in AWS A5.1 that allow a specific maximum-allowable hydrogen level to be specified. These designators are H4, H8, and H16, where "H" indicates hydrogen and "4, 8, and 16" refer to the average maximum-allowable hydrogen level in ml/100 g in the "as-received" condition.[8] In other parts of the world, a similar system is used although the hydrogen levels are H5, H10, and H15. The United States military also has a stricter limit of 2 ml/100 g for some applications.

In addition, AWS has introduced an "R" designator that allows a moisture resistant coating to be specified. The R designator indicates that the electrodes have passed an absorbed moisture test after exposure to an environment of 80ºF (26.7ºC) and 80% relative humidity for a period of not less than 9 hr. Electrodes that meet this requirement have coating moisture limits that are lower than their non-moisture-resistant counterparts. For example, AWS A5.1 requires that E7018-H4R electrodes must have a coating moisture level of less than 0.4% (as opposed to 0.6%).

For in-service welding applications for which low hydrogen levels are required, pipeline operators should consider specifying electrodes with the H4R designator. These are becoming more common and, while there may be a price premium, this is negligible compared to the cost for remedial action that would be required following the discovery or failure of an in-service weld with hydrogen cracks.

C3.2 Packaging

C3.2.1 Packaging Type

Many low-hydrogen electrodes are packaged in hermetically-sealed cans. Cardboard cartons are also used to some extent by some manufacturers and in some parts of the world. These cardboard cartons may be sealed in plastic wrap (Figure C1). With the propensity for electrode coatings to absorb moisture, the concern for low-hydrogen electrodes packaged in cardboard cartons is obvious. Even if plastic wrap is used to seal these cartons, damage may occur in transit or during storage that would allow the electrode coatings to absorb moisture (Figure C2). Some manufacturers that supply low-hydrogen electrodes packaged in cardboard cartons specify that the electrodes must be dried prior to use. While this is common in some parts of the world, it is less common in North America.

For in-service welding applications for which low hydrogen levels are required, the use of electrodes that are packaged in hermetically-sealed cans (i.e., appropriate for use in the as-received condition) would seem to be preferable (Figure C3). If electrodes packaged in cardboard cartons are used, care must be taken to ensure that drying is not required by the manufacturer prior to their use in the as-received condition. If the electrodes are intended to be used in the as-received condition and they are packaged in plastic-sealed cardboard containers, care should be taken to ensure that the plastic wrap is not damaged. If drying is required, care

must be taken to ensure that the drying is carried out properly. Electrode drying is discussed further in Section 5.4.

C3.2.2 Package Size

In North America, a significant percentage of low-hydrogen electrodes are packaged in 50-lb (22.7-kg) hermetically-sealed cans. Many manufacturers also offer low hydrogen electrodes that are packaged in 5- and 10-lb (2.3- and 4.5-kg) cans (Figure C4). Low-hydrogen electrodes in cardboard cartons are typically packaged in 5- to 50-lb (2.3- to 22.7-kg) quantities. Once low-hydrogen electrodes have been removed from a freshly opened package or from an electrode storage oven, they must be used prior to their exposure limit being exceeded (see Section 5.3 below). For in-service welding applications for which low hydrogen levels are required, it may be advantageous to purchase and use low-hydrogen electrodes in smaller quantities [e.g., 10-lb (4.5-kg) cans]. This is particularly true for smaller jobs (e.g., small diameter lines) where it would be difficult to use an entire 50-lb (22.7-kg) can. There is a price premium for this type of packaging, however, which is typically on the order of 40% for 10-lb cans as opposed to 50-lb cans.

C3.2.3 Special Packaging

Taking the small package size concept one step further, several manufacturers offer low-hydrogen electrodes in small quantity, vacuum sealed foil packages. Two examples of this are Lincoln/Smitweld Sahara Ready Packs and ESAB VacPacs (Figures C5 and C6). The concept for this type of packaging is that the entire contents can be used prior to the exposure limit being exceeded. These do not appear to be widely available in North America, however, and there is also a further price premium for this type of packaging.

C4. STORAGE OF ELECTRODES IN UNOPENED CANS/CARTONS

Some manufacturers indicate that unopened cans or cartons will retain the proper moisture content indefinitely when stored in good condition. Other manufacturers indicate that electrodes packaged in plastic-wrapped cardboard cartons can be kept for a maximum of 1 year for normal use if stored properly. This guidance is rather subjective however, as “good conditions” and “stored properly” are not well defined.

In general, unopened cans/cartons of low-hydrogen electrodes should be stored in such a way as to prevent damage to the packaging. A climate-controlled storage room is better than a storage room that is not climate controlled. The storage room should be organized in such a way that allows for rotation of stock (i.e., makes use of the “first in/first out” principle). Hermetically sealed containers should not be opened until the electrodes are needed for use. If the electrodes have been stored in a cold place, they should be allowed to reach ambient temperature before the container is opened.

C5. ELECTRODE HANDLING

Low-hydrogen electrodes must be properly stored and handled to ensure that low hydrogen levels result. Moisture can be absorbed by the electrode coating during storage and handling. Since different low-hydrogen electrodes behave differently with respect to moisture absorption, it is important to follow the specific electrode manufacturer's recommendations for storage and handling.

C5.1 Electrodes Intended for Later Use

Once a container of low-hydrogen electrodes has been opened, it is important that the electrodes that will not be used immediately be transferred to an electrode holding oven, an example of which is shown in Figure C7. For low hydrogen electrodes, the oven temperature should be 250 to 300ºF (121 to 149ºC). Care should be taken to ensure that electrodes of different classifications are stored in clearly marked groups. Low hydrogen electrodes should be stored in this manner until immediately prior to use.

C5.2 Electrodes Intended for Immediate Use

Electrodes intended for immediate use (from containers that have just been opened or electrodes from stationary holding ovens) can be transported by a variety of means. If welding will occur in close proximity to the stationary holding oven from which the electrodes were removed (i.e., on-site welding), the electrodes can be transported in steel buckets, leather quivers, etc. Since these do not protect the electrodes from moisture pick-up, atmospheric exposure time prior to use becomes an issue.

If welding will occur remote from the stationary holding oven (i.e., welding in the field), transportation of electrodes from containers that have been opened is problematic. Electrodes can be transferred to a portable storage oven, examples of which are shown in Figure C8, but these are rarely (if ever) plugged in during transit to the field (or during overnight periods) and they are not hermetically sealed. As an alternative, electrodes from containers that have been opened can be transferred to re-sealable containers, examples of which are shown in Figures C9 and C10, although there is little data pertaining to moisture pick-up in this type of container. If this type of container is used, it may be prudent to limit the amount of time that electrodes can be stored in this manner, since the container materials are somewhat permeable. One manufacturer of re-sealable containers suggests that low-hydrogen electrodes can be stored in this manner for more than 24 hr while maintaining moisture levels to below AWS requirements. Once on site, electrodes from re-sealable containers can be transferred to portable storage ovens (after these have been plugged in). If transported in this manner, atmospheric exposure time prior to use only becomes an issue once the electrodes are removed from the portable oven. If electrodes are transported in portable storage ovens, or in other un-sealed or loosely-sealed containers, atmospheric exposure time should begin once the electrodes are removed from the stationary

holding oven (or from the original container). Unused electrodes from a portable electrode oven can also be transported back to the stationary holding oven in re-sealable containers.

The obvious alternative to transferring electrodes from their original container to stationary holding ovens, to re-sealable containers, and then to portable storage ovens is to transport electrodes to the field in their original un-opened containers and open them there. Electrodes that cannot be used prior to their exposure limit being exceeded must be stored in a portable storage oven (or re-sealable containers).

C5.3 Atmospheric Exposure Limits

Low-hydrogen electrodes, if exposed to the atmosphere, will absorb moisture. This absorbed moisture can contribute to weld hydrogen levels. There are limits that exist for the amount of time that electrodes can be exposed to the atmosphere before they either need to be used, disposed of, or re-dried. Guidelines for atmospheric exposure limits for low-hydrogen electrodes are available from a variety of sources.[1-3] Some are a function of temperature and relative humidity while others are not. Since different brands of low hydrogen electrodes behave differently, the limits specified by the manufacturer for the particular brand of electrode in question should be used. In the absence of specific information, general limits can be used.

AWS D1.1 specifies that low-hydrogen electrodes that meet the requirements of AWS A5.1 (carbon steel electrodes) that are exposed to the atmosphere for more than 4 hr should be re-dried. If the electrodes are supplied with the "R" supplementary designator, the limit is 9 hr. The limits for low-hydrogen electrodes that meet the requirements of AWS A5.5 (low alloy steel electrodes) are 4, 2, and 1 hr for E7018, E8018, and E9018, respectively. The general guidelines in AWS D1.1 do not consider the specific atmospheric conditions of interest, and therefore, may be overly restrictive for areas of low humidity. AWS D1.1 allows longer limits to be established by testing. This allows specific limits for a particular brand of electrode to be established. AWS D1.1 allows electrodes that have been exposed for part of their exposure limit to be returned to a holding oven at 250ºF (120ºC) for 4 hr, after which they may be reissued.

Unless low-hydrogen electrodes are transferred to a storage oven or to a re-sealable container, the exposure time should begin once the hermetic seal on the package is broken. For electrodes that have been stored in an oven or a re-sealable container, the exposure time should begin once the electrodes are removed. Electrodes should be supplied to welders in quantities that can be consumed within atmospheric exposure limits. For this reason, it may be advantageous to purchase and use low-hydrogen electrodes in smaller quantity packages.

C5.4 Electrode Drying/Re-Conditioning

Low-hydrogen electrodes that are packaged in cardboard cartons (plastic-wrapped and otherwise) may require re-conditioning (baking, re-drying) prior to use. The same applies to low-hydrogen electrodes that have exceeded their atmospheric exposure limit. As with storage

and handling, reconditioning guidelines specified by the manufacturer for the particular brand of electrode in question should be followed whenever possible.

Electrode drying/reconditioning should be carried out in a purpose-built oven, an example of which is shown in Figure C11. Drying/reconditioning ovens are capable of attaining temperatures well in excess of those attainable in electrode storage ovens and have the capability for air circulation. Prior to baking, the electrodes should be removed from their container. The electrodes should be spread out in the oven so that all electrodes will reach the final baking temperature. The initial temperature of the oven should not exceed one half of the final baking temperature. The electrodes should be held at that temperature for a minimum of one half hour prior to increasing the temperature to the final baking temperature.

AWS A5.1 (carbon steel electrodes) requires that low-hydrogen electrodes be baked for at least 2 hr between 500 and 800ºF (260 and 430ºC). AWS A5.5 (low alloy steel electrodes) requires that low-hydrogen electrodes be baked for at least one hour between 700 and 800ºF (370 and 430ºC). These are general guidelines, however, and the specific manufacturer's recommendations should be followed when possible.

Some manufacturers recommend that electrodes should not be re-conditioned more than three times. AWS D1.1 specifies that electrodes cannot be re-baked more than once. Any electrode should be discarded if excessive re-drying causes the coating to become fragile and flake or break off while welding, or if there is a noticeable difference in handling or arc characteristics, such as insufficient arc force.

C6. APPLICATION OF GUIDANCE TO FIELD WELDING SITUATIONS

Guidance pertaining to storage and handling of low hydrogen electrodes is good for production welding and is good in principal for in-service welding applications, but the circumstances surrounding an in-service welding application are often unique. In-service welding is normally a one-off job that is performed many miles (kilometers) from where electrodes are stored. It is sometimes carried out under adverse atmospheric conditions (e.g., pipe surface temperature below the ambient dew point). Therefore, some discussion pertaining to how to apply the guidance provided above to actual in-service welding applications is appropriate.

The importance of controlling hydrogen levels for welds made onto in-service pipelines is well established. Many of the potential problems associated with storage and handling of low-hydrogen electrodes can be addressed at the electrode procurement stage. The use of electrodes with the H4R supplemental designator produce weld hydrogen levels that are less than 4 ml/100 g directly from a newly opened package. This precludes the need for baking prior to use. These electrodes also have a moisture resistant coating, so their exposure limits are longer than electrodes without the H4R supplemental designator. Also, the use of electrodes from small quantity packages (e.g., 10-lb cans) results in a high probability that the electrodes will be used

prior to their exposure limit being exceeded. There is also a high probability that, whatever electrodes remain at the end of the day, or after completion of the job, will be small in number, so the cost penalty of discarding these is minimal.

The surface temperature of a buried pipeline that has been exposed for repair or maintenance is often below the ambient dew point. As a result, moisture may condense on the pipe surface, which, if welded over, will contribute to increased weld hydrogen levels. The use of preheating, even though it may not significantly reduce the weld cooling rate, will burn off moisture and other contaminants (e.g., coating residue) prior to welding. Under extreme conditions, an air conditioned habitat can be constructed around the work area to dehumidify the air and reduce moisture condensation.[9] An example of this is shown in Figure C12.

In addition to burning off moisture and other contaminants, preheating allows hydrogen diffusion during and after welding. For this to occur, it is important to maintain the application of heat for some time after the weld is complete. In previous work,[10] it was suggested that preheat maintenance (i.e., post-heating) for 15 min would seem to be a reasonable time for temperatures in the 200 to 250°F (93 to 121°C) range and for the range of thicknesses that are encountered during most typical in-service welding applications. Longer times should be considered for thicker materials [e.g., pipe wall thickness greater than 0.5 inch (12.7 mm) and/or heavy-wall fittings] and/or for lower temperatures. When using post-heating to allow hydrogen diffusion, the post-heating must be applied prior to crack initiation.

C7. SUMMARY

The importance of controlling hydrogen levels for welds made onto in-service pipelines is well established. Many of the potential problems associated with minimizing hydrogen levels for welds made onto in-service pipelines can be addressed at the electrode procurement stage. Low-hydrogen electrodes with the H4R supplemental designator, packaged in small-quantity, hermetically sealed cans are ideally suited for in-service welding. This is particularly true for smaller jobs (e.g., small diameter lines) where it would be difficult to use an entire 50-lb (22.7-kg) can. There is a price premium for this type of packaging, however, and proper handling and use in the field is also important. The ability to closely control weld hydrogen levels will allow HAZ hardness levels that are higher than the limits that have been traditionally imposed (e.g., 350 HV) to be tolerated.

C8. REFERENCES

[1.] Unknown, Storing and Re-drying Electrodes, The Lincoln Electric Company, Cleveland, OH, http://lincolnelectric.com/knowledge/articles/content/storing.asp.

[2.] Unknown, Recommendations for the Storage, Re-drying and Handling of ESAB Consumables, ESAB AB, Göteborg, Sweden, http://www.esab.com/ESABHtml/pdf/Handling%20&Storage%20of%20Consumables(1).pdf.

[3.] AWS D1.1:2004, Structural Welding Code – Steel, American Welding Society, Miami, FL, 2004.

[4.] WTIA Technical Note 3, Care and Conditioning of Arc Welding Consumables, WTIA TN-3-94, Welding Technology Institute of Australia, Silverwater, NSW, 1994.

[5.] Bruce W. A., Boring, M. A., Fiore, S. R., and Nolan, D., Effect of Factors Related to Hydrogen Cracking for In-Service Welds, Part 1 – Weld Hydrogen Level Effects, Final Report for Gas Research Institute, Contract No. GRI-8546, Edison Welding Institute and University of Wollongong, February 2005.

[6.] AWS A5.1-91, Specification for Carbon Steel Electrodes for Shielded Metal Arc Welding, American Welding Society, Miami, FL, 1991.

[7.] AWS A5.5-96, Specification for Low Alloy Steel Electrodes for Shielded Metal Arc Welding, American Welding Society, Miami, FL, 1996.

[8.] Funderburk, S. R., Key Concepts in Welding Engineering – Selecting Filler Metals: Low Hydrogen, http://www.lincolnelectric.com/knowledge/articles/content/fillermetals.asp, Welding Innovation, Vol. XVII, No. 1, 2000.

[9.] Unknown, TDW Technicians Provide More than Customer Expected, TDW Global Solutions, http://www.tdwilliamson.com/EDM/Oct_03/Oct_03web.html, T.D. Williamson, Inc., Tulsa, OK, October 2003.

[10.] Bruce, W. A., and Boring, M. A., "Evaluation of Preheat Requirements for In-Service Welding," Final Report to Pipeline Research Council International for PR-185-0350, Edison Welding Institute, Columbus, OH, July 2005.

Figure C1. Low-hydrogen electrodes packaged in plastic-wrapped cardboard cartons.

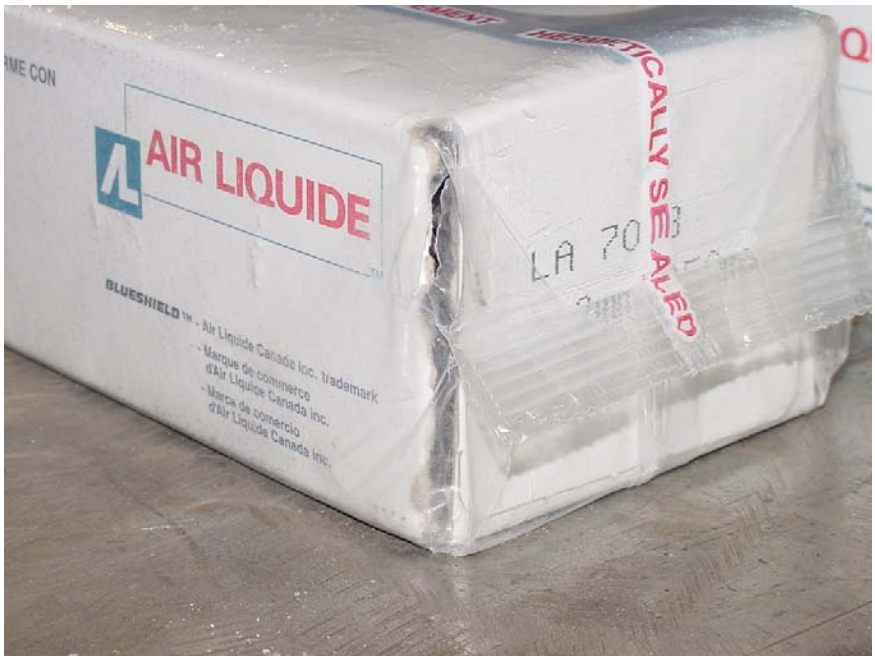

Figure C2. Damage to plastic wrap.

Figure C3. Low-hydrogen electrodes packaged in 50-lb (22.7-kg) hermetically sealed can.

Figure C4. Low-hydrogen electrodes packaged in 10-lb (4.5-kg) hermetically sealed can.

Figure C5. Electrodes packaged in Lincoln/Smitweld Sahara ReadyPacks.

Figure C6. Electrodes packaged in ESAB VacPacs.

Figure C7. Phoenix Type 300 Electrode Holding Oven.

Figure C8. Phoenix DryRod Type 2 Portable Electrode Ovens.

Figure C9. Rod guard storage canister – high-impact polyethylene, threaded cap with neoprene seal.

Figure C10. Phoenix Safetube storage container.

Figure C11. Phoenix Type 400 BT Electrode Re-Drying/Conditioning Oven.

Figure C12. Habitat built on offshore platform where in-service welding is being performed.

DNV Energy

DNV Energy is a leading professional service provider in safeguarding and improving business performance, assisting energy companies along the entire value chain from concept selection through exploration, production, transportation, refining and distribution. Our broad expertise covers Asset Risk & Operations Management, Enterprise Risk Management; IT Risk Management; Offshore Classification; Safety, Health and Environmental Risk Management; Technology Qualification; and Verification.

DNV Energy Regional Offices:

Asia and Middle East
Det Norske Veritas Sdn Bhd
24th Floor, Menara Weld
Jalan Raja Chulan
50200 Kuala Lumpur
Phone: +603 2050 2888

North America
Det Norske Veritas (USA), Inc.
1400 Ravello Drive
Katy, Texas 77449
United States of America
Phone: +281-721-6600

Europe and North Africa
Det Norske Veritas Ltd
Palace House
3 Cathedral Street
London SE1 9DE
United Kingdom
Phone: +44 20 7357 6080

Offshore Class and Inspection
Det Norske Veritas AS
Veritasveien 1
N-1322 Hovik
Norway
Phone: +47 67 57 99 00

Cleaner Energy & Utilities
Det Norske Veritas AS
Veritasveien 1
N-1322 Hovik
Norway
Phone: +47 67 57 99 00

South America and West Africa
Det Norske Veritas Ltda
Rua Sete de Setembro
111/12 Floor
20050006 Rio de Janeiro Brazil
Phone: +55 21 2517 7232

Nordic and Eurasia
Det Norske Veritas AS
Veritasveien 1
N-1322 Hovik
Norway
Phone: +47 67 57 99 00